U.PORTO

PROGRAMA DOUTRORAL EM BIOTECNOLOGIA MOLECULAR E CELULAR
APLICADA ÀS CIÊNCIAS DA SAÚDE

Drugging p53-impaired tumors: impact of new small molecules targeting p73 and mutant p53

Sara Gomes Moreira

D
2019

U.PORTO

Sara Gomes Moreira. Drugging p53-impaired tumors: impact of new small molecules targeting p73 and mutant p53

D.ICBAS **2019**

Drugging p53-impaired tumors: impact of new small molecules targeting p73 and mutant p53
Sara Gomes Moreira

SEDE ADMINISTRATIVA
INSTITUTO DE CIÊNCIAS BIOMÉDICAS ABEL SALAZAR
FACULDADE DE FARMÁCIA

Sara Gomes Moreira

Drugging p53-impaired tumors: impact of new small molecules targeting p73 and mutant p53

Tese de Candidatura ao grau de Doutor em Biotecnologia Molecular e Celular Aplicada às Ciências da Saúde

Programa Doutoral da Universidade do Porto (Instituto de Ciências Biomédicas de Abel Salazar e Faculdade de Farmácia)

Orientador

Doutora Lucília Helena Ataíde Saraiva

Professora Auxiliar

Faculdade de Farmácia da Universidade do Porto

Coorientadores

Doutora Maria Manuel Duque Vieira Marques dos Santos

Professora Auxiliar Convidada

Faculdade de Farmácia da Universidade de Lisboa

Doutor Alberto Inga

Professor Associado

Department of Cellular, Computational and Integrative Biology – CIBIO, University of Trento

Funding

This work was supported by the European Union (FEDER funds POCI/01/0145/FEDER/007728, Programa Operacional Factores de Competitividade – COMPETE), and National Funds (FCT/MCTES, Fundação para a Ciência e Tecnologia and Ministério da Ciência Tecnologia e Ensino Superior), by UID/QUI/50006/2019 and the projects (3599-PPCDT) PTDC/DTP-FTO/1981/2014 – POCI-01-0145-FEDER-016581 and PTDC/QUI-QOR/29664/2017. We also thank FCT for the financial support of the fellowship SFRH/BD/96189/2013 (S. Gomes), and the Programa Operacional Capital Humano (POCH), specifically the BiotechHealth Programme (Doctoral Programme on Cellular and Molecular Biotechnology Applied to Health Sciences; PD/00016/2012). We also acknowledge the support from the Italian Association for Cancer Research, AIRC (IG#18985 to AI).

Acknowledgements

Science is inherently a collaborative process that can only be achieved through the contribution of multiple people. As such, it is important to acknowledge those who have contributed to the completion of this thesis.

First and foremost, I would like to express my deepest gratitude to my supervisor, Professor Lucília Saraiva, for the constant support and guidance she has provided throughout this journey. Thank you for all the growth opportunities, for pushing me out of my comfort zone, and for preparing me for my next step as a scientist. Most of all thank you for always pushing me to improve, never allowing me to settle for less than you thought I was able to achieve.

I would also like to thank my co-supervisor Professor Maria Santos for welcoming me in her lab and providing invaluable training in the daunting field of organic chemistry. The opportunity to work in a different field has certainly given me a lot of perspective and knowledge, for which I'm truly grateful.

I am also deeply grateful to my co-supervisor Professor Alberto Inga for all the support and guidance throughout this journey. Thank you for welcoming in your lab where I've learned so much, and for the constant encouragement and uplifting words.

A big thanks to my lab family, Joana Soares, Liliana Raimundo, Ana Sara Gomes, Cláudia Bessa, Joana Loureiro, and Helena Ramos. Through hard times and big accomplishments your unconditional support has been essential. I'm sure you'll all do great things and that I've made true friends for life. I couldn't have done this without you.

I would also like to acknowledge Valentina Barcherini from the group of Professor Maria Santos at iMed.ULisboa for her essential help in scaling-up the synthesis of SLMP53-2 and the group of Professor Emília Sousa at CIIMAR (in particular Agostinho Lemos and Joana Moreira), for the synthesis of LEM2 and its derivatives.

I also thank Bartolomeo Bosco, Alessandra Bisio, and Yari Ciribilli for all the help with the ChIP and microarray experiments, Dr. Maria Inês Almeida for aiding in the microRNA assays, Bruno Moreira and Dr. Marco Alves for providing support with RT-qPCR assays, Dr. Carla Oliveira and Professor Lucília Domingues for the training and construction of plasmids, Professor Célia Gomes and Professor Flávio Reis for invaluable help and training with *in vivo* experiments, and Matthias Bauer and Professor Sir Alan Fersht, for all the training and help with binding assays.

I would also like to acknowledge the help of the lab technicians from the Laboratory of Microbiology, Cristina and Nuno.

Não poderia deixar de expressar a minha gratidão à minha família, pelo apoio constante durante este longo percurso. A minha mãe e irmãs são verdadeiros exemplos de força e determinação. Obrigada por acreditarem em mim, lembrando-me continuamente que há sempre espaço para melhorar. A maior recompensa que levo é saber que vos deixo orgulhosas, e espero continuar a fazê-lo.

To Bruno, you've endured the most through this ever so long journey and you've stuck with me until the very end. Thank you for all the love and support, and for knowing what I needed even when I didn't. Your encouragement, patience, and incredible sense of humor got me through a lot of hard times. I'm very grateful for being able to share this crazy ride with you.

To Gay and John, thank you for making me feel at home during my time abroad.

To my *minhoto* pal Bryan, thank you for the long talks, encouragement and support, and for being every bit as much of a weirdo as me.

To my friends, Ricardo, Diana, Pedro, Inês, Eduardo, and Rita, it has been a true pleasure getting to know all of you. In some way all of you helped me, in more planes than one, to succeed in this truly epic quest. Here's to many more dungeons to explore, monsters to slay, and dragons to befriend!

The less we see chaos, and the more we see
the pattern, the better we're going to be at
understanding just what we fight
– and just how to defeat it.
— Brandon Sanderson,
The Hero of Ages

Abstract

Cancer is currently a major public health concern with an expected increasing incidence and mortality in the coming decades. It represents a group of diseases with remarkable molecular complexity mostly triggered by alterations of oncogenes and tumor suppressor genes. The use of conventional chemotherapeutics for cancer treatment is limited by the development of chemoresistance and severe toxic side effects. Targeted anticancer therapies represent a crucial advance, since by taking advantage of molecular alterations specifically present in tumor cells, unspecific toxicity is greatly reduced. In this context, p53 family proteins arise as promising therapeutic targets, due to their critical role as tumor suppressors in several hallmarks of cancer. In addition, the antitumor activity of most conventional chemotherapeutics requires a functional p53 pathway. However, alterations of p53 family proteins are frequent in human cancers. In fact, half of human tumors harbor p53 mutations, and most remaining cancers overexpress negative modulators of p53 family proteins. Considering this, the aim of the present thesis was the identification of small molecule modulators of p53 family proteins with antitumor activity in p53-impaired cancers. In particular, two complementary therapeutic strategies were considered:

(i) Activation of TAp73, a p53 paralog, able to compensate for the lack of a functional p53 pathway;

(ii) Reactivation of mutant p53 (mutp53), leading to restoration of its tumor suppressive activity and inhibition of its oncogenic properties.

To this end, a multidisciplinary approach, involving medicinal chemistry, pharmacology, oncobiology, microbiology, biotechnology, and molecular biology, was adopted, resulting in the identification of two new activators of p53 family proteins.

In particular, the work developed in the present thesis led to the identification of the 1-carbaldehyde-3,4-dimethoxyxanthone LEM2, which was shown to activate TAp73 through disruption of its interaction with both *Murine double minute* (MDM)2 and mutant p53. This compound increased the transcriptional activity of TAp73, leading to cell cycle arrest and apoptosis in p53-null and mutp53-expressing tumor cells. Notably, a remarkable antitumor activity of LEM2 against patient-derived neuroblastoma cells, consistent with an activation of the TAp73 pathway, was demonstrated in a work complementary to this thesis. Altogether, besides its potential as an anticancer drug, LEM2 may also be a promising starting point for the development of improved TAp73-activating agents for anticancer therapy, particularly against neuroblastoma. An additional relevant outcome arising from this work was the development of a new yeast cell model that mimics the gain of function

of mutp53 through its inhibitory effect on TAp73. In fact, this work supports the suitability of the yeast model to screen for small molecule inhibitors of the TAp73-mutp53 interaction.

In addition, the tryptophanol-derived oxazoloisoindolinone SLMP53-2 was identified as a reactivator of mutp53. SLMP53-2 restored wild-type-like conformation and transcriptional activity to mutp53, by enhancing its interaction with heat shock protein (Hsp)70. In this way, this compound induced cell cycle arrest, apoptosis, and endoplasmic reticulum stress in mutp53-expressing hepatocellular carcinoma (HCC) cells. Most importantly, SLMP53-2 sensitized HCC cells to the effect of sorafenib and displayed potent *in vivo* antitumor activity against HCC xenografts, with no apparent undesirable toxicity. Altogether, SLMP53-2 represents a new mutp53-reactivating agent with a distinct mechanism of action from those currently reported. It may also represent a new effective anticancer therapeutic option, particularly against HCC, or it may be the basis for new derivatives with increased efficacy.

In conclusion, the work developed in this thesis provides a contribution to the advance of p53 family pharmacology and personalized cancer treatment, with the identification of new TAp73- and mutp53-activating agents with promising anticancer therapeutic applications.

Keywords: Anticancer therapy; Cancer; mutant p53; Small molecule activator; TAp73.

Resumo

O cancro é atualmente um dos principais problemas de saúde pública, esperando-se um aumento da sua incidência e mortalidade nas próximas décadas. O cancro consiste num conjunto de doenças de elevada complexidade molecular, causadas maioritariamente por alterações de oncogenes e genes supressores tumorais. A utilização de quimioterápicos convencionais no tratamento do cancro é limitada pelo desenvolvimento de quimiorresistência e efeitos tóxicos adversos graves. Desta forma, as terapêuticas direcionadas constituem um avanço crucial no tratamento do cancro, uma vez que o seu modo de ação depende da presença de alterações moleculares específicas do tumor, reduzindo significativamente os efeitos tóxicos inespecíficos. Neste contexto, as proteínas da família da p53 revelam-se promissores alvos terapêuticos, devido ao seu papel preponderante como supressores tumorais. Além disso, a atividade antitumoral da maioria dos quimioterápicos convencionais depende da existência de uma via funcional da p53. No entanto, as proteínas da família da p53 estão frequentemente alteradas em tumores humanos. Cerca de metade dos tumores humanos apresenta mutações da p53, e a maioria dos restantes cancros sobre-expressa moduladores negativos de proteínas da família da p53. Tendo isto em consideração, a presente tese teve como objetivo a identificação de pequenas moléculas moduladoras de proteínas da família da p53, com atividade antitumoral em cancros com uma via da p53 comprometida. Em particular, foram consideradas duas estratégias terapêuticas complementares:

(i) Ativação da TAp73, uma proteína da família da p53 cuja atividade poderá compensar a ausência de uma via funcional da p53;

(ii) Reativação de formas mutadas da p53 (mutp53), levando à restauração da atividade supressora tumoral, bem como à inibição das suas propriedades oncogénicas.

Para isso, foi adotada uma abordagem multidisciplinar envolvendo a química medicinal, farmacologia, oncobiologia, microbiologia, biotecnologia e biologia molecular, que resultou na identificação de dois novos ativadores de proteínas da família da p53.

Em particular, o trabalho desenvolvido na presente tese conduziu à identificação da 1-carbaldeído-3,4-dimetoxixantona LEM2, que ativa a TAp73 através da inibição da sua interação com a proteína *Murine double minute* (MDM)2 e mutp53. Este composto aumentou a atividade transcricional da TAp73, causando paragem do ciclo celular e apoptose de células sem expressão de p53 ou com mutp53. Adicionalmente, num trabalho complementar a esta tese, o LEM2 demonstrou uma marcada atividade antitumoral em células de neuroblastoma derivadas de pacientes. Assim, além do seu potencial como fármaco anticancerígeno, o LEM2 poderá representar um promissor ponto de partida para o desenvolvimento de novos agentes ativadores da TAp73 para a terapêutica

anticancerígena, em particular, do neuroblastoma. O desenvolvimento de um novo ensaio fenotípico de levedura que mimetiza o ganho de função da mutp53 através da inibição da TAp73 foi outro resultado importante alcançado com este trabalho. Desta forma, a presente tese evidencia a adequabilidade do modelo de levedura para a pesquisa de pequenas moléculas inibidoras da interação TAp73-mutp53.

Adicionalmente, a oxazoloisoindolinona derivada do triptofanol SLMP53-2 foi identificada como um reativador de mutp53. O composto SLMP53-2 promoveu a interação da mutp53 com a *heat shock protein* (Hsp)70, levando ao restabelecimento da conformação nativa e atividade transcricional da mutp53. Desta forma, este composto induziu paragem do ciclo celular, apoptose, e stresse do retículo endoplasmático em células de carcinoma hepatocelular (HCC) com expressão de mutp53. Além disso, o SLMP53-2 demonstrou um efeito sinérgico com o sorafenib em células de HCC, bem como uma marcada atividade antitumoral *in vivo*, sem sinais aparentes de efeitos tóxicos adversos. Em síntese, o SLMP53-2 representa um novo agente reativador de mutp53 com um mecanismo de ação distinto dos reportados até à presente data. Poderá também representar uma nova opção terapêutica para o tratamento do cancro, particularmente do HCC, bem como a base para o desenvolvimento de derivados com eficácia melhorada.

Em conclusão, o trabalho desenvolvido nesta tese contribui para o avanço da farmacologia das proteínas da família da p53, bem como do tratamento personalizado do cancro, com a identificação de novos agentes ativadores da TAp73 e mutp53 com promissora aplicação na terapêutica anticancerígena.

Palavras-chave: cancro; p53 mutante; pequena molécula ativadora; TAp73; terapêutica anticancerígena

Abbreviations

CETSA	Cellular thermal shift assay
CFU	Colony-forming unit
ChIP	Chromatin immunoprecipitation
CI	Combination index
Co-IP	Co-immunoprecipitation
CTM	Chetomin
DBD	DNA-binding domain
DEG	Differentially expressed gene
DNE	Dominant-negative effect
ER	Endoplasmic reticulum
GOF	Gain of function
HCC	Hepatocellular carcinoma
Hsp	Heat shock protein
HSQC-NMR	Heteronuclear single quantum coherence nuclear magnetic resonance
HTS	High-throughput screening
IP	Immunoprecipitation
IPA	Ingenuity pathway analysis
LOF	Loss of function
MDM	Murine double minute
mut	Mutant
OD	Oligomerization domain
PPI	Protein-protein interaction
PTM	Post-translational modification
RE	Response element
SRB	Sulforhodamine B
TAD	Transactivation domain
TSG	Tumor suppressor gene
UPR	Unfolded protein response
wt	Wild-type
Y2H	Yeast two-hybrid

Table of Contents

List of Figures

List of tables

Chapter 1. Literature Review

Parts of this chapter were based on the following publications:

- Gomes, S., Leão, M., Raimundo, L., Ramos, H., Soares, J. and Saraiva, L., 2016, p53 family interactions and yeast: together in anticancer therapy. Drug Discov Today **21**(4): 616-624. doi: 10.1016/j.drudis.2016.02.007.

- Lopes, E. A., Gomes, S., Saraiva, L. and Santos, M. M. M., 2019, Small Molecules Targeting Mutant P53: A Promising Approach For Cancer Treatment. Current Medicinal Chemistry **25**: 1-13. doi: 10.2174/0929867325666181116124308.

1.1. General concepts on cancer epidemiology and biology

Cancer is currently a global high-priority public health concern, representing the major obstacle to increasing life expectancy in the 21st century (Bray et al., 2018). Both cancer incidence and mortality have been steadily rising worldwide and are predicted to continue increasing in the coming decades (**Figure 1.1**). The growing number of new cancer cases reflects not only population aging, but also several cancer risk factors associated with socioeconomic development (Bray et al., 2018). An estimated 18.1 million new cancers were diagnosed in 2018, with 9.6 million cancer-related deaths on a global scale (Bray et al., 2018). In 2016, cancer was responsible for 213.2 million disability-adjusted life years (DALYs), most of which came from years of life lost (YLLs) (Global Burden of Disease Cancer Collaboration et al., 2018).

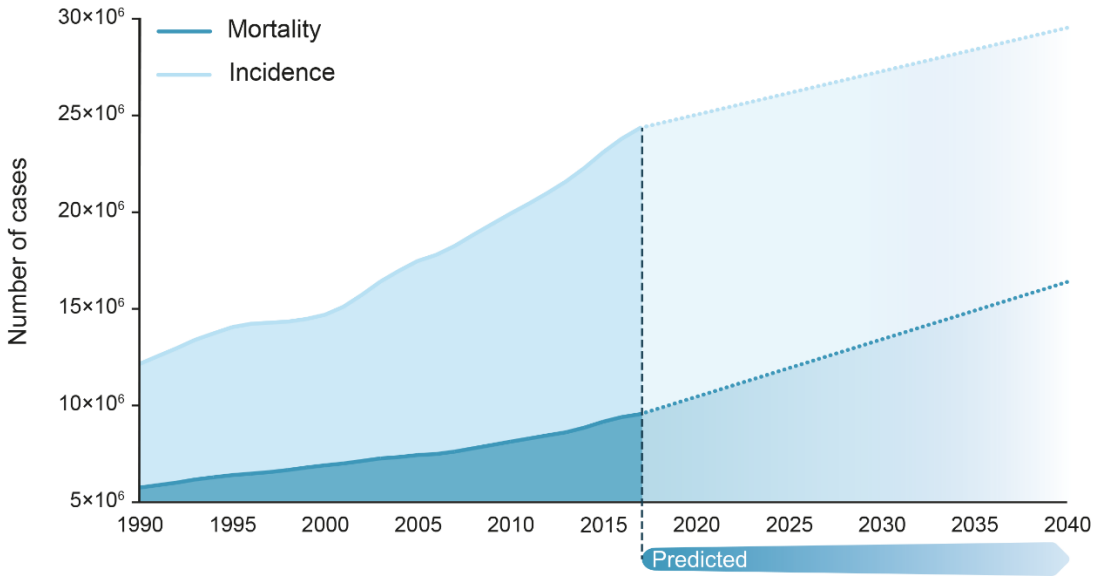

Figure 1.1 Number of incident cases of cancer and cancer-related deaths per year worldwide. Plotted data from 1990 to 2017 were obtained from the GHDx dataset (Institute for Health Metrics and Evaluation, 2017; Global Burden of Disease Cancer Collaboration et al., 2018). Predicted values from 2018 to 2040 were obtained from GLOBOCAN (International Agency for Research on Cancer, 2018b; Ferlay et al., 2019).

In Portugal, malignant neoplasms were the second leading cause of death in 2017 (over 27 thousand deaths, representing 25% of the total mortality), surpassed only by diseases of the circulatory system (INE, 2019). In that period, malignant neoplasms led to an average of 11.2 YLLs (INE, 2019).

Although the most incident types of cancer vary geographically, the 10 cancer types with the highest incidence worldwide in 2018 (**Figure 1.2**) represented 65% of all newly diagnosed cancer cases and deaths in 2018 (Bray et al., 2018).

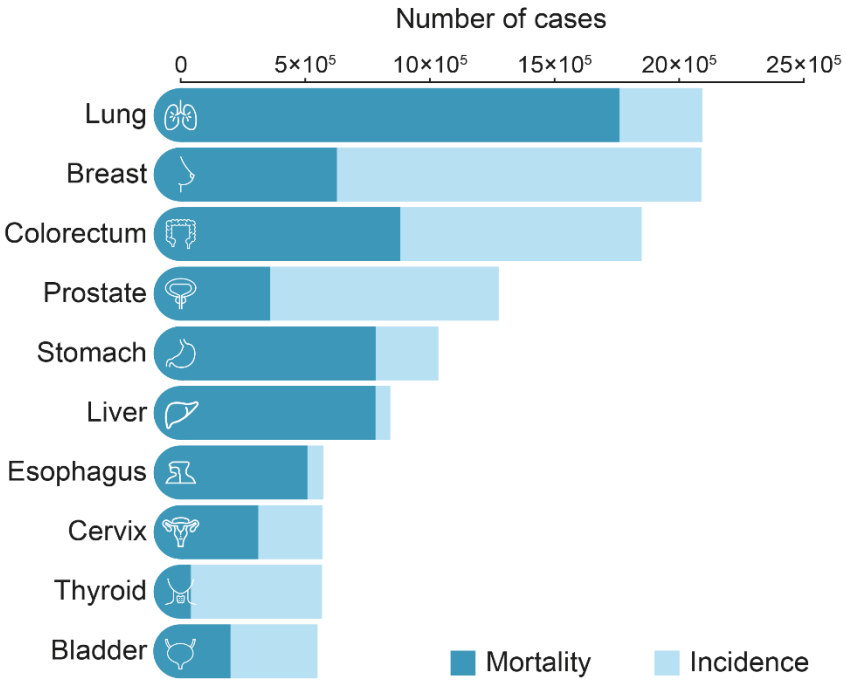

Figure 1.2 Estimated incidence and mortality of the 10 most incident cancer types worldwide in 2018. Plotted data was obtained from GLOBOCAN (Bray et al., 2018; International Agency for Research on Cancer, 2018a).

The huge amount of work on cancer research reflects the outstanding complexity of this multifaceted set of diseases. There have been over 100 reported types of cancer, many of which include subtypes with unique features (Hanahan and Weinberg, 2000). Cancer development occurs through the sequential clonal selection of cells with genetic alterations that confer growth advantages (Mendelsohn et al., 2014). However, tumors are usually heterogenous, containing cells with distinct genetic aberrations. Another layer of complexity arises from the fact that neoplasms are not only composed of tumor cells, but are instead complex tissues in which these interact with other cell types (including immune and endothelial cells), and the extracellular matrix, forming the tumor microenvironment (Mendelsohn et al., 2014).

In order to categorize the myriad of biological features that characterize human cancers, Hanahan and Weinberg devised a set of physiological alterations that define the malignant phenotype and are common to the vast majority of tumors (Hanahan and Weinberg, 2000). This proposed core set of cancer hallmarks consisted of the ability to: (i) promote cell growth and proliferation in the absence of mitogenic stimuli; (ii) evade growth suppressors that would otherwise induce cell senescence; (iii) limit the response to apoptotic triggers thereby resisting cell death; (iv) maintain telomeric DNA length, enabling replicative immortality; (v) stimulate angiogenesis, inducing the formation of blood vessels that provide nutrient and oxygen supplies to the tumor; (vi) invade circumventing tissues and eventually form distant metastases. The ability of tumor cells to reprogram their energetic metabolism to fuel cell growth and division, as well as to avoid destruction by the immune system, have been more recently proposed as emerging cancer hallmarks (Hanahan and Weinberg, 2011).

In addition, two central characteristics that enable the acquisition of the aforementioned hallmarks have also been identified (Hanahan and Weinberg, 2011). In particular, inflammation, which is present in virtually every tumor, can supply growth and survival factors, and promote invasion and angiogenesis, thereby enabling several of the hallmark features. Additionally, tumor cells almost ubiquitously display genomic instability, caused by compromised genomic integrity surveillance and maintenance mechanisms. These mechanisms are regulated by a class of cancer-related tumor suppressor genes (TSGs) called caretakers, which are normally involved in the detection of DNA damage and subsequent mobilization of DNA-repair enzymes (Vogelstein and Kinzler, 2004). Caretaker genes are frequently mutated in human cancers, leading to an increased rate of spontaneous mutation. This contributes to the accumulation of genetic defects in other cancer-related genes, responsible for the acquisition of cancer hallmarks.

Besides caretaker functions, TSGs may also display gatekeeper activity. Gatekeeper TSGs prevent uncontrolled cell proliferation by inducing growth arrest, senescence, or cell death under normal physiological conditions (Kinzler and Vogelstein, 1997). In tumor cells, gatekeeper TSGs often suffer inactivating mutations that lead to loss-of-function (LOF), contributing to the malignant phenotype. Frequent inactivating mutations of TSGs include epigenetic silencing, deletions, and missense and nonsense mutations (Mendelsohn et al., 2014). The contribution of TSG mutations to the malignant phenotype is only observed upon inactivation of both alleles, thus considered recessive mutations. Haploinsufficient TSGs are an exception to this observation, since the remaining wild-type (wt) allele is unable to maintain normal function, and LOF is observed even in a heterozygous context (Mendelsohn et al., 2014).

In contrast to TSGs, proto-oncogenes promote cell growth and proliferation under normal conditions. Oncogenes, generated by mutation of proto-oncogenes, encode constitutively active or overexpressed forms of growth-inducing proteins that promote malignant transformation. These gain-of-function (GOF) alterations are often caused by promoter demethylation, gene amplification, chromosome translocation, or missense mutation (Mendelsohn et al., 2014). Contrary to TSGs, heterozygous mutation is sufficient for the observation of the phenotype (Kinzler and Vogelstein, 1997).

Interestingly, about 80% of cancer-related mutations have been reported to occur in TSGs (Liu et al., 2015). Despite this, the vast majority of the currently available directed anticancer therapies target oncogenes, since the functional rescue of a TSG is less straightforward than the inhibition of an hyperactive protein or pathway (Morris and Chan, 2014). In addition, many TSGs are not considered druggable targets (Liu et al., 2015). Although effective, oncogene-targeted therapies do not address the issue of genomic instability caused by the presence of TSG inactivation, which allows cells to acquire new mutations that may confer therapeutic resistance (Epstein, 2013).

The present thesis focused on the search for pharmacological modulators of the p53 family of TSGs, which displays both caretaker and gatekeeper functions, and includes some of the most ubiquitously altered genes in human cancer.

1.2. The p53 family of tumor suppressors

In mammalian genomes, the p53 family of tumor suppressors comprises three paralogous genes, *TP53*, *TP63*, and *TP73*. *TP5*3 (located on chromosome 17p13.1) encodes the p53 protein that was firstly identified in 1979 as a simian virus (SV40) large T antigen binding protein (Lane and Crawford, 1979; Linzer and Levine, 1979). *TP63* (located on chromosome 3q27-29), and *TP73* (located on chromosome 1p36.2-3), encoding p63 and p73 proteins respectively, were identified 18 years after the discovery of p53 (Jost et al., 1997; Kaghad et al., 1997; Yang et al., 1998). Unlike mammalian genomes, invertebrates possess only one p63/p73-like protein, which is thought to have originated the three genes present in mammalian genomes through two gene duplications (Belyi et al., 2010).

1.2.1. Modular domain organization, gene structure, and isoforms of the p53 family

All p53 family proteins share a similar modular domain organization, consisting mainly of an N-terminal transactivation domain (TAD), a core DNA-binding domain (DBD), and a C-terminal oligomerization domain (OD) (Joerger and Fersht, 2008) (**Figure 1.3**).

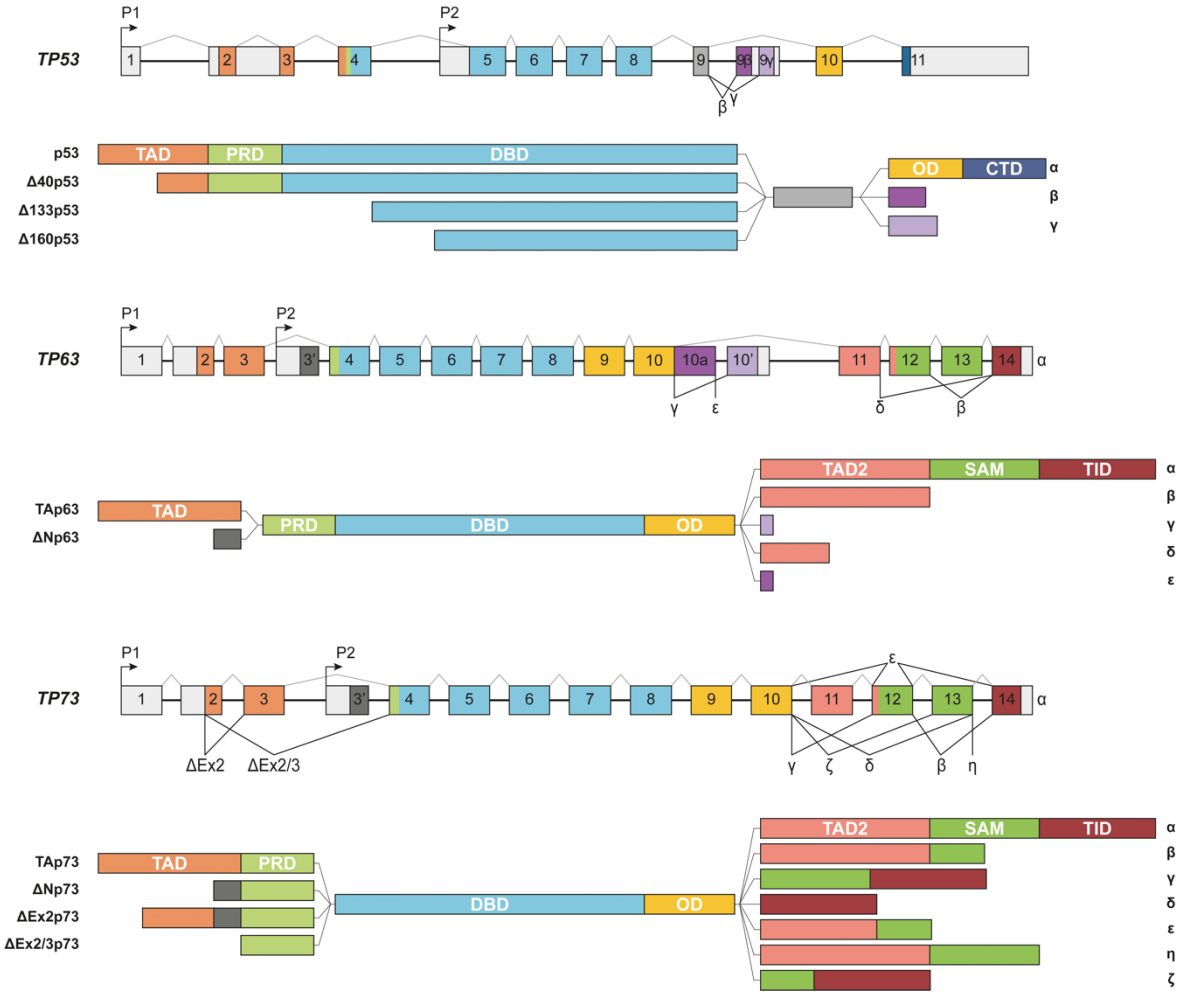

Figure 1.3 Schematic representation of the gene architecture of *TP53, TP63* and *TP73*. Exons are colored according to the encoded protein domains. Promoters and alternative splicing that generate distinct protein isoforms are represented. Modular domain organization of the isoforms of p53, p63 and p73 proteins: TAD, transactivation domain; PRD, proline-rich domain; DBD, DNA-binding domain; OD, oligomerization domain; CTD, C-terminal domain; SAM, sterile alpha motif; TID, transactivation inhibitory domain.

The N-terminal TAD is an intrinsically disordered region that recruits transcriptional coactivators like p300 and CREB-binding protein, directing the transcriptional activity of p53 family proteins (Joerger and Fersht, 2008). Following the TAD, p53 family proteins have a proline-rich domain (PRD), which is known to mediate protein-protein interactions (PPIs), in particular with proteins containing SRC Homology 3 (SH3) motifs (Joerger and Fersht, 2008). The DBD recognizes and binds to specific DNA sequences termed p53-responsive elements (p53REs). Unlike the other domains, the DBD is not intrinsically disordered, and

it is the domain with the highest sequence identity among the three paralogous genes (Wei et al., 2012). In fact, the DBD shares about 80% sequence identity among p53 family proteins, while the TAD and C-terminal regions share only about 30% sequence identity (Wei et al., 2012). The relatively high sequence identity of the DBD justifies the ability of p53 family proteins to transactivate an overlapping set of target genes (Candi et al., 2014). The DBD is also highly conserved, justifying the similarity of DNA-binding specificity observed amongst p53 family proteins of evolutionarily distant species (Brandt et al., 2009; Joerger and Fersht, 2016). The C-terminal OD allows the assembly of p53 family proteins into their active tetrameric conformation (Joerger and Fersht, 2008). Like the TAD, the OD is also an intrinsically disorder region. Although p63 and p73 share similar ODs, they are significantly longer than the p53 OD, containing an additional α-helix (Joerger et al., 2009). Thus, although p63 and p73 can form hetero-tetramers, this difference in the OD length prevents the formation of p53 hetero-tetramers with p63 or p73 (Joerger et al., 2009). Interestingly, a recent work suggests the possibility of p53-p73 hetero-tetramerization, upon phosphorylation of p53 at Thr81 by JNK kinase (Wolf et al., 2018). This post-translational modification (PTM) of p53 is thought to induce a conformational change that allows the interaction of the two ODs. The C-terminal domain (CTD) of p53 establishes non-specific low-affinity interactions with DNA that contribute to the stability of the p53-DNA complex (Vieler and Sanyal, 2018). This region is also intrinsically disordered and subject to many PTMs that are thought to contribute to the fine-tuning of p53 transcriptional activity by interfering with the stability of the p53-DNA complex (Joerger and Fersht, 2008; Laptenko et al., 2015). p63 and p73 display an extended C-terminal region (**Figure 1.3**) that contains a sterile alpha motif (SAM) domain, and a transactivation inhibitory domain (TID) (Thanos and Bowie, 1999; Dötsch et al., 2010). The SAM domain mediates PPIs, essential for tetramerization (Ou et al., 2007; Candi et al., 2014). Conversely, the TID is a regulatory region able to bind to the TAD of another p63/p73 monomer, leading to the formation of an inactive dimer, lacking transactivation ability (Candi et al., 2014).

This modular domain structure, along with the presence of many intrinsically disordered regions, typical of signaling proteins, allows p53 family proteins to establish interactions with several distinct binding partners. In addition, it allows for the fine-tuning of p53 family regulation through many different combinations of PTMs. The adaptability of p53 family proteins, which reflects their crucial role in the regulation of several different cellular processes (Uversky et al., 2014), is further accentuated by the existence of distinct isoforms of each protein with non-redundant roles (**Figure 1.3**).

The p53 family genes contain alternative promoters that generate isoforms with truncated N-terminal domains. In particular, the full-length p53 protein is generated by transcription from the P1 promoter. Alternative splicing of intron 2 generates Δ40 isoforms

lacking a portion of the TAD. On the other hand, transcription of the *TP53* gene from the alternative promoter (P2) at intron 4 generates Δ133p53 or Δ160p53 isoforms, lacking the full TAD. *TP63* and *TP73* also contain two promoters, namely P1 (located at exon 1) that produces TA isoforms, and P2 (located at exon 3) that produces ΔN isoforms lacking the TAD. Additionally, alternative splicing of exons 2 and 3 generates the ΔEx2 and ΔEx2/3 isoforms of p73 that lack exon 2 or exons 2 and 3, respectively (Melino et al., 2002) (**Figure 1.3**).

In general, contrary to TA isoforms (containing the full TAD), N-terminally truncated ΔN isoforms are considered transcriptionally inactive, since they lack the ability to initiate transcription from the canonical p53 family RE. ΔN isoforms have often been reported as dominant-negative regulators of TA isoforms, either through formation of transcriptionally inactive hetero-tetramers, or through competitive binding to DNA (Murray-Zmijewski et al., 2006). Despite this, an alternative TAD (TAD2) encoded in exons 11 and 12 is present in ΔN isoforms (Ghioni et al., 2002), accounting for their reported unique transcriptional activity (Vigano et al., 2006; Marcel et al., 2012).

The α isoforms of p53 family proteins correspond to the full-length proteins, and isoforms varying at the C-terminal region are generated through either alternative splicing or transcriptional termination. Three C-terminal isoforms, α, β, and γ, with different transactivation ability, have been reported for p53 (Zhu et al., 1998; De Laurenzi et al., 1999). Together with the N-terminal isoforms, the *TP53* gene may generate nine different proteins. Alternative splicing of the *TP63* gene generates three C-terminal isoforms, β, γ, and δ, while transcriptional termination at exon 10 generates the ε isoform. The *TP73* gene appears to be the most complex. Termination at exon 13 originates the η isoform, while alternative splicing at 3' generates the β, γ, δ, ε, and ζ isoforms, all with distinct C-terminal regions (Candi et al., 2014) (**Figure 1.3**).

The existence of several different isoforms with distinct transcriptional activities and regulatory domains adds an additional layer of complexity to this family of proteins. The regulation of translation from alternative promoters and of alternative splicing events provides another regulatory level to fine-tune the activity of this crucial family of proteins.

1.2.2. Molecular functions of p53 family proteins

The well-established role of p53 as a tumor suppressor is illustrated by the fact that p53-null mice develop early-onset spontaneous tumors, with 100% penetrance (Donehower et al., 1992; Purdie et al., 1994). Heterozygous $p53^{+/-}$ mice also show increased predisposition for cancer development (Donehower et al., 1992; Purdie et al., 1994).

Despite their structural similarities with p53, the roles of p63 and p73 in human cancer are not as straightforward. Unlike p53, these proteins are vital for normal development and differentiation (Dötsch et al., 2010). In particular, p63 is crucial in the regulation of epithelial morphogenesis (Mills et al., 1999; Yang et al., 1999; Candi et al., 2007; Paris et al., 2012), as evidenced by the severe limb truncations and profound alterations in skin and epithelial appendages that lead to the premature death of p63-null mice (Mills et al., 1999; Yang et al., 1999). p63 is also important for the preservation of genomic integrity in female germ cells (Suh et al., 2006). On the other hand, p73-deficient mice die prematurely as a result of chronic inflammation and recurring infections, supporting the involvement of p73 in immune system regulation (Erster et al., 2006). These animals also display various neuronal defects, corroborating the vital function of p73 in neuronal development (Yang et al., 2000; Pozniak et al., 2002).

Nevertheless, both p63 and p73 (in particular the TA isoforms) share many molecular functions of p53 and are involved in all aspects of cancer progression. In fact, p63 ablation has been reported to increase predisposition for tumor development (Flores et al., 2005), particularly in mice lacking p53 (Guo et al., 2009a). Interestingly, Keyes et al. (2006) did not observe increased tumor predisposition in p63-deficient mice, possibly due to distinct contributions of the p63 isoforms. The ΔNp63 isoforms, reported to contribute to skin carcinogenesis, are often overexpressed in squamous cell carcinomas (Weber et al., 2002; Sniezek et al., 2004; Westfall and Pietenpol, 2004; Wu et al., 2005). In addition, loss of p63 expression has been reported in a subset of invasive bladder carcinomas, correlating with increased invasion and metastasis (Park et al., 2000; Urist et al., 2002). In fact, TAp63 isoforms are crucial for protection against cancer metastasis (Su et al., 2010; Melino, 2011). Regarding p73, ablation of TAp73 isoforms leads to increased tumor susceptibility and genomic instability in mice (Tomasini et al., 2008), while knockout of ΔNp73 isoforms increases susceptibility to DNA-damaging agents (Wilhelm et al., 2010). Consistently, overexpression of ΔNp73 isoforms has been reported in many cancer types, correlating with poor response to chemotherapeutics and unfavorable patient prognosis (Dominguez et al., 2006; Wager et al., 2006).

Under physiological conditions, p53 family proteins are maintained at relatively low levels (Riley et al., 2008). Upon exposure to a variety of cellular stress stimuli p53 family proteins are subjected to PTMs that promote their stabilization and transcriptional activity (**Figure 1.4**) (Giaccia and Kastan, 1998; Hu et al., 2012). The type and intensity of the cellular stress, as well as the cellular context, determine the PTM pattern, which, in turn, determines the transcriptional program triggered by p53 (Riley et al., 2008). Subsequently, p53 tetramers bind to REs, either activating or repressing the transcription of p53 target genes (Riley et al., 2008). These REs consist of two half-site decamers with the sequence

RRRCWWGYYY (in which R represents a purine, W is either an adenine or thymine and Y represents a pyrimidine), separated by a spacer with varying length (Riley et al., 2008). The TA isoforms of p63 and p73 are also known to bind to p53REs, exerting p53-like transcriptional activity (Jost et al., 1997; Kaghad et al., 1997; De Laurenzi et al., 1998; Yang et al., 1998). However, these proteins have also been reported to possess unique transcriptional targets, and many target genes appear to respond differently to distinct p53 family proteins (Levrero et al., 2000). As an additional regulatory layer, small differences in the RE sequence and spacer length confer different binding affinity towards p53, justifying the activation/repression of different sets of target genes under distinct conditions (Resnick-Silverman et al., 1998). The length of the spacer has also been reported to determine the transcriptional program triggered by p73 (Jordan et al., 2008).

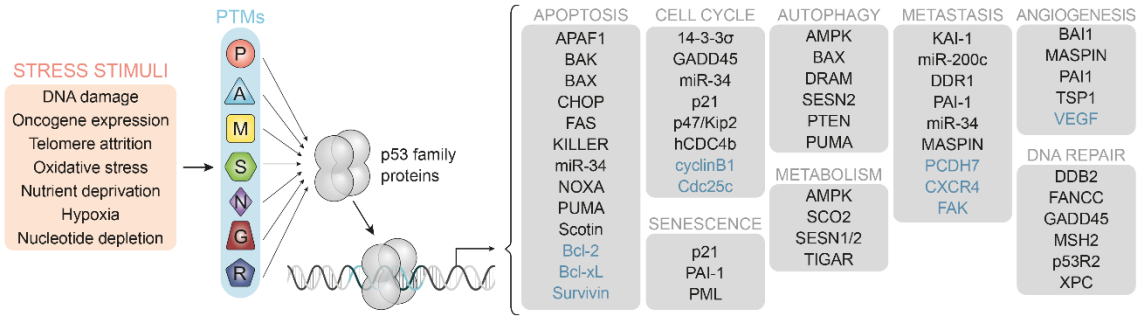

Figure 1.4 Transcriptional targets of p53 family proteins regulate key cellular processes in cancer. p53 family proteins integrate the response to various stress stimuli, which lead to activating PTMs (P: phosphorylation; A: acetylation; M: methylation; S: sumoylation; N: neddylation; G: glycosylation; R: ADP-ribosylation). The type and intensity of the stress stimulus determines the pattern of PTMs, which, in turn, determines the transcriptional program triggered by p53 family proteins, leading to distinct cellular responses (up- and downregulated p53 family transcriptional targets are represented in black and blue, respectively; the arrow above the DNA represents the transcription of genes).

Genetic studies have identified p53REs in approximately 600 distinct genes (Wei et al., 2006b), encoding a complex network of proteins involved in the regulation of several distinct cellular processes that can interfere with virtually all cancer hallmarks (Wei et al., 2006b). In fact, it has been proposed that p53 family proteins function as a central regulatory hub, integrating stress stimuli into a coordinated biological response that prevents cells to acquire cancer hallmark capabilities (Hainaut et al., 2012).

The most well-established functions of p53 family proteins are the control of the cell cycle and cell death. Upon stress exposure, p53 family proteins initially halt cell cycle progression and activate DNA repair mechanisms. Continued exposure to stress or irreparable damage may lead p53 family proteins to trigger senescence or apoptosis (Maddocks and Vousden, 2011).

Regarding cell cycle regulation, p53 family proteins may induce G1 or G2/M arrest. The main effector in G1-phase cell cycle arrest is the cyclin-dependent kinase (Cdk) inhibitor p21 (el-Deiry et al., 1993). In fact, the *CDKN1A* gene, which encodes p21, is a positive transcriptional target of p53 family proteins. Binding of p21 to cyclinE/Cdk2 and cyclinD/Cdk4/6 complexes prevents Rb phosphorylation and release of E2F. In this way, E2F is unable to transactivate genes that would be required for S-phase entry (Harper et al., 1993), leading to G1-arrest. Besides p21, p53 family proteins also transcriptionally upregulate p57/Kip2 (Balint et al., 2002; Guo et al., 2009b) that, like p21, induces cell cycle arrest by inhibiting cyclin/CDK complexes. In addition, hCDC4b, a protein that targets cyclin E for degradation inhibiting S-phase entry, is also transcriptionally upregulated by p53 family proteins (Kimura et al., 2003), contributing to G1-arrest. G2/M-arrest is also triggered by p53 family proteins, since p21 also binds and inhibits the cyclinB1/Cdk1 complex, which is required for progression through mitosis (Smits et al., 2000). p53 family proteins also contribute to G2/M-arrest through transcriptional upregulation of GADD45, which prevents the formation of the cyclinB1/Cdk1 complex (Hollander et al., 1993; Chen et al., 1995; Chin et al., 1997), and of 14-3-3σ, which physically separates cyclinB1/Cdk1 complexes from their target proteins by promoting their nuclear export (Hermeking et al., 1997). p53 and TAp73 have also been reported to downregulate Cdk1, cyclinB1 and Cdc25c (a phosphatase that activates cyclinB1/Cdk1 complexes) (Yun et al., 1999; Krause et al., 2000; Taylor et al., 2001; Innocente and Lee, 2005; Scian et al., 2008) (**Figure 1.4**).

While cell cycle arrest is a reversible process, p53 family proteins can also trigger senescence, which is regarded as a highly stable (albeit not completely irreversible) state of cell cycle arrest, characterized by large cell size, autophagy, and secretion of proinflammatory cytokines (Campisi, 2005). Transcriptional activation of p21 appears to be a critical step in p53 family-induced senescence (Brown et al., 1997). In addition, p53-induced senescence is also associated with transcriptional upregulation of PAI-1 (plasminogen activator inhibitor) and PML (promyelocytic leukemia protein) (Kortlever et al., 2006; Riley et al., 2008) (**Figure 1.4**).

One of the most central roles of p53 family proteins is their ability to induce apoptosis upon irreparable cellular damage, in order to eliminate damaged cells and avoid error propagation (**Figure 1.4**) (Vousden and Prives, 2009). In fact, p53 family proteins are able to trigger both the intrinsic and extrinsic apoptotic pathways (Riley et al., 2008; Zilfou and

Lowe, 2009). p53 is a positive transcriptional regulator of the Fas/CD95/Apo-1 and KILLER/DR5 cell death receptors (Owen-Schaub et al., 1995; Fukazawa et al., 1999; Takimoto and El-Deiry, 2000), which are activated in the first step of the extrinsic apoptotic pathway. Activation of these receptors leads to the recruitment of protein adaptor FADD (Fas-associated protein with death domain) and subsequently of caspase-8, forming the death-inducing signaling complex (DISC). Interestingly, p53 is also a transcriptional activator of caspase-8 (Liedtke et al., 2003). p63 and p73 have also been reported to transcriptionally activate cell death receptors (Zaika et al., 2002; Ramadan et al., 2005). Regarding the intrinsic or mitochondrial apoptotic pathway, p53 family proteins transcriptionally activate BH3 domain-only proapoptotic proteins (PUMA, NOXA, BAX, and BAK). These proteins translocate to the mitochondria, where they trigger mitochondrial outer membrane permeabilization. In particular, BAX and BAK insert into the outer mitochondrial membrane forming pores that allow cytochrome *c* release. Cytochrome *c* binds APAF-1, promoting the formation of the apoptosome complex, which ultimately leads to the recruitment of executioner caspases to induce cell death. PUMA and NOXA release BAX and BAK from inhibitory interactions with antiapoptotic Bcl-2 family proteins (Chen, 2016). Interestingly, p53 family proteins have also been reported to transcriptionally downregulate antiapoptotic Bcl-2 family proteins, namely Bcl-2 and Bcl-xL. Besides its transcriptional role in apoptosis induction, p53 can act directly at the mitochondria, binding to Bcl-2 and Bcl-xL with subsequent BAX and BAK release (Mihara et al., 2003).

p53, TAp63, and TAp73 are also involved in endoplasmic reticulum (ER) stress-related apoptotic cell death. ER stress occurs when the homeostasis of the ER is disrupted, leading to accumulation of unfolded proteins in the ER lumen (Kim et al., 2008). Under these circumstances, the unfolded protein response (UPR) is triggered, in an attempt to restore ER homeostasis (Kim et al., 2008). Three ER stress sensors, PERK, IRE1α, and ATF6, cooperate in this response (Verfaillie et al., 2012). Under physiological conditions, these ER proteins are kept inactive by the chaperone BiP/GRP78. Accumulating unfolded proteins compete for BiP/GRP78, releasing PERK, IRE1α, and ATF6. Upon activation, PERK promotes phosphorylation of eIF2α (Marciniak et al., 2006). Phosphorylated eIF2α (p-eIF2α) is unable to form complexes with $tRNA^{Met}$, required for translation initiation. In this way, PERK temporarily halts protein translation, reducing the ER load, and allowing homeostasis restoration. Upon activation, the C-terminal endoribonuclease domain of IRE1α catalyzes the processing of XBP1 into spliced XBP1 (sXBP1). sXBP1 is then able to transactivate a set of UPR genes (Lee et al., 2003). In addition, released ATF6 is cleaved at the Golgi, generating an active N-terminal fragment able to homodimerize or heterodimerize with NF-Y or sXBP1 at the nucleus, directing the transcription of UPR genes (Yamamoto et al., 2007). The UPR genes stimulated through the IRE1α and ATF6

pathways include chaperones, to aid in protein folding, and proteins involved in the ER-associated degradation pathway (ERAD), to promote degradation of terminally misfolded proteins. When the UPR is unable to restore ER homeostasis, chronic UPR activation leads to apoptotic cell death (Tabas and Ron, 2011). The major event involved in the switch to apoptosis is the activation of CHOP following sustained activation of PERK. CHOP inhibits Bcl-2, and increases oxidative stress, promoting apoptosis (McCullough et al., 2001). In addition, CHOP activates GADD34, which dephosphorylates p-eIF2α thereby restoring normal protein translation, which overloads the ER promoting cell death (Brush et al., 2003). CHOP also induces the expression of TRIB3, which promotes apoptosis through Akt inhibition (Ohoka et al., 2005). p53 transcriptionally activates CHOP, consistent with an involvement in ER stress-mediated cell death (Liu et al., 2007). Despite this, the role of p53 in this mechanism is not straightforward, since ER stress has been reported to enhance p53 nuclear export and degradation (Pluquet et al., 2005). However, this may occur only at the first stage of the UPR response, before the switch to apoptosis. In addition, cytoplasmic p53 is able to localize to the ER at specialized regions that contact with the mitochondria. Upon activation, p53 promotes the release of Ca^{2+} from the ER to the mitochondria, promoting the intrinsic apoptotic pathway (Giorgi et al., 2015). p53 stabilization upon ER stress has also been reported, in particular through NF-κB, leading to apoptosis through PUMA and NOXA induction (Pluquet and Hainaut, 2001; Lin et al., 2012b). In addition, p53 family proteins transcriptionally induce the expression of scotin, a protein that causes apoptotic cell death in response to ER stress (Bourdon et al., 2002; Terrinoni et al., 2004; Zocchi et al., 2008).

Besides cell proliferation and death, p53 family proteins regulate a complex network of target genes that lead to the regulation of many other cellular processes, including autophagy and energetic metabolism, activation of DNA repair pathways, inhibition of cell migration and invasion, and downregulation of angiogenesis (**Figure 1.4**) (Hainaut et al., 2012).

1.3. Impairment of p53 family proteins in human cancer

TP53 is the most frequently altered gene in human tumors, regardless of cancer type (Petitjean et al., 2007). Mutation in the *TP53* gene occurs in approximately 50% of all cancers, and even in their absence, p53 activity is usually impaired by upregulation of its negative modulators (Hainaut et al., 2012). In addition, although *TP63* and *TP73* mutations are rare in human cancers, these proteins are frequently inactivated by negative modulators (Candi et al., 2014). This observation supports that p53 family inactivation is a major event

in tumor progression (Hainaut et al., 2012). As such, understanding the mechanisms of p53 family impairment in human cancer is paramount for its therapeutic targeting.

1.3.1. Overexpression of negative modulators

The activity of p53 family proteins is tightly inhibited by interacting partners, including murine double minute (MDM)2 and MDMX (also named MDM4). The frequent overexpression of MDMs in cancers retaining wtp53 correlates with high-grade tumors, poor prognosis, and therapeutic resistance (Muller and Vousden, 2013). Interestingly, soft-tissue sarcomas, hepatoblastomas, and urothelial cell carcinomas, with frequent MDM2 amplification, have also been shown to display MDMX deregulation (Bartel et al., 2005; Veerakumarasivam et al., 2008; Arai et al., 2010). MDMX overexpression is a common feature in retinoblastomas (Laurie et al., 2006) and melanomas (Gembarska et al., 2012). Animal models have revealed important roles for both MDM2 and MDMX in cancer development. In fact, MDM2 overexpression increases spontaneous tumorigenesis in mice, with a tumor spectrum similar to that observed in p53-knockout mice (Jones et al., 1998). MDMX overexpression has also shown to increase tumor development in mice, particularly of sarcomas (Xiong et al., 2010).

The mechanisms by which MDM2 and MDMX interact with and inhibit p53 are well characterized. Both MDMs bind to the p53 TAD, inhibiting its transcriptional activity (Zdzalik et al., 2010). Three p53 amino acid residues are crucial for this interaction, namely phenylalanine 19, tryptophan 23, and leucine 26, which bind to the hydrophobic pockets present at the N-terminus of both MDM2 and MDMX (Kussie et al., 1996). In addition, MDM2 contains an acidic domain that binds the p53 DBD, blocking its interaction with DNA, thereby efficiently preventing p53 transcriptional activity (Cross et al., 2011). In contrast, the acidic domain of MDMX has only a slight inhibitory effect on the p53-DNA interaction (Cross et al., 2011). Furthermore, the C-terminal region of MDM2 contains a RING domain with E3-ligase activity (Clegg et al., 2008), crucial for p53 ubiquitination. In fact, MDM2 induces p53 monoubiquitination, promoting its nuclear export, and consequent inhibition of its transcriptional activity (Brooks and Gu, 2011; Duffy et al., 2014). In addition, MDM2 can catalyze the polyubiquitination of p53 at several C-terminal lysine residues, targeting p53 for proteasomal degradation (Iwakuma and Lozano, 2003; Meek and Anderson, 2009; Jain and Barton, 2010). MDM2 also facilitates p53 degradation by enabling its direct interaction with the proteasome (Kulikov et al., 2010). Conversely, the RING domain present at the C-terminal region of MDMX does not exhibit E3 ligase activity (Sharp et al., 1999a; Tanimura et al., 1999; Shadfan et al., 2012). Therefore, MDMX is not able to ubiquitinate p53 or to induce its proteasomal degradation. Despite this, the RING domain of MDMX is crucial for

the formation of MDM2/MDMX heterodimers, which have been reported to induce p53 degradation (Sharp et al., 1999a; Tanimura et al., 1999; Shadfan et al., 2012). In fact, it has been reported that while MDM2 homodimers mostly mediate p53 monoubiquitination, MDM2/MDMX heterodimers mainly induce p53 polyubiquitination required for proteasome degradation (Wang et al., 2011). This suggests that despite their similarities in structure and function, MDM2 and MDMX collaborate in a non-redundant manner to regulate p53 levels and transcriptional activity (Wade and Wahl, 2009). These non-redundant roles of MDM2 and MDMX have been corroborated by the observation that both MDM2 and MDMX knockout lead to p53-dependent embryonic lethality in mice, suggesting that neither protein can compensate for the loss of the other (Parant et al., 2001).

Given their structural and functional similarities with p53, the interactions between p63/p73 and MDM2/MDMX have also been investigated. Although controversial, the interaction of the p63 TAD with both MDMs was demonstrated *in vitro*, showing to be weaker than that observed with the p53 and p73 TADs (Zdzalik et al., 2010). In the same study, p63 bound to MDM2 with lower affinity than to MDMX. In fact, p63-MDMs interactions had been previously reported in tumor cells (Kadakia et al., 2001). In that study, although both MDMs inhibited p63, only MDM2 induced p63 nuclear export, albeit without degradation. Surprisingly, in a subsequent study, the p63-MDM2 interaction was suggested to cause p63 activation rather than inhibition (Calabro et al., 2002).

Early studies demonstrated that both MDMs are also able to bind the p73 TAD, inhibiting its transcriptional activity, as with p53 (Wang et al., 2001). Surprisingly, the p73-MDM2 interaction has also been reported to enhance, rather than inhibit, p73 growth suppressive functions (Ongkeko et al., 1999). The p73-MDMs interactions were thereafter confirmed *in vitro*, showing that p73 had higher affinity towards MDMX than MDM2 (Zdzalik et al., 2010). As observed with p53, MDM2 also catalyzes p73 ubiquitination through its RING domain (Wu and Leng, 2015). However, as with p63, MDM2 did not trigger p73 degradation *per se*, but instead promoted p73 proteasomal degradation through interaction with ITCH, a NEDD-4-like ubiquitin ligase (Rossi et al., 2005; Wu and Leng, 2015). Interestingly, ITCH has also been reported to target p63 for proteasomal degradation (Rossi et al., 2006).

Another feature in the p53 family-MDMs regulatory network relies on the existence of a p53-responsive promoter upstream of the *MDM2* gene (Wu et al., 1993; Barak et al., 1994). The stimulation of this promoter creates an autoregulatory feedback loop that is essential both for the maintenance of low p53 levels in unstressed cells, and for the restoration of normal p53 levels upon re-establishment of homeostasis after cellular stress. This promoter can also be activated by p63 and p73 (Moll and Slade, 2004). Furthermore,

a p53RE can also be found in the *MDMX* gene, creating a similar autoregulatory feedback loop (Wei et al., 2006a).

1.3.2. Mutant p53: a TSG turned oncogene

Approximately half of human cancers harbor mutations in the *TP53* gene. The frequency of p53 mutation varies among different cancer types, with ovary, lung, pancreas, and colorectal cancers presenting the highest frequency of p53 mutation (between 50 and 95%) (Bouaoun et al., 2016). Besides sporadic mutations, germline *TP53* mutations are a cause of Li Fraumeni syndrome, a disease characterized by an extraordinarily high susceptibility to cancer development, corroborating the critical role of mutant (mut)p53 in tumorigenesis (Malkin, 1993). Regardless of being sporadic or inherited, p53 mutation is usually followed by loss of the remaining wtp53 allele (loss of heterozygosity, LOH), resulting in complete inactivation of the p53 pathway (Bieging et al., 2014). In addition, tumors expressing mutp53 have been reported to display more malignant features, including genomic instability, and increased invasion and metastasis (Bieging et al., 2014).

The vast majority (80%) of p53 mutations are missense, and 97% occur within the DBD (Weisz et al., 2007), therefore affecting all p53 isoforms. Additionally, the most prevalent mutp53 in human cancers affect mainly six hotspot residues, namely R175, G245, R248, R249, R273, and R282 (Bisio et al., 2014) (**Figure 1.5**). Depending on whether the amino acid substitution leads to p53 conformational distortion or removes an amino acid residue that establishes direct contacts with DNA, without significant structural alterations, p53 mutations can be classified as either structural (e.g. R175H, Y220C, G245S, G245D, R249S, and R282W), or DNA-contact (e.g. R248W, R273H, R273C, and R280K), respectively (Khoo et al., 2014). Regardless of the type of mutation, cancer-related mutp53 loses its ability to interact with p53RE DNA sequences, resulting in the loss of transcriptional activity (LOF) (Khoo et al., 2014) (**Figure 1.6**).

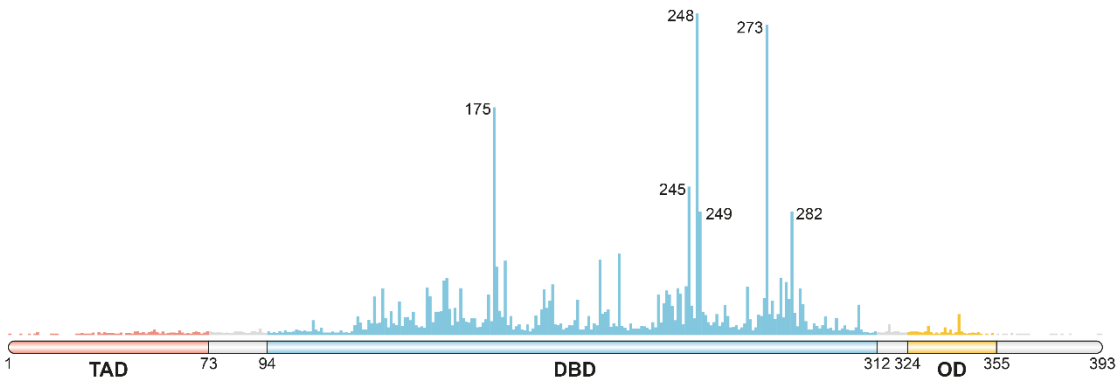

Figure 1.5 Distribution of sporadic mutations of p53. The figure displays the prevalence of sporadic mutations in human tumors, at each amino acid residue. Mutations are most frequent at the

DBD, mainly at the six mutation hotspots labelled in the figure (data from the IARC *TP53* database, version R19, July 2018).

Additionally, in heterozygous cells, mutp53 can exert dominant-negative effect (DNE) on the remaining wtp53, repressing its normal activity. The high level of mutp53 in tumor cells, caused by its prolonged half-life compared with wtp53, could explain the pronounced DNE (Chan et al., 2004). The major mechanisms of DNE on wtp53 are the formation of inactive mut/wtp53 co-tetramers (Chan et al., 2004) and the incorporation of wtp53 into mutp53 supratetrameric aggregates (Xu et al., 2011) (**Figure 1.6**). Additionally, the DNE depends on several factors, including the wt:mut subunit ratio within the co-tetramers, the mutp53 conformation, the DNA-binding affinity of the mutp53 subunits within the co-tetramers, and the DNA-binding site (Chène, 1998). Approximately 80% of the most common mutp53 are able to exert DNE over wtp53, whereas only 45% of the less frequent mutp53 have this effect (Petitjean et al., 2007). This suggests a pivotal role of the DNE in the selection of mutations in sporadic cancers.

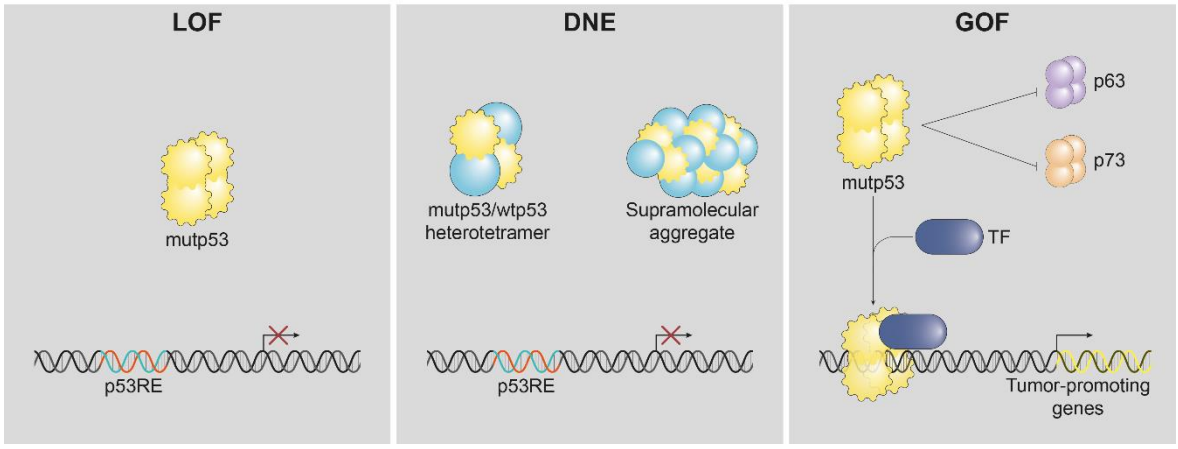

Figure 1.6 Functional profiles of mutp53. p53 mutations lead to loss of DNA-binding and subsequent p53 transcriptional activity, termed loss of function (LOF). In addition, through the formation of heterotetramers of supramolecular aggregates with wtp53, mutp53 has a dominant-negative effect (DNE) over wtp53 in a heterozygous context. Mutp53 also acquires oncogenic capabilities collectively termed gain of function (GOF), through inhibition of p63 and p73, and recruitment of transcription factors (TFs) to upregulate the expression of tumor-promoting genes. The arrow above the DNA represents the transcription of genes.

Besides LOF and DNE, some mutp53 also display GOF capabilities that turn them into oncogenes. This concept was first proposed in 1993, in a work that showed the ability of some mutp53 to induce malignant transformation of p53-null cells (Dittmer et al., 1993). Furthermore, it has been reported that knock-in mice expressing hotspot mutp53 develop tumors with more invasive and metastatic phenotype compared to $p53^{-/-}$ or $p53^{+/-}$ mice (Lang et al., 2004; Olive et al., 2004). This concept was further corroborated by the observation that patients with germline missense mutp53 develop tumors significantly earlier than patients with germline mutations that lead to loss of p53 expression (Bougeard et al., 2008; Zerdoumi et al., 2013).

The molecular mechanisms responsible for mutp53 GOF are still not fully elucidated and may differ according to specific mutations. Despite this, several mechanisms that lead to GOF have been described, and it is proposed that multiple pathways may cooperate to trigger the GOF phenotype (Bisio et al., 2014). Although mutp53 loses the ability to transactivate wtp53 target genes, studies have suggested that mutp53 are able to bind DNA in a structure-specific manner that requires the intact C-terminus (rarely mutated in human cancers), regulating the expression of genes (He et al., 2017). In fact, large scale transcriptome analyzes suggested that mutp53 is a potent transcriptional activator of several oncogenic-related genes (Weisz et al., 2007). Furthermore, mutp53 can recruit different transcription factors, coordinating the expression of their target genes (**Figure 1.6**). In fact, the interaction of mutp53 with transcription factors including NF-Y, ETS2, E2F1, and STAT2, results in the regulation of a wide array of genes that stimulate cell proliferation, inhibit cell death, and promote invasion and migration [reviewed in (Bisio et al., 2014; He et al., 2017)].

Another important GOF activity of both contact and structural mutp53 is the interaction with p63/p73 (**Figure 1.6**). In fact, the involvement of DBDs in these PPIs justifies the loss of p63/p73 transcriptional activity (Gaiddon et al., 2001). The mechanisms related to the mutp53–p63 interaction are mostly implicated in the promotion of tumor cell migration, invasion, and metastasis, which are cellular events suppressed by p63 (Muller and Vousden, 2013). Several proteins can differently interfere with this GOF by either promoting the mutp53–p63 interaction [e.g., topoisomerase IIb binding protein (TopBP1); peptidylprolyl cis/trans isomerase NIMA-interacting 1 (PIN1); and SMAD2], or blocking it [e.g., ankyrin repeat domain 11, (ANKRD11); MDM2] (Muller and Vousden, 2013; Stindt et al., 2015). It was also demonstrated that mutp53 uses p63 as a critical molecular chaperone to promote the expression of oncogenes (Neilsen et al., 2011). Nevertheless, this regulation is restricted to a set of genes, suggesting that the co-recruitment of both proteins is mediated by additional transcriptional factors within the complex. Consequently, the cancer cell transcriptome is reprogrammed, leading to oncogenesis. Additionally, the

chemoresistance commonly associated with mutp53 has been partly attributed to its inhibitory interaction with p73 (Bergamaschi et al., 2003). Accumulating data have shown that the mutp53 polymorphism at residue 72 [arginine (R) versus proline (P)] promotes the mutp53–p73 interaction, increasing p73 downregulation (Bergamaschi et al., 2003). Consistently, patients with squamous cell carcinomas expressing the mutp53 allele R72 had a poorer response to cisplatin (a known p73 inducer) treatment and overall worse survival, compared with those expressing the P72 allele (Bergamaschi et al., 2003). However, this correlation was not observed by other groups (Gaiddon et al., 2001; Willis et al., 2003), suggesting that other factors might interfere with the role of this polymorphism. Recently, it was also reported that MDM2 might enhance p73 inhibition by promoting its interaction with mutp53 (Stindt et al., 2015). The interaction of mutp53 with ΔNp63/ΔNp73 isoforms has also been explored, but to a lesser extent. It was reported that mutp53 establishes a stronger interaction with TAp63 than with ΔNp63, suggesting that, in addition to the DBD, the TAD may also contribute to these PPIs (Gaiddon et al., 2001). However, a recent work reported a similar binding affinity of mutp53 towards p63/p73 TA and ΔN isoforms and revealed an important role of the p63/p73 C-terminal in the interaction with mutp53 (Stindt et al., 2015). Given the controversy surrounding the functions of ΔNp63/ΔNp73 in tumor cells (Muller and Vousden, 2013), it is understandable that the role of mutp53 in the regulation of these isoforms remains far from being elucidated.

1.4. Strategies to target p53 family proteins in human cancer therapy

As previously mentioned, targeting p53 family proteins is an extremely appealing approach for anticancer therapy, considering their frequent inactivation in cancer, and their tumor-suppressive activity in several hallmarks of cancer. In mutp53-expressing tumors, therapeutic strategies aimed restoring wt-like activity to mutp53 and/or circumventing GOF are preferred. Conversely, in wtp53-expressing tumors, the inhibition of p53 interaction with negative regulators arises as a promising therapeutic approach. In addition, the activation of TAp73 by blocking its interaction with negative regulators has also been considered an encouraging strategy in anticancer therapy to compensate for the lack of a functional p53 pathway in tumors.

1.4.1. Inhibition of the interaction between p53 family proteins and negative modulators

As stated above, the main negative regulators of p53 family proteins, MDM2 and MDMX, are often upregulated in human cancers, leading to the impairment of the p53 family pathway. Extensive research has been developed in the search for inhibitors of the p53-MDM2 and p53-MDMX interactions, resulting in the identification of numerous peptides and small molecules.

Regarding MDM2, a common strategy has been the design of molecules that mimic the structure of the three key p53 amino acid residues (phenylalanine 19, tryptophan 23, and leucine 26) that bind to the MDM2 hydrophobic pocket. The first identified p53-MDM2 inhibitor was nutlin-3a (Vassilev et al., 2004), a molecule that binds the MDM2 hydrophobic pocket, displacing p53. Following pre-clinical validation, analogs with improved bioavailability and toxicity profiles, RG7112 (Ray-Coquard et al., 2012; Andreeff et al., 2016) and RG7388 (Ding et al., 2013), were developed and advanced to phase I/II clinical trials both as single agents and in combination regimens (Obrador-Hevia et al., 2015). The efficacy and safety profiles of other inhibitors of the p53-MDM2 interaction are currently being assessed in clinical trials, including SAR405838, AMG232, MK-8242, CMG097, DS3032b, and HDM201 [reviewed in (Merkel et al., 2017)], both as single agents and in combination with other chemotherapeutics.

In spite of this, resistance to p53-MDM2 inhibitors through MDMX amplification has been reported, since these compounds do not interfere with the p53-MDMX interaction. In fact, limited efficacy against tumors with MDMX overexpression (e.g. retinoblastoma) has been reported for this class of compounds (Patton et al., 2006). To circumvent this issue, inhibitors of the p53-MDMX interaction were developed. SJ-172550, the first MDMX inhibitor, forms covalent adducts with MDMX preventing its binding to p53, and triggering apoptosis in retinoblastoma cells (Reed et al., 2010). Nevertheless, no inhibitor of the p53-MDMX interaction has reached clinical trials.

Molecules able to suppress the inhibitory effect of both MDM2 and MDMX would represent an improved strategy relatively to MDM2- or MDMX-only inhibitors for p53 activation. To this end, the compound RO-5963 was designed to fit both the MDM2 and MDMX pockets, by avoiding the regions of the pocket that differ the most between the two proteins (the leucine subpocket) (Graves et al., 2012). Although RO-5963 was equally effective against MDM2 and MDMX in cell-free *in vitro* assays, in cancer cells this compound displayed increased efficacy towards the p53-MDMX interaction. ALRN-6924 is a stapled peptide designed to mimic p53, disrupting both the p53-MDM2 and p53-MDMX interactions. This peptide displayed high affinity towards both MDM2 and MDMX and is currently in phase I/II clinical trials (Burgess et al., 2016).

TAp73 has also proved to be a particularly appealing therapeutic target. In fact, TAp73 overexpression has been reported in the majority of solid tumors, but the presence of negative modulators impairs its tumor-suppressive activity (Maas et al., 2013). Interestingly, nutlin-3a has been shown to disrupt the TAp73-MDM2 interaction, leading to activation of TAp73 transcriptional activity, growth suppression, and apoptosis in p53-null and mutp53-expressing tumor cells (Lau et al., 2007). Besides MDM2 and MDMX, ΔN isoforms of p63 and p73 are known to inhibit their TA counterparts. In fact, cisplatin treatment has been reported to induce c-Abl-dependent phosphorylation of TAp73, prompting its dissociation from ΔNp63, and subsequent activation of TAp73 transcriptional activity and apoptosis (Rocco et al., 2006; Leong et al., 2007). In addition, the COX-2 inhibitor celecoxib has been reported to increase TAp73 levels while decreasing ΔNp73 levels, resulting in increased TAp73 transcriptional activity that leads to apoptosis (Lau et al., 2009). A different approach has been pursued through the 37AA peptide, which releases TAp73 from its inhibitory interaction with iASPP (Bell et al., 2007). This peptide causes p73-dependent tumor regression in a mouse xenograft model. As stated above, TAp73 can also be inhibited by interaction with mutp53. The disruption of this interaction represents a valuable anticancer therapeutic strategy. In fact, SIMPs (short interfering mutp53 peptides) were shown to disrupt the interaction between mutp53 and TAp73α, leading to TAp73α activation and sensitization of mutp53-expressing cells to chemotherapeutic agents (Di Agostino et al., 2008). Similarly, prodigiosin (Hong et al., 2014), benzyl isothiocyanate (Xie et al., 2016), and RETRA (Kravchenko et al., 2008), with *in vivo* antitumor activity, have also been reported to restore TAp73 transcriptional activity by inhibiting TAp73 interaction with mutp53.

1.4.2. Restoration of wt-function to mutp53

Since p53 mutations disrupt the normal mechanisms of p53 degradation by MDM2, mutp53 is usually expressed at high levels in tumor cells. In addition, with the exception of germline mutations, mutp53 expression is restricted to the tumor tissue, making mutp53 targeting therapies highly selective towards tumor cells. Several different approaches have been proposed for the therapeutic targeting of mutp53.

Considering the DNE of mutp53 through formation of supratetrameric aggregates that trap tumor suppressor proteins, pharmacological inhibition of mutp53 aggregation is an appealing therapeutic strategy. In fact, ReACp53, a peptide inhibitor of mutp53 aggregation, has displayed promising *in vivo* antitumor activity (Soragni et al., 2016).

Another relevant therapeutic approach is the inhibition of mutp53 GOF capabilities through pharmacological inhibition of mutp53 stabilizing proteins, leading to mutp53

depletion. Particularly, the heat-shock protein (Hsp) 90 forms a complex with mutp53 that leads to its stabilization. As such, inhibitors of Hsp90, including geldanamycin, 17AAG, and ganetespib, have been reported to destabilize mutp53, displaying promising antitumor activity (Alexandrova et al., 2015). Similarly, histone deacetylase (HDAC) inhibitors, such as vorinostat, are able to destabilize Hsp90-mutp53 complexes (Li et al., 2011). Consistently, vorinostat has shown preferential cytotoxicity in tumor cells expressing mutp53.

However, reactivation of mutp53 has been considered the most encouraging strategy, since it not only eliminates the pro-oncogenic functions of mutp53, but also re-establishes wt-like tumor-suppressive functions. In addition, since many chemotherapeutics rely on a functional p53 pathway for induction of tumor cell death, the combination of mutp53 reactivators with conventional chemotherapeutics might greatly improve their efficacy in mutp53-expressing tumors. Extensive research has been carried out in the search for mutp53 reactivators, with the identification of multiple compounds with distinct mechanisms of mutp53 reactivation (**Table 1.1**; **Figure 1.7**).

1.4.2.1. Covalent modification of cysteine residues

One important mechanism of mutp53 reactivation relies on the covalent modification of cysteine residues within the DBD. In fact, this domain contains 10 cysteine residues, three of which (cysteines 124, 182 and 277) have been implicated in mutp53 refolding (Bykov et al., 2018).

The first reported mutp53 reactivator, CP-31398, has been shown to induce mutp53 refolding to a wt-like conformation, restoring transcriptional activity and leading to cell death (Foster, 1999). This molecule has a reactive carbon-carbon double bond and has been reported to form adducts with thiol groups. This led to the hypothesis that cysteine modification might be responsible for CP-31398-mediated mutp53 reactivation. Despite this, CP-31398 has been reported to induce DNA-damage (Rippin et al., 2002), suggesting other mechanisms underlying its tumor-suppressive activity. Similarly, the mechanisms of mutp53 reactivation by MIRA-1 and STIMA-1 have been reported to involve their thiol-alkylating activity (Bykov, 2005; Zache et al., 2008; Lambert et al., 2009a).

Through a cellular screening, PRIMA-1 was identified due to its mutp53-dependent growth inhibitory activity (Bykov et al., 2002). PRIMA-1 was shown to restore wt-like folding and transcriptional activity to mutp53, leading to cell death. More recently, a more lipophilic and cell permeable PRIMA-1 derivative, APR-246 (PRIMA-1^{MET}) has been developed (Bykov, 2005). The activity of both PRIMA-1 and APR-246 depends on their hydrolysis to methylene quinuclidinone (MQ), a potent electrophile that reacts with cysteines in the p53

DBD, in particular cysteine 124 (Lambert et al., 2009a). APR-246 is currently undergoing phase Ib/II clinical trials (Bykov et al., 2018).

The compound PK11007 also targets cysteine residues in the mutp53 DBD, although leading to the alkylation of the thiol groups through nucleophilic aromatic substitution (Bauer et al., 2016). This molecule has been shown to stabilize and refold mutp53-Y220C, leading to the restoration of wt-like transcriptional activity.

More recently, the curcumin analog HO-3867 was identified as another mutp53 reactivator that also targets cysteine residues (Madan et al., 2018). HO-3867 was shown to covalently bind to the p53 DBD, reacting with cysteines 182 and 277. This compound restored wt-like folding and transcriptional activity to mutp53, displaying preferential cytotoxicity towards tumor cells. In addition, HO-3867 displayed *in vivo* antitumor activity.

1.4.2.2. Non-covalent binding to mutp53

The analysis of the crystal structure of the mutp53-Y220C DBD domain revealed that the tyrosine to cysteine amino acid substitution generates a hydrophobic crevice that destabilizes this mutp53 (Boeckler et al., 2008). This has been exploited for the development of mutp53-Y220C-binding compounds that stabilize this protein. The mutp53-Y220C ligand PhiKan083 was identified through virtual screening and rational drug design (Boeckler et al., 2008). In biophysical assays, this compound was able to stabilize mutp53-Y220C, raising its melting temperature. PK7088 was also identified as a mutp53-Y220C ligand, able to stabilize mutp53-Y220C (Liu et al., 2013b). In addition, PK7088 displayed growth inhibitory activity in mutp53-Y220C-expressing tumor cells, through restoration of wt-like p53 conformation and activity. More recently, the ability of compounds MB-710 and MB-725 to bind and stabilize mutp53-Y220C, leading to its reactivation in human tumor cells, has been reported (Baud et al., 2018).

Other molecules that reactivate mutp53 through direct binding have been reported. In particular, CDB3 is a peptide derived from a p53 binding protein that functions as a chaperone, binding the mutp53-R249S DBD and restoring its wt-like conformation and DNA-binding *in vitro* (Friedler et al., 2002). Similarly, the small molecule SCH529074 has been reported to bind to the mutp53 DBD restoring wt-like DNA-binding and transcriptional activity. Interestingly, SCH529074 has also been shown to prevent MDM2-mediated p53 ubiquitination, leading to p53 stabilization (Demma et al., 2010). Additionally, the small molecule SLMP53-1 has been identified as a reactivator of mutp53-R280K, able to restore wt-like transcriptional activity. SLMP53-1 also activates wtp53, displaying *in vivo* p53-dependent antitumor activity (Soares et al., 2016). Recently, SLMP53-1 was shown to bind to the mutp53-R280K DBD, leading to its stabilization, and to reactivate other mutp53 forms (Gomes et al., 2019a).

Table 1.1 Summary of mutp53 reactivators described to date. Mutp53 reactivators are organized by mechanism of mutp53 reactivation and stage of development (from preclinical assays to clinical trials).

Molecule	Mechanism	Stage of development	Reference
Covalent modification of cysteine residues			
CP-31398	Covalent binding to mutp53 leading to refolding and stabilization	• Biophysical evidence • Activity in cell assays • *In vivo* antitumor activity	(Foster, 1999)
STIMA-1	Restoration of wt-like transcriptional activity and cell death	• Biophysical evidence • Activity in cell assays	(Zache et al., 2008) (Lambert et al., 2009a)
MIRA-1	Restoration of wt-like transcriptional activity and cell death	• Biophysical evidence • Activity in cell assays	(Bykov, 2005) (Lambert et al., 2009a)
PRIMA-1	Covalent binding to cysteine residues restoring conformation	• Biophysical evidence • Activity in cell assays • *In vivo* antitumor activity	(Bykov et al., 2002) (Lambert et al., 2009a)
APR-246 (PRIMA-1^{MET})	Covalent binding to cysteine residues restoring conformation	• Biophysical evidence • Activity in cell assays • *In vivo* antitumor activity • Phase Ib/II clinical trials	(Bykov and Wiman, 2014) (Lambert et al., 2009a)
PK11007	Alkylation of mutp53 cysteines leading to stabilization	• Biophysical evidence • Activity in cell assays	(Bauer et al., 2016)
HO-3867	Covalent binding to cysteine residues restoring conformation	• Biophysical evidence • Activity in cell assays • *In vivo* antitumor activity	(Madan et al., 2018)
Non-covalent binding to mutp53			
PhiKan083	Binding and stabilization of mutp53-Y220C	• Biophysical evidence	(Boeckler et al., 2008)
PK7088	Binding and stabilization of mutp53-Y220C	• Biophysical evidence • Activity in cell assays	(Liu et al., 2013b)
MB710/MB725	Binding and stabilization of mutp53-Y220C	• Biophysical evidence • Activity in cell assays	(Baud et al., 2018)
CDB3 (peptide)	Binding and stabilization of mutp53; restoration of DNA binding	• Biophysical evidence	(Friedler et al., 2002)
SCH529074	Binding to mutp53 and restoration of wt-like activity and function	• Biophysical evidence • Activity in cell assays • *In vivo* antitumor activity	(Demma et al., 2010)
SLMP53-1	Binding and stabilization of mutp53-R280K	• Biophysical evidence • Activity in cell assays • *In vivo* antitumor activity	(Soares et al., 2016) (Gomes et al., 2019a)
Zinc chelators			
ZMC1 (NSC319726)	Restoration of wt-like conformation and transcriptional activity to mutp53-R175H	• Activity in cell assays • *In vivo* antitumor activity	(Yu et al., 2014) (Yu et al., 2012)
COTI-2	Restoration of wt-like transcriptional activity to mutp53	• Activity in cell assays • *In vivo* antitumor activity • Phase I clinical trials	(Salim et al., 2016)
Alternative mechanisms of mutp53 reactivation			
NSC87511 (Stictic acid)	Restoration of wt-like transcriptional activity to mutp53-R175H	• *In silico* data • Activity in cell assays	(Wassman et al., 2013)
P53R3	Restoration of wt-like DNA binding and transcriptional activity	• Activity in cell assays	(Weinmann et al., 2008)
WR-1065	Restoration of wt-like conformation	• Activity in cell assays	(North et al., 2002)
KSS9	Restoration of wt-like conformation and transcriptional activity to mutp53	• Activity in cell assays	(Punganuru et al., 2016)
PEITC	Restoration of wt-like conformation and transcriptional activity to mutp53-R175H	• Activity in cell assays • *In vivo* antitumor activity	(Aggarwal et al., 2016)
Goniothalamin	Restoration of wt-like conformation and transcriptional activity to mutp53	• Activity in cell assays	(Punganuru et al., 2018)
CTM	Binding to Hsp40, enhancing its interaction with mutp53-R175H with consequent refolding and reactivation	• Biophysical evidence • Activity in cell assays	(Hiraki et al., 2015)

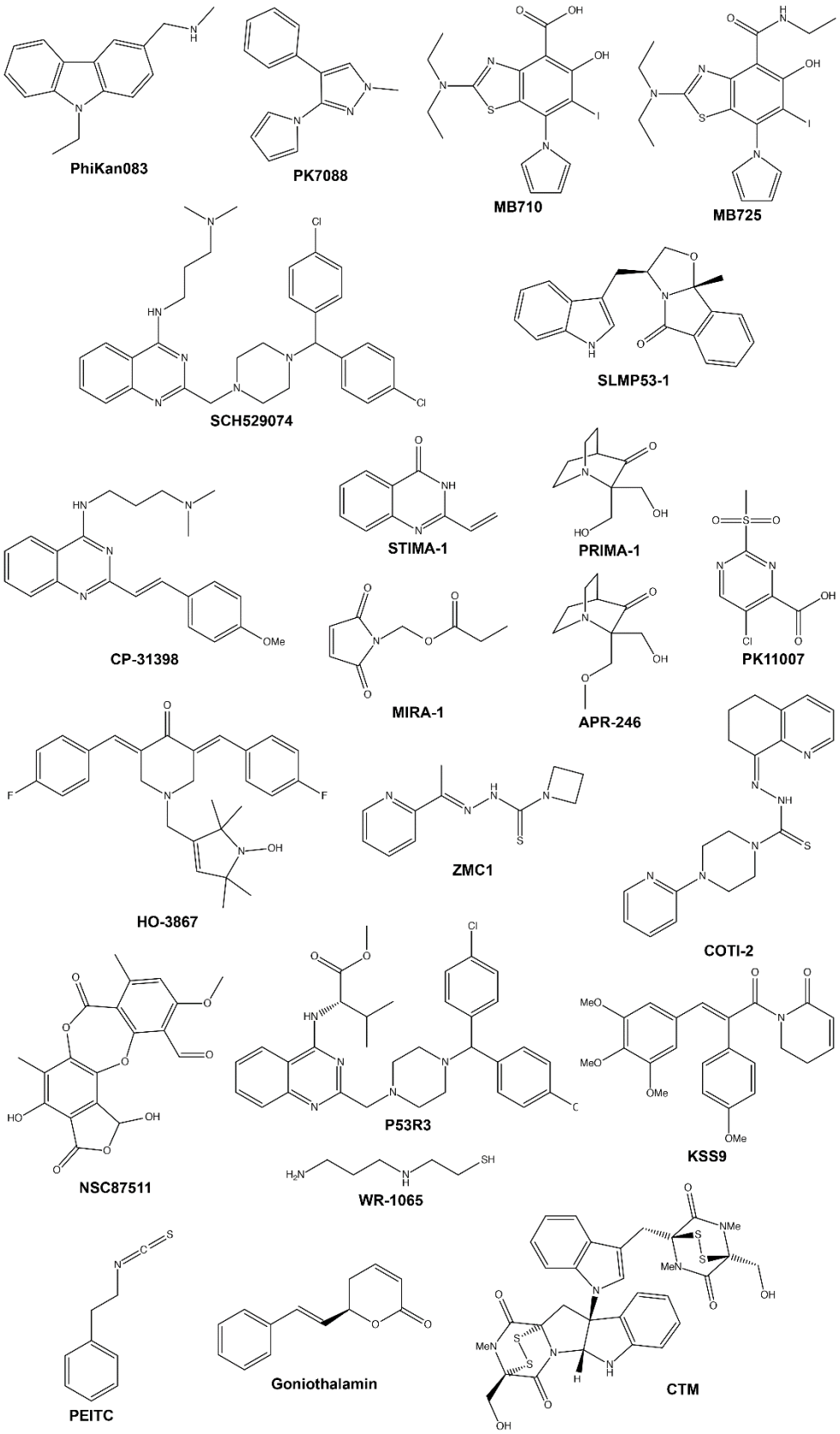

Figure 1.7 Chemical structures of mutp53 reactivators.

1.4.2.3.Zinc (Zn^{2+}) ion chelators

The p53 protein contains a Zn^{2+} ion coordinated by cysteines 176, 238, and 242, and histidine 179, in a tetrahedral geometry, near the DNA-binding surface. The Zn^{2+} ion is essential for correct p53 folding and DNA binding, and many mutp53, including R175H, lose Zn^{2+} coordination ability (Merkel et al., 2017). Considering this, Zn^{2+} chelators have been employed for mutp53 reactivation. In particular, the metallochaperone ZMC1 has been reported to buffer intracellular Zn^{2+} concentration promoting Zn^{2+} binding and consequent reactivation of mutp53-R175H (Yu et al., 2012) and other Zn^{2+}-binding deficient mutp53s (C176F, C238S, C242S, and G245S) (Yu et al., 2014). More recently, COTI-2 (a molecule from the same chemical family as ZMC1), currently in phase I clinical trials (Bykov et al., 2018), has been reported as a mutp53 reactivator with potent antitumor activity in human tumor cells and in mouse xenograft models (Salim et al., 2016). Despite this, COTI-2 has also been reported to inhibit the PI3K/Akt/mTOR pathway, suggesting other mechanisms underlying its antitumor activity (Maleki Vareki et al., 2018).

1.4.2.4. Alternative mechanisms of mutp53 reactivation

The compounds NSC87511, P53R3, WR-1605, KSS9, PEITC, and goniothalamin have been shown to restore wt-like transcriptional activity to several mutp53 forms, although the precise molecular mechanism of mutp53 reactivation remains unclear (North et al., 2002; Weinmann et al., 2008; Wassman et al., 2013; Aggarwal et al., 2016; Punganuru et al., 2016; Punganuru et al., 2018).

Recently, the natural compound chetomin (CTM) was identified as a reactivator of mutp53-R175H with growth inhibitory activity in human tumor cells (Hiraki et al., 2015). The authors showed that CTM binds Hsp40, enhancing its interaction with mutp53-R175H, with subsequent refolding and reactivation of mutp53-R175H transcriptional activity.

1.4.3. Yeast as a cell model to screen for p53 family targeted therapy

The yeast *Saccharomyces cerevisiae* has long been established as a valuable model to study human disease-related proteins (Guaragnella et al., 2014). In fact, given the remarkable conservation of cellular processes with human cells, the heterologous expression of human proteins in yeast has provided relevant clues about their biology and pharmacology. In particular, the simplicity of the yeast cellular background has contributed to the study of complex families of human proteins, such as the p53 family, due to the absence of orthologs of these proteins in yeast (Guaragnella et al., 2014; Leão et al., 2015a).

1.4.3.1. Yeast transactivation assays

The discovery that p53 was also a transcription factor in yeast enabled the development of simplified assays to evaluate its transcriptional activity, such as Functional Analysis of Separated Alleles in Yeast (FASAY) (Ishioka et al., 1993). In this technique, a p53 cDNA collected from human tumors is expressed in a yeast strain transformed with a plasmid containing a reporter gene (e.g., *ADE2*, *URA3*, or Luciferase) downstream of a human p53RE. In 2011, a dual-luciferase optimized version was adapted for the high-throughput screening (HTS) of factors interfering with p53 activity, including small molecules, mutations, and interacting proteins, such as MDM2 (Andreotti et al., 2011). This assay was later extended to p63 and p73, with overlapping transactivation profiles in yeast (Ciribilli et al., 2013) (**Figure 1.8**).

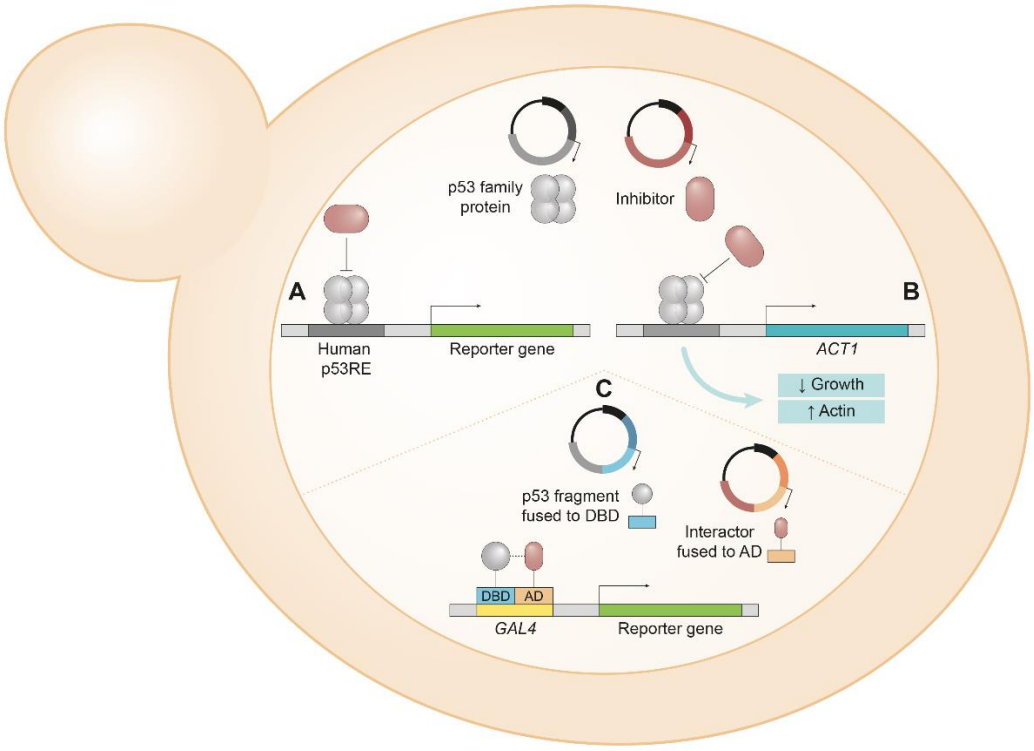

Figure 1.8 Yeast assays developed to study the impact of protein interacting partners and small molecules on the function of p53 family proteins. These assays use *Saccharomyces cerevisiae* cells co-expressing a human p53 family protein and a protein interacting partner (e.g., MDM2, MDMX, or mutp53). **(A) Yeast transactivation assay.** The impact of interacting protein partners and small molecules on p53 family transcriptional activity is evaluated using a reporter gene (e.g., *ADE2* or Luciferase) under the regulation of a human p53 family response element (RE). **(B) Yeast phenotypic assay.** Expression of a p53 family protein induces yeast growth inhibition associated with an increase of actin expression. The impact of interacting protein partners and small molecules on p53 function is evaluated by quantification of yeast cell growth and actin protein expression levels. **(C) Yeast two-hybrid assay.** A protein (bait; e.g., p53) is fused to the *GAL4* DNA-binding domain (DBD) and the interacting protein partner (prey; e.g., MDM2) is fused to the *GAL4*-

transactivation domain (AD). If the bait and prey establish a physical interaction, the function of *GAL4* is restored, enabling it to bind to a specific sequence and leading to the transcription of a reporter gene (e.g., *HIS3*, *ADE2*, or *LacZ*); this effect is abolished by small molecule inhibitors of the bait-prey interaction.

In addition to understanding the impact of mutations on p53 function (Fronza et al., 2000), the yeast transactivation assays have also been used to study the interference of mutp53 on wtp53, p63, and p73 activity. The first systematic study to evaluate mutp53 DNE was performed in yeast by measuring the ability of several mutp53 to inhibit the wtp53 transcriptional activity on its consensus RE (Brachmann et al., 1996). Moreover, with these assays, a correlation between mutp53 LOF and DNE was established (Dearth et al., 2007). Additionally, the transactivation potential and DNE of several germline mutp53 alleles were evaluated (Monti et al., 2011). This technique enabled the identification of LOF, partial function (PF), and DNE status of mutp53 from prostate cancer, and provided evidence that mutp53 alleles with PF did not have a DNE over wtp53 (Shi et al., 2002). The lack of predictable patterns for these alleles suggested that each mutation uniquely affects p53 function. In fact, this yeast system revealed that dominant mutations affect key residues that are essential for DBD stabilization or DNA binding (Inga et al., 1997). Additionally, it showed that the residue location was more important than the amino acid substitution in determining whether a mutant was dominant (Monti et al., 2002). These functional assays further evidenced that mutp53 DNE was associated with more aggressive tumor profiles and cancer recurrence (Hassan et al., 2008). They have also contributed to the study of mutp53 GOF, particularly of the impact of distinct mutp53 on p73 transcriptional activity, further supporting the fact that the interference detected was not exclusive to mutations located in specific topological regions of the p53 DBD (Monti et al., 2003).

Collectively, with the study of the molecular epidemiology of p53 mutations associated with carcinogenesis, and their impact on the function of p53 family proteins, this technique has become a powerful clinical tool. Indeed, with knowledge of the type and function of mutp53, tumor prognosis and treatment outcomes could be predicted.

A correlation between p53 transcriptional activity and the actin protein and mRNA expression levels was recently established in yeast (Leão et al., 2013b). The identification of a putative p53RE located upstream of the *ACT1* gene, and the enhancement of actin expression by wtp53 (not observed with inactive mutp53 forms) that is inhibited by MDM2/X (**Figure 1.8**) and pifithrin-α (a selective inhibitor of p53 transcriptional activity), supported the direct transactivation of the yeast *ACT1* by p53, as observed in human cells (Leão et al., 2013b). Later, the upregulation of *ACT1* by TAp63, TAp73, and ΔNp63 was also

demonstrated in yeast (Leão et al., 2015a). Collectively, these studies led to the identification of *ACT1* as a yeast endogenous p53 family transcriptional target. This opened the way to simplified yeast transcriptional assays to analyze the impact of interfering factors on p53 family activity, without requiring artificial reporter gene constructions.

1.4.3.2. Yeast two-hybrid assays

The yeast two-hybrid (Y2H) assay was the first molecular genetic tool developed to study PPIs in a cellular context. By taking advantage of the modular nature of yeast transcription factors, it has enabled the identification of protein interactors (prey) of a protein of interest (bait), through HTS of large cDNA libraries (**Figure 1.8**). However, because the Y2H system is based on reconstitution of a transcription factor, it might not be suitable for the interaction analysis of proteins (bait) that can directly activate transcription of the reporter gene in the absence of a PPI with a prey. Therefore, two alternative Y2H systems, based on repression of transactivation and on the use of the alternative polymerase III transcription pathway, were developed to circumvent this limitation (Bruckner et al., 2009).

With Y2H, the p53 fragment responsible for oligomerization (the OD) was identified, and its involvement in mutp53 oligomerization with wtp53 was revealed (Iwabuchi et al., 1993). This provided a molecular explanation for the mutp53 DNE. The ability of different p63/p73 isoforms to form homo- (De Laurenzi et al., 1998; Ikawa et al., 1999) and hetero-oligomers (not observed with wtp53) (Kojima et al., 2001), and the occurrence of ΔNp63–wtp53 interactions responsible for a reduction in the half-life of ΔNp63 (Ratovitski et al., 2001), were also evidenced by Y2H.

The contribution of Y2H to the characterization of the interactions of p53 family proteins with MDMs is also undeniable. In particular, with this assay, the four amino acid residues of MDM2 essential for the interaction with p53 (Gly58, Asp68, Val75, and Cys77) were determined (Freedman et al., 1997). Although no p63–MDMs interactions were detected by Y2H, the p73–MDMs interactions were corroborated by this technique (Kojima et al., 2001). It also demonstrated that MDM2 and MDMX form hetero-oligomers through their C-terminal RING finger domains (Sharp et al., 1999b), which protects MDM2 from proteasomal degradation, enhancing its inhibitory activity on p53. In addition, using Y2H, protein regulators of the p53–MDM2 interaction were identified, in particular the ribosomal protein L26, which forms a ternary complex with p53 and MDM2, causing p53 stabilization through MDM2 inhibition (Zhang et al., 2010), and UBE4B, an ubiquitin ligase required for MDM2-induced p53 polyubiquitination (Wu et al., 2011).

Y2H was also used to detect mutp53 in tumors based on its inability to bind to p53-binding protein 1 (53BP1), an interacting partner and enhancer of wtp53 transcriptional

activity also identified by Y2H (Schwartz et al., 1998). Moreover, using this technique, the interaction of mutant p53-binding protein 1 (MBP1) with mutp53, but not with wtp53, was evidenced (Gallagher et al., 1999). This mutp53-specific binding partner enhances mutp53 oncogenic activity, contributing to its GOF. Collectively, accumulating data have supported the potential of Y2H to identify binding partners and to study their impact on p53 family proteins.

1.4.3.3. Yeast phenotypic assays: contribution to the discovery of activators of p53 family proteins

Several studies have reported the growth inhibitory effect of human p53 (Guaragnella et al., 2014), TAp63, TAp73, and ΔNp63 (Leão et al., 2015a) expressed in yeast.

The interference of MDM2 with endogenous yeast pathways was demonstrated through analysis of p53 ubiquitination and ensuing degradation in yeast (Di Ventura et al., 2008). Subsequently, the inhibitory effect of MDM2 and MDMX on p53 family-induced yeast growth inhibition was shown (Leão et al., 2013b; Leão et al., 2013c; Leão et al., 2015a). In particular, the slight effect of MDMs on TAp63 was reinforced, and the ΔNp63–MDMX interaction was reported for the first time (Leão et al., 2015a). Collectively, these studies enabled the development of simplified growth-inhibitory screening assays, well adaptable to HTS, and highly efficient for the identification of inhibitors of the interactions between p53 family proteins and MDMs (**Figure 1.8**).

In fact, using the yeast growth inhibitory assays, two new scaffolds of p53–MDM2 interaction inhibitors were identifed: xanthones [pyranoxanthone 1 (Leão et al., 2013c), α-mangostin, and gambogic acid (Leão et al., 2013a)] and oxazoloisoindolinones (Soares et al., 2014). These assays also revealed that prenylation enhances the tumor cytotoxicity of chalcones by improving their ability to disrupt the p53–MDM2 interaction (Leão et al., 2015b). Notably, these assays also led to the discovery of three new dual inhibitors of p53–MDM2/X interactions, the tryptophanol-derived oxazolopiperidone lactam OXAZ-1 (Soares et al., 2015), the tryptophanol-derived oxazoloisoindolinone DIMP53-1 (Soares et al., 2017), and the tryptophanol-derived bicyclic lactam SYNAP (Raimundo et al., 2018).

The effectiveness of the yeast growth-inhibitory assay to search for p73–MDM2 interaction inhibitors was recently demonstrated using the known inhibitor of this PPI, nutlin-3a (Leão et al., 2015a). Interestingly, a potential disruption of the p73–MDMX interaction by the known inhibitor of the p53–MDMX interaction, SJ-172550, was also suggested (Leão et al., 2015a). Therefore, similar assays developed for p63–MDMs interactions (Leão et al., 2015a). might contribute to the discovery of inhibitors of these interactions, which remain unknown.

In addition, the observation that unlike wtp53, mutp53 did not induce yeast growth inhibition (Leão et al., 2013b), allowed the development of a phenotypic assay to screen for potential mutp53 reactivators. In this assay, a mutp53 reactivator would restore wt-like yeast growth inhibitory activity to mutp53, as demonstrated with the mutp53-Y220C reactivator, PhiKan083, in yeast cells expressing human mutp53-Y220C (Soares et al., 2016). In fact, using this assay, the reactivator of mutp53-R280K, tryptophanol-derived oxazoloisoindolinone SLMP53-1, was discovered (Soares et al., 2016).

A possible limitation of these assays is the fact that they are dependent on the occurrence of a measurable phenotype proportional to the degree of activation/inhibition of a given molecular target. Nevertheless, accumulating evidence has attested to the unquestionable contribution of the yeast model as a targeted screening approach for the discovery of molecules targeting p53 family proteins.

1.5. Aims

As previously referred, in addition to its high incidence and mortality rates, cancer represents a group of diseases with remarkable molecular complexity, caused by a complete reprogramming of cells that results from alterations of oncogenes and TSGs. In this context, p53 family proteins arise among the most promising therapeutic targets in cancer. Taking this into consideration, with the present thesis, it was intended to identify new modulators of p53 family proteins with antitumor activity against p53-impaired cancers. In particular:

i. Activators of TAp73 (**Chapter 3**);
ii. Reactivators of mutp53 (**Chapter 4**).

To carry out the proposed goals, this thesis encompassed a multidisciplinary research approach, including medicinal chemistry, pharmacology, microbiology, oncobiology, biotechnology, and molecular biology.

Collectively, this thesis aimed to advance the knowledge on p53 family biology and pharmacology. Most importantly, it intended to provide new improved therapeutic opportunities, by targeting p53 family proteins, to be used alone or in combination with conventional chemotherapeutics in personalized cancer therapy.

Chapter 2. Materials and Methods

2.1. Compounds

Synthesis of LEM2, LEM2ox, and LEM2red is described in Appendix A (**Figure A.1**). Nutlin-3a, cyclophosphamide, and APR-246 were purchased from Sigma-Aldrich (Sintra, Portugal). Etoposide was purchased from Calbiochem (VWR, Carnaxide, Portugal). Sorafenib was purchased from Santa Cruz Biotechnology (Heidelberg, Germany). All compounds were dissolved in dimethyl sulfoxide (DMSO; Sigma-Aldrich).

2.2. Synthesis of SLMP53-2

General methods: All reagents and solvents were obtained from commercial suppliers and used without further purification. Reactions were performed under a nitrogen atmosphere. Melting point was determined using a Kofler camera Bock monoscope M. Thin layer chromatography was performed using Merck Silica Gel 60 F_{254} plates and visualized by UV light. For flash column chromatography Merck Silica Gel with high purity grade (200-400 mesh) was used. ^{1}H and ^{13}C-NMR spectra were recorded on a Bruker Fourier 300 Avance at 300MHz (^{1}H NMR) and at 75MHz (^{13}C NMR). ^{1}H and ^{13}C NMR chemical shifts are reported in parts per million (ppm, δ) referenced to the solvent used. Proton coupling constants (*J*) are expressed in hertz (Hz). Multiplicities are given as: s (singlet), dd (double doublet), and m (multiplet). The specific rotation value was measured in a PerkinElmer 241 MC polarimeter at room temperature (New University of Lisbon, PT). Compound SLMP53-2 showed purity ≥ 90% by LC-MS, performed in a Waters Alliance 2695 HPLC with a Waters SunFire C18 column (100 × 2.1 mm; 5 µM) at 35 ºC, using a gradient from 95% solution A (Milli-Q water containing 0.5% formic acid (v/v)) to 95% solution B (acetonitrile) as mobile phase and employing a photodiode array detector to scan wavelength absorption from 210 to 600 nm; MS experiments were performed on Micromass® Quattro Micro triple quadrupole (Waters®, Ireland) with an electrospray in positive ion mode (ESI+), ion source at 120 ºC, capillary voltage of 3.0 kV and source voltage of 30 V, at the Liquid Chromatography and Mass Spectrometry Laboratory, Faculty of Pharmacy, University of Lisbon.

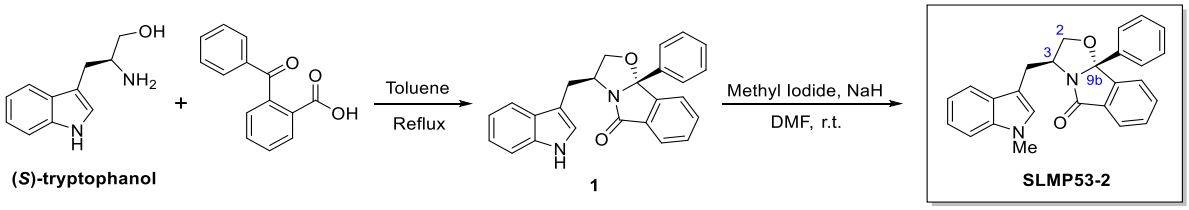

Figure 2.1 Synthetic pathway and reaction conditions to obtain SLMP53-2.

Chemical synthesis of SLMP53-2 (Figure 2.1): Compound **1** was prepared from (*S*)-tryptophanol (0.16 g, 0.84 mmol, 1.0 equiv.) and 2-benzoylbenzoic acid (0.21 g, 0.93 mmol, 1.1 equiv.) in 10 mL of toluene, according to the protocol described in (Pereira et al., 2015). To a stirred solution of compound **1** (0.10 g, 0.27 mmol) in anhydrous DMF (3 mL) at 0 °C, and under inert atmosphere of nitrogen, 0.014 g of NaH (0.60 mmol, 2.2 equiv., 95% anhydrous reagent) was added. After stirring for 30 minutes, 0.025 mL of methyl iodide (0.41 mmol, 1.5 equiv.) was added and the reaction was slowly allowed to warm to room temperature for 1 hour. Ethyl acetate (10 mL) was added, and the organic phase washed with water (6 × 10 mL), with an aqueous saturated solution of $NaHCO_3$ and then with a brine solution. The organic phase was dried with Na_2SO_4 and concentrated. After flash chromatography (ethyl acetate/*n*-hexane 1:1) and recrystallization from EtOAc, SLMP53-2 was obtained as a white crystalline solid (0.096 g, 89.3%); mp: 134-136 ºC; $[\alpha]^{20}_D$ =+ 84.5 (*c*=0.37, CH_2Cl_2). ^{1}H NMR (300MHz, $CDCl_3$) δ 7.84 – 7.77 (m, 1H, ArH), 7.67 – 7.59 (m, 2H, ArH), 7.53 – 7.45 (m, 3H, ArH), 7.42 – 7.35 (m, 3H, ArH), 7.22 (m, 3H, ArH), 7.12 – 7.05 (m, 1H, ArH), 6.96 (s, 1H, ArH), 4.69 (m, 1H, H-3), 4.46 (dd, J = 8.6, 7.6 Hz, 1H, H-2), 3.98 (dd, J = 8.6, 6.8 Hz, 1H, H-2), 3.72 (s, 3H, NCH_3), 3.21 (dd, J = 14.7, 5.5 Hz, 1H, CH_2-indole), 2.65 (dd, J = 14.7, 9.3 Hz, 1H, CH_2-indole) (Appendix B, **Figure B.1**); ^{13}C NMR (75 MHz, $CDCl_3$) δ 174.72 (C=O), 147.29 (Cq), 138.98 (Cq), 136.98 (Cq), 133.38 (ArCH), 131.22 (Cq), 130.20 (ArCH), 128.87 (ArCH), 128.76 (ArCH), 128.01 (Cq), 127.01 (CH-indole), 125.92 (ArCH), 124.48 (ArCH), 123.56 (ArCH), 121.75 (ArCH), 119.01 (ArCH), 110.29 (Cq), 109.26 (ArCH), 101.06 (C-9b), 76.43 (CH-2), 55.91 (CH-3), 32.77 (N-CH_3), 30.15 (CH_2-indole) (Appendix B, **Figure B.1**); MS (ESI) m/z calculated for $C_{26}H_{22}N_2O_2$: 394, found 395 $[M + H]^+$.

2.3. Yeast transformation, growth, and screening assay

Saccharomyces cerevisiae CG379 cells expressing human TAp73α alone or co-expressed with human MDM2 were previously obtained and used as described (Leão et al., 2015a).

To obtain the screening system of yeast cells co-expressing TAp73α with mutp53-R273H, the pRS314-(*TRP1*)-TAp73α and pLS76-(*LEU2*)-mutp53-R273H plasmids were used, as well as the respective empty vectors (negative controls). Yeast plasmid pRS314-(*TRP1*) encoding human TAp73α under the *GAL1-10* inducible promoter and the respective empty vector were kindly provided by Dr. Alberto Inga (Centre for Integrative Biology, University of Trento, Italy). Yeast plasmid pLS76-(*LEU2*) encoding human mutp53-R273H

under the *ADH1* constitutive promoter and the respective empty vector were kindly provided by Dr. Gilberto Fronza (IST Istituto Nazionale per la Ricerca sul Cancro, Genoa, Italy). Plasmids were first amplified in *Escherichia coli* DH5α (Lucigen, Frilabo, Porto, Portugal), and thereafter purified using the GenElute™ HP Plasmid Miniprep Kit (Sigma-Aldrich). After extraction, *Saccharomyces cerevisiae* CG379 cells were transformed using the LiAc/SS Carrier DNA/PEG method as described (Gietz and Schiestl, 2007). For selection of transformed yeast, cells were routinely grown in selective minimal medium with 2% (w/v) glucose (Panreac, Frilabo), 0.7% (w/v) yeast nitrogen base without amino acids (Difco, Enzifarma), and all the amino acids required for yeast growth (50 µg/mL), except leucine and tryptophan, and incubated at 30 ºC, under continuous orbital shaking (200 rpm). Expression of human proteins was confirmed by western blot, as in 2.11.

To study the growth of the transformed yeast cultures, cells were diluted to 0.05 OD_{600} and grown in induction selective medium [2% (w/v) galactose (AppliChem, Frilabo), 1% (w/v) raffinose (Acros Organics, Frilabo), 3% (v/v) glycerol (José Manuel Gomes dos Santos, Lda.), 0.7% (w/v) yeast nitrogen base without amino acids (Difco, VWR), and all the amino acids required for yeast growth (50 µg/mL)], for 72 h. Cell growth was analyzed at selected time-points by colony-forming unit (CFU) counts. For the yeast screening assay, cells were grown in induction selective medium with LEM2 or 0.1% DMSO for 48 h; cell growth was analyzed by CFU counts, as described (Leão et al., 2015a).

2.4. Human cell lines and growth conditions

All human cell lines used in the present thesis are listed in **Table 2.1**. The HCT116 $p53^{+/+}$ cell line and its p53-null isogenic derivative (HCT116 $p53^{-/-}$) were kindly provided by Dr. Vogelstein (The Johns Hopkins Kimmel Cancer Center, Baltimore, USA). HuH-7 cells were obtained from the JCBR Cell Bank (Osaka, Japan). p53 knock-out (KO) HuH-7 cells were generated using CRISPR editing (Baud et al., 2018). All remaining tumor cell lines were purchased from ATCC (Rockville, MD, USA). Cell lines were grown in RPMI-1640 with UltraGlutamine (Lonza, VWR) with 10% FBS (Gibco, Alfagene, Carcavelos, Portugal), except for HFF-1 cells, which were cultured in DMEM:F12 (Lonza) with 10% FBS. All cells were maintained in a humidified incubator at 37 °C with 5% CO_2. Routine testing for *Mycoplasma* infection was carried out using the MycoAlert™ PLUS *Mycoplasma* detection kit (Lonza).

Table 2.1 Human cell lines and their respective p53 status.

Cell line	Tissue/Disease	p53 status
HCT116 p53$^{+/+}$	Colon adenocarcinoma	wtp53
HCT116 p53$^{-/-}$	Colon adenocarcinoma	p53-null
SK-BR-3	Breast adenocarcinoma	mutp53-R175H
MDA-MB-231	Breast adenocarcinoma	mutp53-R280K
MDA-MB-468	Breast adenocarcinoma	mutp53-R273H
HT-29	Colorectal adenocarcinoma	mutp53-R273H
SW-837	Rectal adenocarcinoma	mutp53-R248W
NCI-H1299	Non-small cell lung carcinoma	p53-null
HuH-7	Hepatocellular carcinoma	mutp53-Y220C
HuH-7 p53KO	Hepatocellular carcinoma	p53-null
HCC1419	Breast ductal carcinoma	mutp53-Y220C
HFF-1	Foreskin fibroblasts	wtp53

2.5. Transfection of human tumor cells

For ectopic TAp73α expression in HT-29 cells, the pCI-neo-TAp73α, kindly provided by Dr. Alberto Inga (Centre for Integrative Biology, University of Trento, Italy) was used. For ectopic mutp53 expression in NCI-H1299 cells, pCDNA3 plasmids encoding mutp53-R175H, -Y220C, -G245S, or -R280K were used (Gomes et al., 2019a). In each case, the empty pCI-neo or pCDNA3 vector was used as a negative control. HT-29 and NCI-H1299 cells in suspension were simultaneously transfected using the ScreenFectA reagent (NZYTech, Porto, Portugal) and seeded, according to manufacturer's instructions.

For TAp73α knockdown, HCT116 p53$^{-/-}$ cells were transfected with the ON-TARGETplus Human *TP73* (7161) siRNA SMARTpool (sip73, ThermoScientific, Dharmacon, Bioportugal, Porto, Portugal), using Lipofectamine 2000 (Invitrogen, Alfagene), according to manufacuter's instructions. For Hsp70 knockdown, HuH-7 cells were transfected with the ON-TARGETplus Human HSPA1A (3303) siRNA SMARTpool (siHsp70, ThermoScientific) using the ScreenFectA reagent, according to manufacturer's instructions. In both cases, nonspecific siRNAs (siCTRL, Non-targeting Pool, ThermoScientific) was used as a negative control.

Efficiency of knockdown and ectopic protein expression were confirmed by western blot as described in 2.11.

2.6. Cell proliferation, viability, and combination therapy assays

Sulforhodamine B (SRB) assay: Cells were seeded in 96-well plates at 5.0×10^3 (HCT116, parental and transfected HT-29, HuH-7, SW-837, HuH-7, NCI-H1299), 7.5×10^3 (SK-BR-3, MDA-MB-468), and 1.0×10^4 (MDA-MB-231, HCC1419, HFF-1) cells/well, and allowed to adhere overnight. Cells were then treated with serial dilutions of compounds for 48 h. Afterward, cells were fixed in 10% trichloroacetic acid for 1 h at 4 °C, and stained with 0.4% SRB (Sigma-Aldrich) for 30 min at room temperature. After washing unbound dye with 1% acetic acid, bound dye was solubilized with 10 mM Tris-base (Sigma-Aldrich) and the absorbance at 510 nm was measured using a microplate reader (Biotek Instruments Inc., Synergy MX, USA). The maximum concentration of DMSO (0.25%) was included as a control. IC_{50} (concentration that causes 50% growth inhibition) values were determined using the GraphPad Prism software v7.0 (La Jolla, CA, USA). In combination therapy assays, combination index (CI) values were determined using the CompuSyn software v1.0 (Chou and Talalay, 1984; Raimundo et al., 2018).

Colony formation assay: MDA-MB-468 and transfected HCT116 $p53^{-/-}$ cells were seeded in 6-well plates, at 5.0×10^2 cells/well density and immediately treated with 0.4-3.0 μM LEM2 or DMSO for 24 h. Colonies were grown for 10 days in compound-free medium. HuH-7 cells (parental and transfected with siCTRL or siHsp70) were seeded in 6-well plates at 2.0×10^3 cells/well density and treated with 0.9-28 μM SLMP53-2 for 14 days. Colonies were fixed with 10% methanol and 10% acetic acid for 10 min, followed by staining with 0.5% crystal violet (Sigma-Aldrich) in 1:1 methanol/H_2O for 15 min. Colonies with more than 20 cells were counted.

2.7. Cell cycle and apoptosis

Cells were seeded in 6-well plates at 1.5×10^5 (HCT116 $p53^{-/-}$ and HuH-7) and 2.25×10^5 (MDA-MB-468) cells/well density and allowed to adhere overnight. Cells were then treated with LEM2 (HCT116 $p53^{-/-}$ and MDA-MB-468), SLMP53-2 (HuH-7) or DMSO. For cell cycle analysis, after 24 h (HCT116 $p53^{-/-}$ and MDA-MB-468) or 48 h (HuH-7), cells were fixed with ice-cold 70% ethanol for 15 min, followed by incubation with 20 μg/mL RNase A (Sigma-Aldrich) for 15 min at 37 °C. Cells were then incubated with 50 μg/mL propidium iodide (PI; Sigma-Aldrich) for 30 min, followed by flow cytometry analysis. Apoptosis analysis was performed after 48 h (HCT116 $p53^{-/-}$ and MDA-MB-468) or 72 h (HuH-7) treatment, using the Annexin V-FITC Apoptosis Detection Kit I (BD Biosciences Enzifarma,

Porto, Portugal), according to manufacturer's instructions. In both cases, data acquisition was performed using the Accuri™ C6 flow cytometer and the BD Accuri C6 software (BD Biosciences, Enzifarma). Cell cycle phases were quantified using FlowJoX 10.0.7 (Treestar, Ashland, OR, USA).

2.8. Generation of colon cancer spheroids

1×10^3 HCT116 $p53^{-/-}$ cells/well were seeded in ultra-low attachment 24-well plates in DMEM:F12 medium supplemented with 10 ng/mL bFGF, 20 ng/mL EGF (Bio-techne, Citomed Lda, Lisboa, Portugal), 1× B27 (Life Technologies, Porto, Portugal) and 5 µg/mL insulin (Sigma Aldrich), as described (Bessa et al., 2018), in the presence of 0.5, 1, or 2 µM LEM2 or DMSO; spheroids were grown for 7 days. Alternatively, spheroids were allowed to grow in compound-free medium for 3 days, followed by treatment with 0.5, 1, or 2 µM LEM2 for 3 days (Raimundo et al., 2018). Spheroids were monitored and photographed using an inverted Nikon TE 2000-U microscope at 100× magnification, with a DXM1200F digital camera and NIS-Elements imaging software.

2.9. Microarray experiments

2.0×10^5 HuH-7 cells/well were seeded in 6-well plates and allowed to adhere overnight, followed by 24 h treatment with 28 or 42 µM SLMP53-2 or DMSO. Total RNA was extracted using Illustra™ RNAspin Mini (GE Healthcare, VWR), according to manufacturer's instructions. RNA purity and concentration were measured by Nanodrop™ and Agilent 2100 Bioanalyzer (Agilent Technologies, Santa Clara, CA, USA). Samples with RIN (RNA integrity number) ≥ 8 were used for the one-Color Microarray-Based Gene Expression Analysis protocol (Agilent Technologies) and hybridized on Agilent-014850 4×44K Whole Human Genome Microarrays. Slides were scanned on the Agilent DNA Microarray Scanner (G2505C) using the Agilent HD_GX_1Color Profile of Agilent ScanControl v8.1.3. Four biological replicates per treatment were prepared and analyzed. Microarray data were deposited in Gene Expression Omnibus database (GSE124021). The scanned TIFF images were analyzed numerically and background-corrected using the Agilent Feature Extraction Software (v10.7.7.1), according to the Agilent GE1_107_Sep09 standard protocol. The output of Feature Extraction was analyzed with the R software environment for statistical computing (http://www.r-project.org/) and the Bioconductor packages (http://www.bioconductor.org/). The arrayQualityMetrics package was used to

check the quality of the arrays. Low signal Agilent probes, identified by a repeated "not detected" flag across the majority of the arrays in every condition, were filtered out from the analysis. Signal intensities across arrays were background corrected (Edwards method) and normalized with the quantile normalization method. Differentially Expressed Genes (DEGs) were determined using a double threshold based on: (1) the magnitude of the change (fold change greater than ±2); (2) the statistical significance of the change, measured with a multiple-test-correction adjusted *p*-value less than 0.05) using limma package. The Ingenuity Pathway Analyzes (IPA, v2017) resource was used for enrichment analysis of the transcriptome DEGs lists. The IPA Ontologies are derived from manually curated collections of experimental data and are utilized to infer functional enrichment of different type of relationships. The significance of gene list over-representations was determined using a Fisher exact *p*-value threshold of 0.05 with multiple-test-correction. In particular, we utilized the bio-functions and the up-stream regulators analysis. The graphical representation of the IPA results was performed in R/Bioconductor environment.

2.10. RNA-extraction and RT-qPCR

Cells were seeded in 6-well plates at 1.5×10^5 (HCT116 $p53^{-/-}$ and HuH-7) or 2.25×10^5 (MDA-MB-468) cells/well and allowed to adhere overnight. Cells were thereafter treated with 2 µM LEM2 for 24 or 48 h (HCT116 $p53^{-/-}$ and MDA-MB-468) or 14 and 28 µM SLMP53-2 for 24 h (HuH-7).

For gene expression analysis, total RNA was extracted using the Illustra™ RNAspin Mini RNA Isolation Kit (GE Healthcare). RNA purity and concentration were measured by Nanodrop™. 1 µg total RNA was used for cDNA synthesis using M-MuLV reverse transcriptase and the Revert Aid cDNA Synthesis kit (Thermo Fisher), according to manufacturer's instructions. cDNA was used for qPCR reactions, which were carried out on a CFX Touch™ Real-Time PCR Detection System (Bio-Rad), using 2× KAPA SYBR® FAST qPCR Kit (Kapa Biosystems) and specific primers for each analyzed gene, listed in **Table 2.2** (Eurofins, MWG, Italy). *GAPDH* and *B2M* were used as reference genes.

Table 2.2 Sequences of primers used in RT-qPCR experiments

Primer	Sequence (5' – 3')
AREG Fw	TTGATACTCGGCTCAGGCCAT
AREG Rv	CACAGGGGAAATCTCACTCCC
ASNS Fw	CCTCGCAGGCATGATGAAAC
ASNS Rv	GAAGAAAATCTGGGCGTAAGCA
AURKA Fw	ATATCTCAGTGGCGGACGAG
AURKA Rv	TGAGACCCTCTAGCTGTAATAAGT
B2M Fw	AGGCTATCCAGCGTACTCCA
B2M Rv	ATGGATGAAACCCAGACACA
BIRC5 Fw	AGGACCACCGCATCTCTACA
BIRC5 Rv	TTTCCTTTGCATGGGGTCGT
BAX Fw	CCTGGAGGGTCCTGTACAATCT
BAX Rv	GCACCTAATTGGGCTCCATCT
BMF Fw	CCCTCCTTCCCAATCGAGTCT
BMF Rv	CTCCATCTCTCCTGGGTGACT
CDKN1A Fw	CTGGAGACTCTCAGGGTCGAA
CDKN1A Rv	GATTAGGGCTTCCTCTTGGAG
CHOP Fw	AGAACCAGGAAACGGAAACAGA
CHOP Rv	TCTCCTTCATGCGCTGCTTT
DDIT4 Fw	CTAGCTGCGGCTTCTACGC
DDIT4 Rv	CCAAAGGCTAGGCATGGTGA
GADD45 Fw	TCAGCGCACGATCACTGTC
GADD45 Rv	CCAGCAGGCACAACACCAC
GAPDH Fw	TCCAAAATCAAGTGGGGCGA
GAPDH Rv	AGTAGAGGCAGGGATGATGT
MDM2 Fw	GGCCTGCTTTACATGTGCAA
MDM2 Rv	GCACAATCATTTGAATTGGTTGTC
SESN2 Fw	CTCCTCCTTCGTGTTTGGCT
SESN2 Rv	CTCAAAGCCCCCAGAGTTGT
SCL3A2 Fw	AGCTGGAGTTTGTCTCAGGC
SCL3A2 Rv	GGCCAATCTCATCCCCGTAG
TNFRSF10B Fw	TGACTCATCTCAGAAATGTCAATTCTTA
TNFRSF10B Rv	GGACACAAGAAGAAAACCTTAATGC
TRIB3 Fw	AGACTCGCAGCGGAAGTGG
TRIB3 Rv	CTCGCATCTCGCCCCGTC
sXBP1 Fw	CTGAGTCCGAATCAGGTGCAG
sXBP1 Rv	ATCCATGGGGAGATGTTCTGG
uXBP1 Fw	CAGCACTCAGACTACGTGCA
uXBP1 Rv	ATCCATGGGGAGATGTTCTGG
tXBP1 Fw	TGGCCGGGTCTGCTGAGTCCG
tXBP1 Rv	ATCCATGGGGAGATGTTCTGG

For miRNA analysis, total RNA was extracted using TRIzol reagent (Invitrogen) according to manufacturer's instructions. RNA concentration and purity were measured in NanoDrop™ 1000 (ThermoFisher Scientific). 260/280 nm and 260/230 nm ratios ranged around 1.8-2.2. RNA integrity was assessed by gel electrophoresis. miRNA levels were evaluated using TaqMan miRNA assays (Applied Biosystems). cDNA was synthesized (MyCycler Thermal Cycler, Bio-Rad) using RNA, TaqMan MicroRNA Reverse Transcription Kit (Applied Biosystems) and stem-loop Reverse Transcription primers (hsa-miR-34a-5p; Applied Biosystems). qPCR reactions were performed in CFX96 Touch™ Real-Time PCR Detection System (Bio-Rad) using cDNA, miR-34a or snRNA U6 TaqMan probes (Applied Biosystems) and SsoAdvanced™ Universal Probes Supermix (Bio-Rad). snRNA U6 was used as reference gene.

Relative expression levels were calculated using the quantification cycle (Cq) method, according to MIQE guidelines (Bustin et al., 2009).

2.11. Western blot

Yeast: Cells were inoculated in induction selective medium and incubated at 30 °C, 200 rpm for 48 h. Yeast cells were then harvested and incubated with lyticase (Sigma-Aldrich) for 15 min at 37 °C, followed by incubation with the Cellytic™ Y Cell Lysis Reagent (Sigma-Aldrich), with EDTA-free protease inhibitor cocktail (Sigma-Aldrich), for 30 min at room temperature, and removal of cell debris by centrifugation.

Human tumor cell lines: 1.5×10^5 (HCT116 $p53^{-/-}$, HuH-7, NCI-H1299, HT-29) or 2.25×10^5 (MDA-MB-468) cells/well were seeded in 6-well plates and allowed to adhere overnight. Cells were then treated with LEM2 (HCT116 $p53^{-/-}$ and MDA-MB-468) or SLMP53-2 (HuH-7), for 16, 24, or 48 h. Thereafter, cells were harvested and whole cell lysates were obtained by incubation with RIPA buffer with EDTA-free protease inhibitor cocktail (Sigma-Aldrich) for 1 h at 4 °C, followed by removal of cell debris by centrifugation.

Protein extracts obtained from both yeast and human tumor cell lines were quantified using the Pierce™ BCA Protein Assay Kit (Thermo Scientific), according to manufacturer's instructions. Protein samples were prepared using 40 µg protein extract and 5× sodium dodecyl sulfate-polyacrylamide gel electrophoresis (SDS-PAGE) Sample Loading Buffer (NZYTech). Protein samples were then separated by SDS-PAGE and transferred to a nitrocellulose membrane (GE Healthcare). Membranes were blocked with 5% milk, incubated with primary antibody (**Table 2.3**) overnight at 4 °C, followed by 2 h incubation with secondary antibody (**Table 2.3**) at room temperature. Signal detection was carried out

using the ECL Prime Amersham kit (GE Healthcare) and the ChemiDoc™ MP Imaging System (Bio-Rad). Pgk1p and GAPDH were used as loading controls for yeast and human tumor cells, respectively.

Table 2.3 List of primary and secondary antibodies used in western blot.

Antibody	Dilution	Supplier	Reference
Primary antibodies			
α-actinin (Mouse monoclonal)	1:6000	Santa Cruz Biotechnology	**sc-17829**
γH2AX (Rabbit polyclonal)	1:10000	Abcam	**ab2893**
BAX (6A7; Mouse monoclonal)	1:100	Thermo Scientific	**MA5-14003**
Bcl-2 (C-2; Mouse monoclonal)	1:200	Santa Cruz Biotechnology	**sc-7382**
eIF2α (Rabbit polyclonal)	1:500	Abcam	**ab26197**
p-eIF2α (Rabbit polyclonal)	1:500	Abcam	**ab32157**
GADD45A (Rabbit polyclonal)	1:500	Millipore	**ABE2696**
GAPDH (6C5; Mouse monoclonal)	1:10000	Santa Cruz Biotechnology	**sc-32233**
Hsp40 (B-3; Mouse monoclonal)	1:200	Santa Cruz Biotechnology	**sc-398766**
Hsp70 (Rabbit polyclonal)	1:1000	Sigma-Aldrich	**SAB2702387**
Hsp90 (F-8; Mouse monoclonal)	1:500	Santa Cruz Biotechnology	**sc-13119**
Killer (Rabbit polyclonal)	1:500	Thermo Scientific	**PA5-19895**
MDM2 (SMP14; Mouse monoclonal)	1:100	Santa Cruz Biotechnology	**sc-965**
PARP (C2-10; Mouse polyclonal)	1:2000	Santa Cruz Biotechnology	**sc-53643**
Pgk1p (22C5D8; Mouse monoclonal)	1:10000	Invitrogen	**459250**
PUMA (B-6; Mouse monoclonal)	1:100	Santa Cruz Biotechnology	**sc-377015**
p21 (C-19; Rabbit polyclonal)	1:100	Santa Cruz Biotechnology	**sc-397**
p53 (DO-1; Mouse monoclonal)	1:5000	Santa Cruz Biotechnology	**sc-126**
p63 (4A4; Mouse monoclonal)	1:200	Santa Cruz Biotechnology	**sc-8431**
TAp73 (E-4; Mouse monoclonal)	1:1000	Santa Cruz Biotechnology	**sc-17823**
Survivin (EP2880Y; Rabbit monoclonal)	1:15000	Abcam	**ab76424**
VEGF (Mouse monoclonal)	1:200	Thermo Scientific	**MA1-16629**
Secondary antibodies (HRP-conjugated)			
Anti-mouse	1:5000	Santa Cruz Biotechnology	**sc-2005**
Anti-rabbit	1:5000	Santa Cruz Biotechnology	**sc-2006**

2.12. Immunofluorescence

XBP1 staining: HuH-7 cells were seeded in 24-well plates at 1.5×10^5 cells/well density and allowed to adhere overnight, followed by 24 h treatment with 28 μM SLMP53-2 or DMSO. After treatment, cells were fixed with 4% formaldehyde/PBS for 20 min at room temperature, blocked with BSA 5% and Triton 0.1% for 1 h at room temperature, incubated with anti-XBP1 antibody (**Table 2.4**) overnight at 4 °C, followed by incubation with an Alexa Fluor 488-conjugated secondary antibody (**Table 2.4**) for 1 h at room temperature, and staining with Hoechst (ThermoFisher Scientific; 1:10000). Images were visualized with a

Zeiss Axio Observer Z1 microscope (Carl Zaiss, Oberkochen, Germany) using Zeiss AxioVision v.4.8.1. Nuclear signal was quantified using CellProfiler™ software (Broad Institute, Cambridge, MA, USA).

PAb240/PAb1620 staining: HuH-7 cells were seeded in chambered cell culture slides at 1×10^4 cells/well density and allowed to adhere overnight, followed by 36 h treatment with 42 μM SLMP53-2 or DMSO. After treatment, the cell monolayer was fixed with 4% formaldehyde/PBS for 30 min at room temperature, permeabilized with 0.1% Triton for 20 min at 4 °C and blocked with 5% BSA for 1 h at room temperature. Thereafter, cells were incubated with PAb240, PAb1620, or DO-1 anti-p53 antibodies (**Table 2.4**) overnight at 4 °C, followed by incubation with Alexa Fluor 488-conjugated secondary antibody (**Table 2.4**) for 1 h at room temperature, and staining with DAPI. Cells were photographed (Nikon DS-5Mc camera; Nikon Eclipse E400 fluorescence microscope; Nikon ACT-2U software, Izasa).

Table 2.4 List of primary and secondary antibodies used in immunofluorescence.

Antibody	Dilution	Supplier	Reference
Primary antibodies			
p53 (DO-1; Mouse monoclonal)	1:500	Santa Cruz Biotechnology	**sc-126**
p53 (PAb1620; Ab-5; Mouse monoclonal)	1:100	Millipore	**OP33**
p53 (PAb240; Ab-3; Mouse monoclonal)	1:200	Millipore	**OP29**
XBP1 (Mouse monoclonal)	1:250	Santa Cruz Biotechnology	**sc-8015**
Secondary antibody (Alexa Fluor 488-conjugated)			
Anti-mouse	1:1000	ThermoFisher Scientific	**A-11001**

2.13. Immunoprecipitation (IP) and co-immunoprecipitation (co-IP)

2×10^6 HCT116 $p53^{+/+}$, HCT116 $p53^{-/-}$, MDA-MB-468, or HuH-7 cells were seeded in 75 cm^2 flasks and allowed to adhere overnight. HCT116 $p53^{+/+}$ and HCT116 $p53^{-/-}$ cells were treated with 4 and 5 μM LEM2 for 24 h. MDA-MB-468 cells were treated with 1 and 2 μM LEM2 for 24 h. HuH-7 cells were then treated with 14, 28, and 42 μM SLMP53-2, for 36 h. In each case, DMSO was included as a control.

For co-IP in yeast, transformed cells obtained in 2.3 were grown in induction selective medium in the presence of 10, 20, and 25 μM LEM2 for 48 h.

The Pierce™ Magnetic IP/Co-IP Kit (Thermo Scientific) was used, according to manufacturer's instructions. Basically, cells were harvested and lysed in IP Lysis/Wash Buffer. Protein extracts were quantified using the Pierce™ BCA Protein Assay Kit. For each IP/co-IP reaction, 1 mg samples of protein extract were incubated with 1 μg/mL antibody

(antibodies used for IP/co-IP are listed in **Table 2.5**). Samples were then incubated with Pierce™ Protein A/G magnetic beads. After washing, beads were resuspended in Lane marker sample buffer with 50 mM DTT and boiled at 95 °C for 10 min, to elute bound proteins. Immunoprecipitated fractions (IP) and whole cell lysates (input) were then analyzed by western blot, as described in 2.11.

Table 2.5 List of antibodies used for IP and co-IP experiments.

Antibody	Supplier	Reference
p53 (DO-1; Mouse monoclonal)	Santa Cruz Biotechnology	**sc-126**
p53 (PAb1620; Ab-5; Mouse monoclonal)	Millipore	**OP33**
p53 (PAb240; Ab-3; Mouse monoclonal)	Millipore	**OP29**
TAp73 (E-4; Mouse monoclonal)	Santa Cruz Biotechnology	**sc-17823**

2.14. Chromatin immunoprecipitation (ChIP)

1.5×10^6 HuH-7 cells were seeded in 150 mm dishes and allowed to adhere overnight, followed by 24 h treatment with 28 µM SLMP53-2 or DMSO. ChIP was performed based on the Myers lab protocol (Alessandrini et al., 2018). Briefly, after treatment, cross-linking was performed with 1% formaldehyde (Sigma-Aldrich) for 10 min at room temperature, followed by quenching with 0.125 M glycine. Cells were then harvested and lysed in SDS-containing lysis buffer. Lysates were processed using a Bioruptor for chromatin fragmentation. The size of sonicated fragments was confirmed by gel electrophoresis (150-500 bp). IP was performed using Dynabeads Protein G (Thermo Scientific) and 1 µg anti-p53 antibody (DO-1) or mouse IgG (negative control), according to manufacturer's instructions. The bead pellet was then incubated overnight at 65 °C to reverse cross-linking and recover immunoprecipitated DNA. Samples were incubated with RNaseA (37 °C, 30 min) and proteinase K (56 °C, 20 min). DNA was then purified using the QIAquick PCR Purification Kit (Qiagen), according to manufacturer's instructions. p53 occupancy at the p21 promoter was measured by RT-qPCR (as described in 2.10) using specific primers (forward: GTGGCTCTGATTGGCTTTCTG; reverse: CTCCTACCATCCCCTTCCTC).

2.15. Cellular thermal shift assay (CETSA)

HCT116 $p53^{+/+}$ and MDA-MB-468 cells were lysed by dounce homogenization in 25 mM Tris pH 7.4 buffer, containing 10 mM $MgCl_2$ and 2 mM DTT. Lysates were then treated with 0.5-25 µM LEM2 for 1 h at room temperature, heated at different temperatures for 3

min, cooled to room temperature for 3 min, and placed on ice. Insoluble (denatured) protein was separated by centrifugation. Soluble protein was analyzed by western blot, as described in 2.11.

2.16. Comet assay

1.5×10^5 HCT116 $p53^{-/-}$ cells were seeded in 6-well plates and allowed to adhere overnight. Cells were then treated with 1 and 2 μM LEM2 or 50 μM etoposide (ETOP, positive control) for 48 h. The OxiSelect Comet Assay kit (Cell Biolabs, Meditecno, Carcavelos, Portugal) was used according to manufacturer's instructions. Images were acquired using a Nikon Eclipse E400 fluorescence microscope, Nikon DS-5Mc camera and Nikon ACT-2U software (Izasa). Tail DNA quantification was performed using Fiji Software (Open Comet/ImageJ).

Cells with more than 5% of DNA in the tail were considered comet-positive. 100 cells were quantified in each sample.

2.17. Cytokinesis-block micronucleus assay

Fresh peripheral blood samples, collected from heathy volunteers into heparinized vacutainers, were suspended in RPMI-1640 with 10% FBS and seeded in 6-well plates. Cells were then exposed to 1 and 2 μM LEM2, or 100 μg/mL cyclophosphamide (CP; positive control; Sigma-Aldrich) for 44 h, followed by a 28 h incubation with 3 μg/mL cytochalasin B (for cytokinesis block; Sigma-Aldrich). Isolation of lymphocytes was carried out by density gradient separation using Histopaque-1077 and -1119 (Sigma-Aldrich), followed by fixation with 3:1 methanol/acetic acid, and staining with Wright stain (Sigma-Aldrich). Samples were analyzed using a Nikon AlphaPhotoF2 YS2 light optical microscope. The number of micronuclei per 1000 binucleated lymphocytes was recorded.

2.18. Recombinant protein expression and purification

The stabilized [containing 4 stabilizing mutations M133L/V203A/N239Y/N268D (Nikolova et al., 1998)] DBD of mutp53-Y220C (T-p53C-Y220C) was expressed and purified as described (Bauer et al., 2016). Basically, *Escherichia coli* C41(DE3) (Lucigen) transformed with a pET24 plasmid encoding T-p53C-Y220C were grown in M9 minimal medium with $^{15}NH_4Cl$ (1 g/L) as sole nitrogen source, at 37 °C, until OD_{600} of 1.2. At this

point, protein expression was induced with 1 mM IPTG, and cultures were incubated for 16 h at 25 °C. Cells were then harvested by centrifugation and flash-frozen in liquid nitrogen. Pellets were suspended in phosphate buffer with protease inhibitor cocktail, subjected to Dounce homogenization, and lysed in a French press. Cell lysates were cleared by centrifugation and filtered through 0.45 µm filter before proceeding with purification. Protein purification consisted of three sequential purification steps: (i) a nickel affinity chromatography (the protein was fused with a poly-histidine tag, which was then removed by TEV cleavage before proceeding to the next purification step); (ii) a heparin affinity chromatography; (iii) gel filtration. All purification steps were carried out using an Äkta Protein Purification System (GE Healthcare). Purified protein was analyzed by SDS-PAGE.

2.19. Heteronuclear single-quantum coherence (HSQC)-NMR

^{1}H-^{15}N HSQC spectra of ^{15}N-labeled T-p53C-Y220C (70 µM) and different compound concentrations were recorded and analyzed as described (Bauer et al., 2016). Briefly, SLMP53-2 was diluted from a stock solution in DMSO-d6 to a final concentration of 5% (v/v) DMSO-d6 in buffer. SLMP53-2 was added to the protein solution immediately before NMR measurement. SLMP53-2 was tested at 127 and 500 µM. Spectra were recorded on a Bruker Avance-800 spectrometer using a 5 mm inverse cryogenic probe. Analysis of spectra was performed using Sparky 3.11430 and Bruker Topspin 2.0 software.

2.20. *In vivo* antitumor and toxicity assays

Animal experiments were conducted following the EU Directive 2010/63/EU and National Authorities. The study was approved by the local Animal Welfare Body (ORBEA-5-2016). Female swiss nude mice and Wistar rats (Charles River Laboratories, Barcelona, Spain) were housed under pathogen-free conditions in ventilated cages.

For toxicological analysis, female Wistar rats were treated with 50 mg/kg SLMP53-2 or vehicle (DMSO) by intraperitoneal injection, twice a week. After five administrations, blood samples were collected for toxicological analysis. Each experimental group was composed of five animals.

For xenograft antitumor analysis, 7.5×10^{6} HuH-7 cells (in PBS/Matrigel 1:1; Corning, Enzifarma) were subcutaneously inoculated in the dorsal flank of nude mice (5 animals/group). Tumors were routinely measured using a caliper for tumor volume calculation [$(a \times b^2)/2$; a and b represent the longest and shortest tumor axes, respectively].

Twice-weekly intraperitoneal injections of 50 mg/kg SLMP53-2 or vehicle were started for tumors with approximately 100 mm^3 (5 days after the grafts). Five administrations were performed with continuous monitoring of tumor volume, animal weight, and signs of morbidity. At the end of treatment, animals were sacrificed by cervical dislocation, organs (kidneys, liver, heart, and spleen) were weighed, and tumor samples were collected for immunohistochemical analysis.

2.21. Immunohistochemical analysis

For immunohistochemical analysis, xenograft tumor samples were fixed in 10% formalin, embedded in paraffin and sectioned at 4 µm. Sections were thereafter subjected to deparaffination and rehydration, and then boiled for 20 min in 10 mM citrate buffer (pH 6.0; for BAX and Ki-67 detection) or 10 mM EDTA buffer (pH 8.0; for VEGF detection), for antigen retrieval. Sections were incubated with UltraVision Hydrogen Peroxide Block and UltraVision Protein Block solution, according to manufacturer's instructions (Thermo Scientific, Taper, Sintra, Portugal), followed by incubation with primary antibodies (**Table 2.6**), overnight at 4 °C. For staining, the UltraVision Quanto Detection System HRP DAB, (Thermo Scientific, Taper) was used according to the manufacturer's instructions. Sections were then counterstained with Gill's hematoxylin (Thermo Scientific, Taper), dehydrated, clarified, and mounted. Images were acquired using a Nikon Eclipse E400 microscope (400× magnification) with the Nikon DS-5Mc camera and Nikon ACT-2U software (Izasa).

Table 2.6 List of primary antibodies used for immunohistochemistry.

Antibody	Dilution	Supplier	Reference
BAX (6A7; Mouse monoclonal)	1:100	Thermo Scientific	**MA5-14003**
Ki-67 (SP6; Rabbit monoclonal)	1:500	Thermo Scientific	**MA5-14520**
VEGF (Mouse monoclonal)	1:200	Thermo Scientific	**MA1-16629**

2.22. Statistical analysis

Data were statistically analyzed using the GraphPad Prism software v7.0 (La Jolla). Appropriate statistical tests were applied to each dataset (indicated in figure legends); $p<0.05$ was considered statistically significant.

Chapter 3. New inhibitor of the TAp73 interaction with MDM2 and mutant p53 with promising antitumor activity

Parts of this chapter were based on the following publications:

- Gomes, S.[*], Raimundo, L. [*], Soares, J. [*], Loureiro, J. B., Leão, M., Ramos, H., Monteiro, M. N., Lemos, A., Moreira, J., Pinto, M., Chlapek, P., Veselka, R., Sousa, E., Saraiva, L. 2019, New inhibitor of the TAp73 interaction with MDM2 and mutant p53 with promising antitumor activity against neuroblastoma. Cancer Letters **446**: 90-102. doi: 10.1016/j.canlet.2019.01.014.
  [*]Authors contributed equally to this work.

In p53-impaired tumors, TAp73 activation may compensate for the lack of a functional p53 pathway, suppressing tumor proliferation and increasing chemotherapeutic efficiency (Wu and Leng, 2015). In these tumors, disruption of the TAp73 interaction with mutp53 and MDM2 represents an encouraging therapeutic strategy, alternative to p53 activation.

Herein, we report the identification of 1-carbaldehyde-3,4-dimethoxyxanthone (LEM2**,** **Figure 3.1**), a new activator of TAp73 with promising antitumor activity.

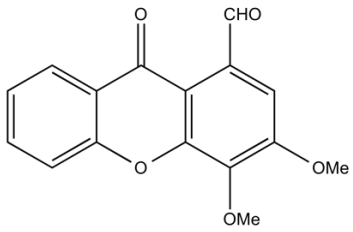

Figure 3.1 Chemical structure of LEM2.

3.1. Results

3.1.1. LEM2 is a non-genotoxic drug with p53-independent growth inhibitory activity in human tumor cells

The antitumor activity of LEM2 (**Figure 3.1**) was evaluated in human wtp53-expressing HCT116 $p53^{+/+}$ and respective p53-null isogenic derivative HCT116 $p53^{-/-}$ cells, by SRB assay (**Figure 3.2A**). The results showed that LEM2 had potent p53-independent tumor growth inhibitory effect, with similar IC_{50} values in $p53^{+/+}$ (0.98 ± 0.12 μM) and $p53^{-/-}$ (0.68 ± 0.08 μM) HCT116 cells. In HCT116 $p53^{-/-}$ cells, further analysis revealed that 2 μM LEM2 induced G_2/M-phase cell cycle arrest (**Figure 3.2B**) and apoptosis (demonstrated by the increase in Annexin V-positive cells (**Figure 3.2C**) and PARP cleavage (**Figure 3.2D**). Consistently, in a 3D-model of HCT116 $p53^{-/-}$ cells, 0.5-2 μM LEM2 also markedly inhibited spheroid growth (**Figure 3.2E**) and prevented their formation, when added upon seeding (**Figure 3.2F**).

We next interrogated whether the antiproliferative effect of LEM2 was associated with induction of DNA damage. However, compared to solvent, and unlike the positive controls, 1 and 2 μM LEM2 did not increase the number of micronuclei in human lymphocytes (**Figure 3.2G**), nor the percentage of comet-positive HCT116 $p53^{-/-}$ cells (**Figure 3.2H, I**).

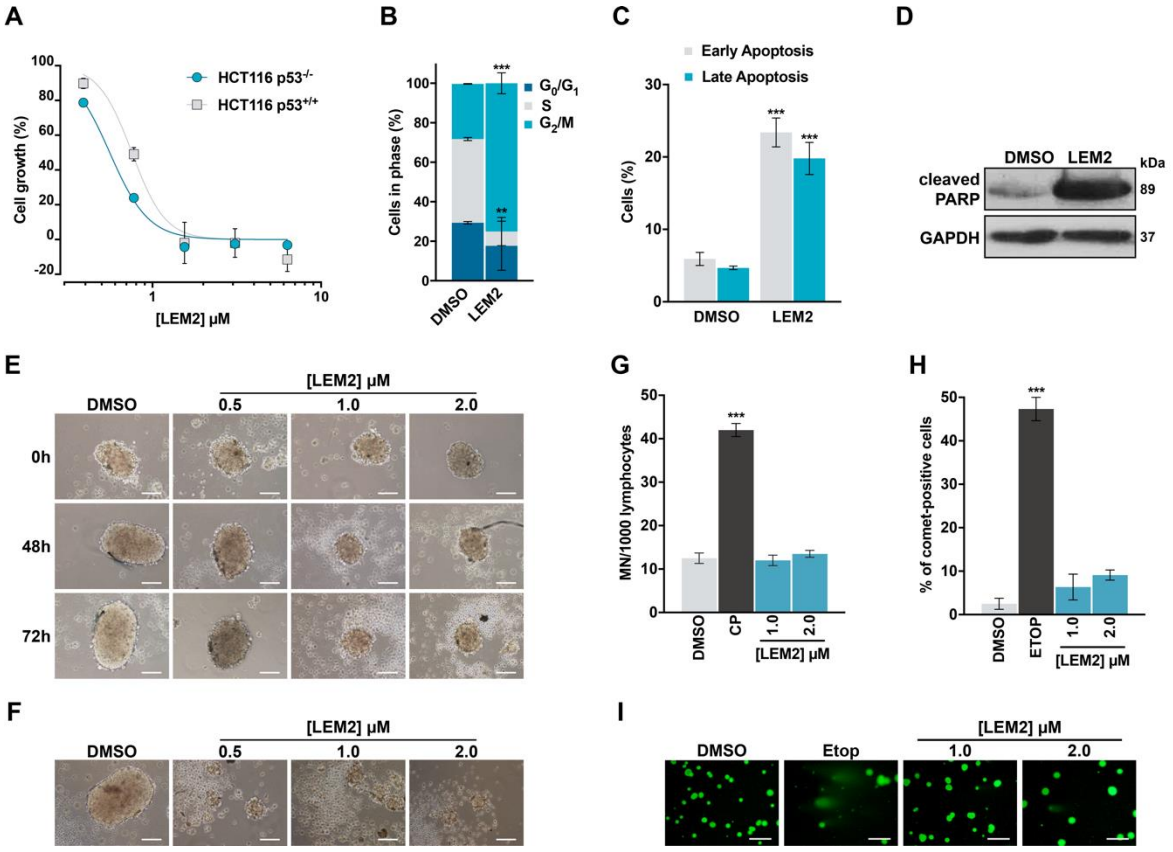

Figure 3.2 LEM2 is non-genotoxic and displays p53- and p63-independent growth inhibitory activity in human tumor cells. (A) Dose-response curves for the growth inhibitory activity of 0.39-6.25 µM LEM2 in $p53^{+/+}$ and $p53^{-/-}$ HCT116 cells, determined by SRB assay, after 48 h treatment. Data are mean±SEM (n=4). **(B)** Effect of 2 µM LEM2 on cell cycle progression of HCT116 $p53^{-/-}$ cells after 24 h treatment. Data are mean±SEM (n=3); values significantly different from DMSO: $^{**}p<0.01$, $^{***}p<0.001$ (two-way ANOVA with Dunnett's multiple comparison test). **(C)** Effect of 2 µM LEM2 on apoptosis of HCT116 $p53^{-/-}$ cells after 48 h treatment. Data are mean±SEM (n=4); values significantly different from DMSO: $^{***}p<0.001$ (one-way ANOVA with Dunnett's multiple comparison test). **(D)** Levels of cleaved PARP in HCT116 $p53^{-/-}$ cells after 48 h treatment with 1 µM LEM2 or solvent, visualized by western blot. Immunoblots represent one of three independent experiments; GAPDH was used as a loading control. **(E)** Brightfield imaging of 3-day-old HCT116 $p53^{-/-}$ spheroids, treated with LEM2 or solvent for 48 and 72 h. **(F)** Brightfield imaging of HCT116 $p53^{-/-}$ spheroids formed after 7 days. Spheroids were seeded in the presence of LEM2 or solvent. In E and F, images are representative of 3 independent experiments; scale bar=100 µm; magnification=100×. **(G)** Analysis of the genotoxicity in human lymphocytes measured by cytokinesis-block micronucleus assay, following 72 h treatment with 5 µg/mL cyclophosphamide (CP; positive control), or LEM2 (n=3); values significantly different from DMSO: $^{***}p<0.001$ (one-way ANOVA with Dunnett's multiple comparison test). **(H, I)** DNA damage was measured in HCT116 $p53^{-/-}$cells by comet assay after 48 h treatment with 50 µM etoposide (ETOP; positive control) or LEM2. In **H**, quantification of comet-positive cells (containing more than 5% of DNA in the tail); one hundred cells were analyzed in each group (n=3); values significantly different from DMSO: $^{***}p<0.001$ (one-way ANOVA with Dunnett's multiple comparison test). In **I**, representative images of the comet assay (scale bar=50 µm; magnification=100×).

3.1.2. LEM2 has TAp73-dependent growth inhibitory activity in human tumor cells, activating TAp73 through disruption of its interaction with MDM2

A western blot analysis revealed that LEM2-induced growth inhibition in HCT116 p53$^{-/-}$ cells was associated with regulation of several p53-family transcriptional targets. In fact, 1 µM LEM2 increased the protein levels of TAp73α, MDM2, p21, Killer, and BAX, while reducing Bcl-2 and vascular endothelial growth factor (VEGF) protein levels (**Figure 3.3A**). Accordingly, 2 µM LEM2 increased the mRNA levels of *CDKN1A*, *BAX*, *TNFRSF10B*, and *MDM2* (**Figure 3.3B**). Since HCT116 p53$^{-/-}$ cells do not express p53 nor p63 (Vilgelm et al., 2010), we hypothesized that LEM2 growth inhibitory activity in these cells might relate to interference with p73. To test such hypothesis, TAp73α-silenced HCT116 p53$^{-/-}$ cells were obtained using siRNA (**Figure 3.3C**). By colony formation assay, we observed that p73-silenced cells were less susceptible to the inhibitory effect of LEM2 than cells transfected with control siRNA (**Figure 3.3D**). These results supported a p73-dependent growth inhibitory activity of LEM2 in HCT116 p53$^{-/-}$ cells.

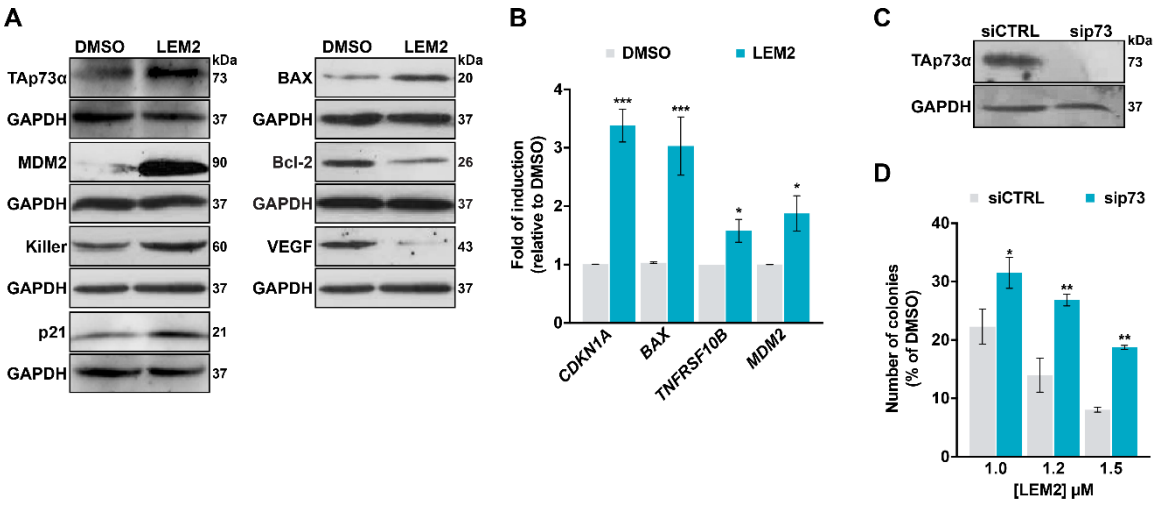

Figure 3.3 LEM2 has TAp73-dependent growth inhibitory activity and activates TAp73 transcriptional activity in human tumor cells. (A) Protein levels of TAp73 transcriptional targets in HCT116 p53$^{-/-}$ cells, after 16 h (p21 and BAX) 24 h (MDM2, Killer, Bcl-2, VEGF) or 48 h (TAp73α) treatment with 1 µM LEM2 or solvent, visualized by western blot. **(B)** mRNA levels of TAp73 transcriptional targets measured by RT-qPCR in HCT116 p53$^{-/-}$ cells after 24 h treatment with 2 µM LEM2 or solvent. Fold of induction is relative to solvent. Data are mean±SEM (n=3); values significantly different from solvent: *p<0.05, ***p<0.001 (two-way ANOVA with Dunnett's multiple comparison test). **(C)** The immunoblot shows TAp73α protein levels in HCT116 p53$^{-/-}$ cells transfected with sip73 or siCTRL; immunoblot represents one of three independent experiments. GAPDH was used as loading control. **(D)** Effect of LEM2 on the colony formation of HCT116 p53$^{-/-}$ cells transfected with siRNA targeting p73 (sip73) or control siRNA (siCTRL). Cells were treated with LEM2 or solvent for 24 h, and colonies were allowed to grow for 10 days. Data are mean±SEM (n=3); values significantly different from siCTRL: *p<0.05, **p<0.01 (two-way ANOVA with Sidak's multiple comparison test).

Since MDM2 is a well-known inhibitor of TAp73, we investigated the potential mode of action of LEM2 by testing its impact on the TAp73α-MDM2 interaction. For this, we first used a previously developed yeast assay (Leão et al., 2015a). In this assay, TAp73α-MDM2 interaction inhibitor would restore the TAp73α-induced yeast growth inhibition previously abolished by MDM2. Consistently, LEM2 caused dose-dependent growth inhibition in yeast cells co-expressing TAp73α and MDM2, while not interfering with the growth of control yeast (empty-vectors) and yeast expressing TAp73α or MDM2 alone (**Figure 3.4A**). To confirm these results, co-immunoprecipitation was performed. As expected, 4 and 5 μM LEM2 markedly reduced the amount of MDM2 precipitated with TAp73α (**Figure 3.4B**), while not affecting the amount of MDM2 precipitated with p53 in HCT116 $p53^{+/+}$ cells (**Figure 3.4C**). These results corroborated the ability of LEM2 to disrupt the TAp73α-MDM2 interaction, having a p53-independent growth inhibitory effect in tumor cells. Additionally, it was verified by CETSA that 5-25 μM LEM2 induced thermal stabilization of TAp73α at 56 ºC in HCT116 $p53^{-/-}$ cells (**Figure 3.4D**). Conversely, LEM2 did not increase the melting temperature of MDM2, even at the concentration that caused maximum TAp73α thermal stabilization (25 μM) (**Figure 3.4E**). These data support a potential interaction of LEM2 with TAp73α and not with MDM2.

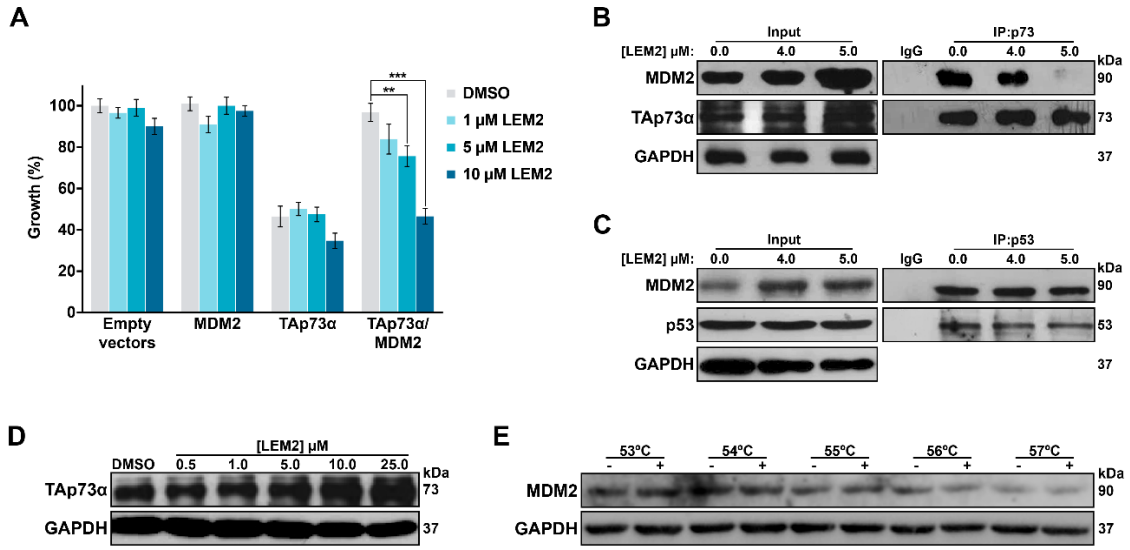

Figure 3.4 LEM2 induces disruption of TAp73 interaction with MDM2 and TAp73 thermal stabilization. (A) Effect of LEM2 on the growth of control yeast (empty vectors), yeast expressing TAp73α alone, and yeast co-expressing TAp73α and MDM2, after 40 h treatment. Results were plotted setting the growth of untreated control yeast as 100%; data are mean±SEM (n=4); values significantly different from DMSO: **p<0.01, ***p<0.001 (two-way ANOVA with Dunnett's multiple comparison test). **(B)** Co-immunoprecipitation in HCT116 $p53^{-/-}$ cells treated with 4 and 5 μM LEM2 or solvent for 24 h, using anti-immunoglobulin G (IgG) or anti-TAp73α (IP:p73) antibodies followed

by immunoblotting with anti-MDM2. **(C)** Co-immunoprecipitation in HCT116 $p53^{+/+}$ cells treated with 4 and 5 μM LEM2 or solvent for 24 h, using anti-immunoglobulin G (IgG) or anti-p53 (IP:p53) antibodies followed by immunoblotting with anti-MDM2. **(D,E)** CETSA in HCT116 $p53^{-/-}$ cell lysates treated with LEM2 or solvent; soluble protein was analyzed by western blot. In **D**, lysate samples were treated with 0.5-25 μM LEM2 and heated at 56 °C. In **E**, lysate samples were treated with 25 μM LEM2 (+) or solvent (-) and heated at increasing temperatures. In **B-E**, immunoblots represent one of three independent experiments; GAPDH was used as a loading control.

3.1.3. LEM2 has TAp73-dependent growth inhibitory activity in mutp53-expressing human tumor cells, activating TAp73 through disruption of its interaction with mutp53

The effect of LEM2 on the growth of human tumor cells expressing distinct mutp53 forms was also investigated by SRB assay (**Figure 3.5A**). The IC_{50} values (around 1-3 μM) revealed a potent antiproliferative effect of LEM2 against SK-BR-3 (mutp53-R175H), MDA-MB-231 (mutp53-R280K), MDA-MB-468 (mutp53-R273H), SW-837 (mutp53-R248W), and HuH-7 (mutp53-Y220C) cells. The only exception were HT-29 cells (mutp53-R273H), in which the IC_{50} of LEM2 (20 μM) was much higher than those in the remaining mutp53-expressing tumor cells, particularly in MDA-MB-468 cells (1.5 μM), which express the same mutp53 (**Figure 3.5A**). Interestingly, in HT-29 cells, TAp73α protein levels are much lower than in MDA-MB-468 cells (**Figure 3.5B**). This raised the hypothesis that, in mutp53-expressing tumor cells, LEM2 antiproliferative activity might also be mediated by TAp73 activation. In fact, the ectopic expression of TAp73α in HT-29 cells (**Figure 3.5C**) significantly enhanced LEM2 antiproliferative activity (**Figure 3.5D**).

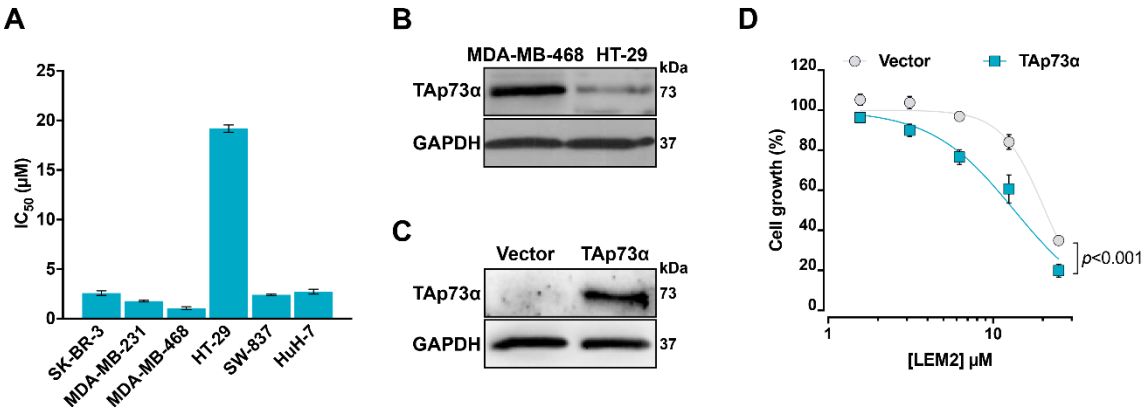

Figure 3.5 LEM2 has TAp73-dependent growth inhibitory activity in human mutp53-expressing tumor cells. (A) IC_{50} values of LEM2 in human tumor cells expressing different mutp53 forms, determined by SRB assay, after 48 h treatment with 0.39-25.0 μM LEM2. Data are mean±SEM (n=4). **(B)** Protein levels of TAp73α in MDA-MB-468 and HT-29 cells, visualized by western blot. **(C)** Protein levels of TAp73α in HT-29 cells transfected with the pCI-neo plasmid encoding TAp73α or

with the empty-vector, visualized by western blot. In **B** and **C**, immunoblots represent one of three independent experiments; GAPDH was used as a loading control. **(D)** Dose-response curves for the growth inhibitory activity of LEM2 in human HT-29 transfected with the pCI-neo plasmid encoding TAp73α or with the empty vector, determined by SRB assay, after 48 h treatment with 0.39-25.0 μM LEM2. Data are mean±SEM (n=4); p<0.001, extra sum-of-squares F test.

Consistently, in MDA-MB-468 cells, the pronounced LEM2 growth inhibitory activity observed by SRB (**Figure 3.5A**) and colony formation (**Figure 3.6A**) assay, was associated with pronounced G_2/M-phase cell cycle arrest (**Figure 3.6B**) and apoptosis (**Figure 3.6C**), and regulation of several TAp73 transcriptional targets. In fact, in these cells, 1.5 μM LEM2 increased TAp73α, p21, Killer, and PUMA protein levels, while decreasing Bcl-2 and VEGF (**Figure 3.6D**). Likewise, LEM2 increased mRNA levels of *CDKN1A*, *BAX,* and *TNFRSF10B* in MDA-MB-468 cells (**Figure 3.6E**). In MDA-MB-468 cells, the involvement of TAp73α in LEM2 growth inhibitory activity was further supported by CETSA. In this assay, 1-25 μM LEM2 induced TAp73α thermal stabilization at 52 ºC (**Figure 3.6F**), while no increase in the mutp53 melting temperature was observed even at the concentration that caused maximum TAp73α thermal stabilization (25 μM) (**Figure 3.6G**). Collectively, these results supported the involvement of TAp73 in LEM2 growth inhibitory activity in mutp53-expressing tumor cells.

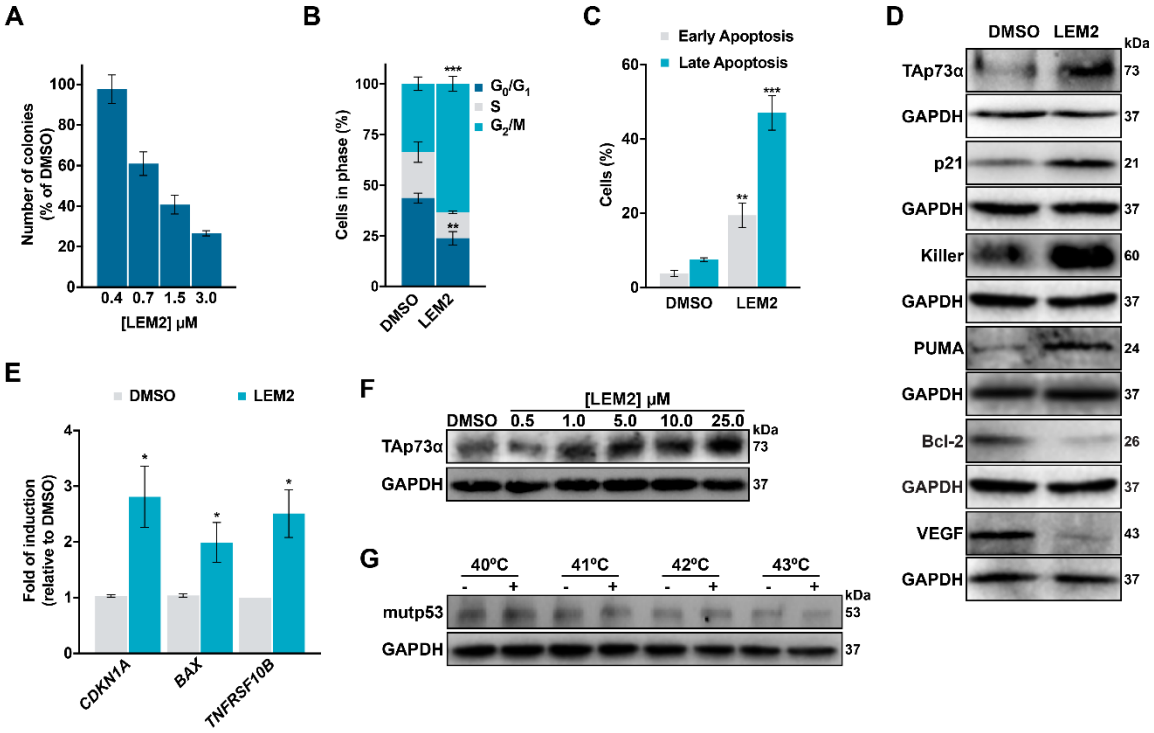

Figure 3.6 LEM2 activates TAp73 transcriptional activity and induces its thermal stabilization in human mutp53-expressing tumor cells. (A) Effect of LEM2 on the colony formation of MDA-MB-468 cells. Cells were treated with LEM2 or solvent for 24 h, and colonies were allowed to grow for

10 days. Data are mean±SEM (n=3). **(B)** Effect of 1.5 μM LEM2 on cell cycle progression of MDA-MB-468 cells after 24 h treatment. Data are mean±SEM (n=3); values significantly different from DMSO: ***p*<0.01, ****p*<0.001 (two-way ANOVA with Dunnett's multiple comparison test). **(C)** Effect of 1.5 μM LEM2 on apoptosis of MDA-MB-468 cells after 48 h treatment. Data are mean±SEM (n=4); values significantly different from DMSO: ***p*<0.01, ****p*<0.001 (one-way ANOVA with Dunnett's multiple comparison test). **(D)** Protein levels of TAp73 transcriptional targets in MDA-MB-468 cells, after 16 h (PUMA and TAp73α), 24 h (VEGF), or 48 h (p21, Killer, Bcl-2) treatment with 1.5 μM LEM2 or solvent, visualized by western blot. Immunoblots represent one of three independent experiments; GAPDH was used as a loading control. **(E)** mRNA levels of TAp73 transcriptional targets measured by RT-qPCR in MDA-MB-468 cells after 24 h (*MDM2*) or 48 h (*BAX* and *TNFRSF10B)* treatment with 2 μM LEM2 or solvent. Fold of induction is relative to solvent. Data are mean±SEM (n=3); values significantly different from solvent: **p*<0.05 (two-way ANOVA with Dunnett's multiple comparison test). **(F,G)** CETSA in MDA-MB-468 cell lysates treated with LEM2 (+) or solvent (-); soluble protein was analyzed by western blot. In **F**, lysate samples were treated with 0.5-25 μM LEM2 and heated at 52 °C. In **G**, lysate samples were treated with 25 μM LEM2 and heated at increasing temperatures.

Since mutp53 interacts with and inhibits TAp73, we interrogated whether LEM2 would also disrupt the TAp73-mutp53 interaction. To answer this question, we developed a new yeast assay, consisting of yeast cells expressing human TAp73α and/or mutp53-R273H, and control yeast (empty-vectors) (**Figure 3.7A**). In this assay, TAp73α expression induced marked yeast growth inhibition, which was reverted by co-expression with mutp53 (**Figure 3.7B**). As such, a reestablishment of TAp73α-induced yeast growth inhibition would reflect the disruption of its interaction with mutp53. This was obtained with 20 and 25 μM LEM2 in yeast cells co-expressing TAp73α and mutp53-R273H, while no effect was observed in control yeast or yeast expressing TAp73α or mutp53 alone (**Figure 3.7C**). To confirm that the reestablishment of TAp73α-induced yeast growth inhibition by LEM2 was due to disruption of the TAp73α-mutp53 interaction, co-immunoprecipitation was performed. In this assay, 10-25 μM LEM2 visibly decreased the amount of TAp73α precipitated with mutp53 in yeast (**Figure 3.7D**). Consistently, in MDA-MB-468 cells, 1 and 2μM LEM2 also visibly decreased the amount of TAp73α precipitated with mutp53, further supporting the ability of LEM2 to disrupt the TAp73α-mutp53 interaction in human tumor cells (**Figure 3.7E**).

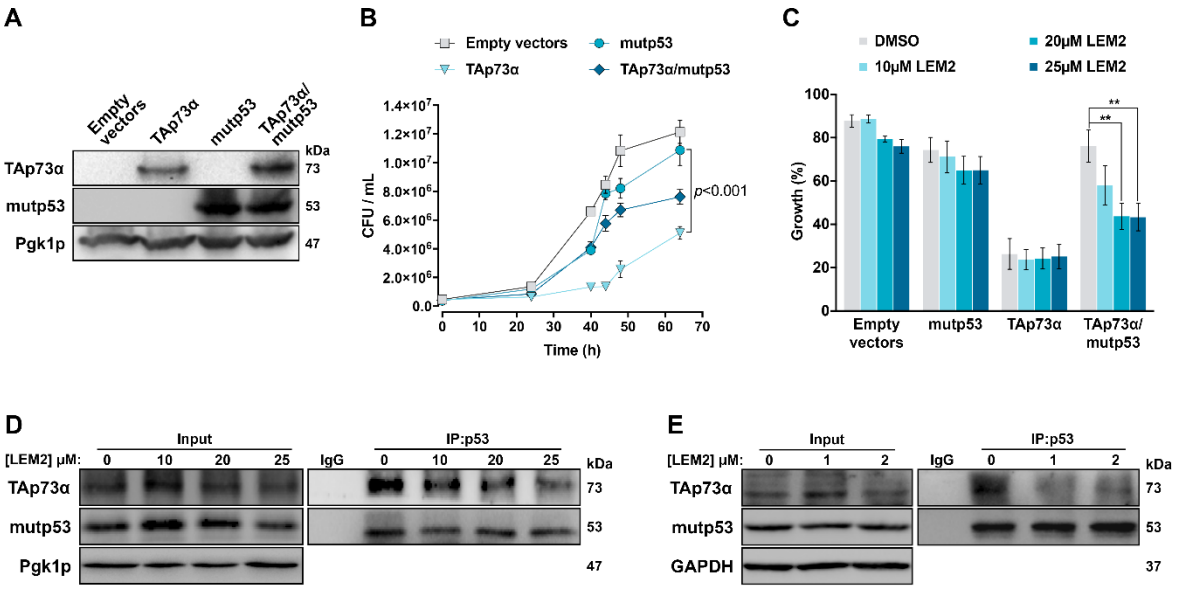

Figure 3.7 LEM2 disrupts the TAp73 interaction with mutp53 in yeast and human mutp53-expressing tumor cells. (A) Expression of TAp73α alone and combined with mutp53 in yeast was confirmed by western blot. **(B)** Yeast cells individually expressing TAp73α or mutp53-R273H, co-expressing TAp73α and mutp53-R273H, and control yeast (empty vectors) were grown for up to 64 h. Growth curves were obtained by CFU counts; data are mean±SEM (n=5); $p<0.001$ (two-way ANOVA). **(C)** Effect of LEM2 on yeast cells individually expressing TAp73α or mutp53-R273H, co-expressing TAp73α and mutp53-R273H, and control yeast. Yeast cells were treated with LEM2 or solvent for 44 h. Results are plotted setting the growth of untreated yeast as 100%. Data are mean±SEM (n=4); values significantly different from DMSO: $^{**}p<0.01$ (two-way ANOVA with Dunnett's multiple comparison test). **(D)** Co-immunoprecipitation in yeast cells co-expressing TAp73α and mutp53-R273H treated with LEM2 or solvent for 44 h, using anti-immunoglobulin G (IgG) or anti-p53 (IP:p53) antibodies, followed by immunoblotting with anti-TAp73α and anti-p53 antibodies. **(E)** Co-immunoprecipitation in MDA-MB-468 cells treated with LEM2 or solvent for 24 h, using anti-immunoglobulin G (IgG) or anti-p53 (IP:p53) antibodies, followed by immunoblotting with anti-TAp73α and anti-p53 antibodies. In **A**, **D** and **E**, immunoblots represent one of three independent experiments; Pgk1p **(A,D)** or GAPDH **(E)** were used as loading controls.

3.1.4. Putative metabolites of LEM2 display markedly reduced activity

Cellular metabolism of aldehydes is a process largely dependent on the aldehyde and on the cellular content of aldehyde-metabolizing enzymes. Reduction and oxidation are the major metabolic routes for aromatic aldehydes (O'Brien et al., 2005). It could be hypothesized that the alcohol and/or carboxylic acid derivatives of LEM2 might be the active species responsible for TAp73 activation, instead of LEM2 itself. To test this hypothesis, the biological activity of the alcohol 1-(hydroxymethyl)-3,4-dimethoxy-9*H*-xanthen-9-one (LEMred) and carboxylic acid 3,4-dimethoxy-9-oxo-9*H*-xanthene-1-carboxylic acid (LEMox) putative LEM2 metabolites (**Figure 3.8A**) was evaluated. In yeast, none of the two compounds was able to inhibit the TAp73-MDM2 interaction (**Figure 3.8B**). Concerning the

TAp73-mutp53 interaction, although a significant inhibitory effect was observed with LEMred, its activity was much lower than that obtained with LEM2 (**Figure 3.8C**). Most importantly, both compounds displayed weak antitumor activity, with much higher IC_{50} values (superior to 25 µM, maximal concentration tested) than LEM2 in both HCT116 $p53^{-/-}$ and MDA-MB-468 tumor cells (**Figure 3.8D**). These results support that the biological activity obtained with LEM2 treatment can be attributed to the molecule itself and not to its alcohol and carboxylic acid derivatives.

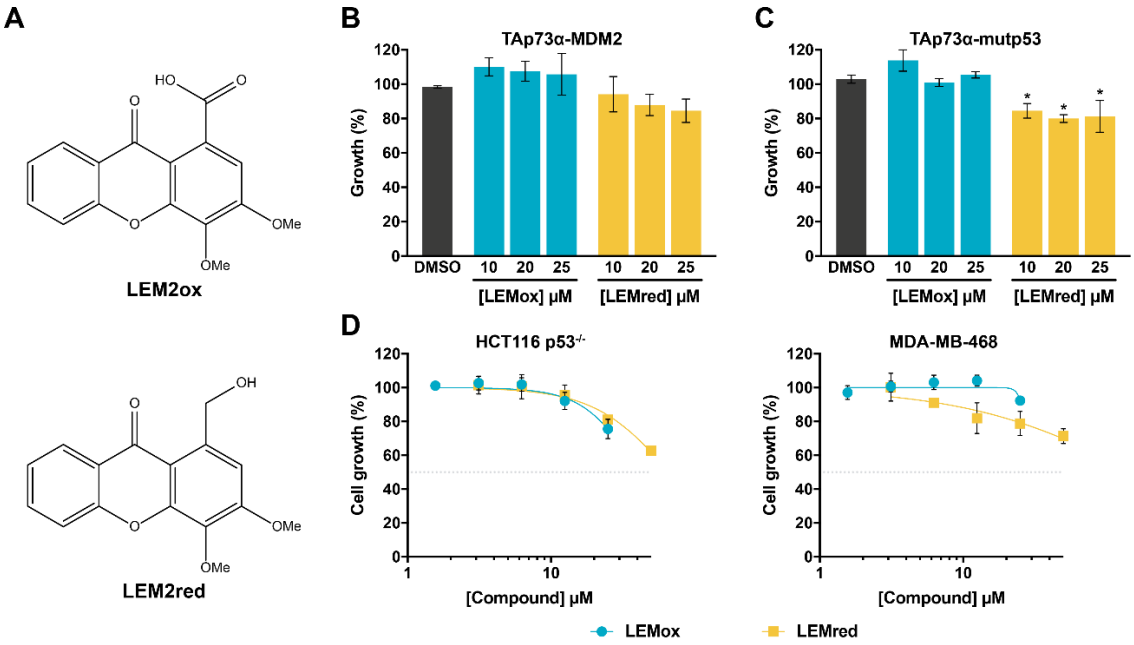

Figure 3.8 LEM2ox and LEM2red show markedly reduced growth inhibitory effect compared to LEM2. (A) Chemical structures of LEM2ox and LEM2red. **(B, C)** Effect of LEMox and LEMred on the growth of yeast co-expressing TAp73α and MDM2 **(B)** or TAp73α and mutp53 R273H **(C)**, after 40 h **(B)** or 44 h **(C)** treatment. Results were plotted setting the growth of untreated control yeast as 100%; data are mean±SEM (n=4); values significantly different from DMSO: **p*<0.05 (two-way ANOVA with Dunnett's multiple comparison test). LEMox and LEMred had no effect on the growth of control yeast (transformed with the empty vectors) or yeast expressing TAp73α, MDM2, or mutp53 R273H alone (data not shown). **(D)** Dose-response curves for the growth inhibitory activity of 1.56-25 µM LEMox and LEMred in HCT116 $p53^{-/-}$ and MDA-MB-468 cells, determined by SRB assay, after 48 h treatment. Data are mean±SEM (n=4).

3.2. Discussion

TAp73 is a key tumor suppressor protein, particularly in p53-disrupted tumor cells. Besides its ability to transactivate p53 target genes, regulating cellular processes as cell cycle and apoptosis, additional tumor suppressor properties have been attributed to TAp73, which are not shared by p53 (Di Como et al., 1999). This has strengthened the concept of functional replacement of impaired p53 by TAp73 in anticancer therapy (Wu and Leng, 2015).

Xanthones are a relevant class of *O*-heterocycles in Medicinal Chemistry, with several representatives in clinical research (Gomes et al., 2016). Herein, we report the xanthonic derivative LEM2, as a new TAp73 activator with potent antitumor activity. In p53-null and mutp53-expressing tumor cells, LEM2 displayed pronounced TAp73-dependent antiproliferative effect through cell cycle arrest and apoptosis. Moreover, it inhibited the growth of tumor cell spheroids, with no genotoxicity. Interestingly, in these cells, LEM2 downregulated the angiogenesis-inducing factor VEGF, suggesting a potential antiangiogenic activity.

In an attempt to further understand its mechanism of TAp73 activation, LEM2 was shown to disrupt the TAp73 interaction with MDM2 and mutp53, both in yeast and in human tumor cells. The peculiar ability of LEM2 to inhibit both the TAp73-MDM2 and TAp73-mutp53 interactions may be explained by its possible interference with TAp73, as evidenced by LEM2-induced TAp73 thermal stabilization. This dual LEM2 activity allows to predict promising therapeutic applications in a wide variety of cancer types. Additionally, since normal cells typically express low TAp73 levels, its activation by release of inhibitory interactions has been proposed as a selective anticancer therapeutic strategy, with minimal toxicity on normal cells (Maas et al., 2013).

In conclusion, despite the relevance of TAp73 in anticancer therapy, effective TAp73-activating agents are still mostly unavailable. In this work, we report the TAp73-activating agent LEM2 capable of inhibiting the TAp73 interaction with both MDM2 and mutp53.

Chapter 4. SLMP53-2 restores wild-type-like function to mutant p53 through Hsp70: promising activity in hepatocellular carcinoma

Parts of this chapter were based on the following publications:

- Gomes, S., Bosco B., Loureiro, J. B., Ramos, H., Raimundo, L., Soares, J., Nazareth, N., Barcherini, V., Bisio, A., Piazza, S., Bauer, M. R., Brás, J. P., Almeida, M. I., Gomes, C., Reis, F., Fersht, A. R., Inga, A., Santos, M. M. M., Saraiva, L. **(Work submitted for publication)**

- Saraiva L., Santos, M. M. M., Pereira, N. A. L., Pereira, C., Gomes, S., Leão, M., Monteiro, A., Soares, J. Tryptophanol-derived oxazoloisoindolinones: small-molecule p53 activators. **European patent nº EP3013833; US patent nº 20160347765**

In this chapter, a tryptophanol-derived oxazoloisoindolinone, SLMP53-2, is identified as a new mutp53 reactivator with encouraging anticancer activity, particularly against hepatocellular carcinoma (HCC).

4.1. Results

4.1.1. SLMP53-2 displays mutp53-dependent growth inhibitory effect in human tumor cells, leading to cell cycle arrest, apoptosis, and ER stress

In our previous work, the tryptophanol-derived oxazoloisoindolinone SLMP53-1 was identified as a reactivator of mutp53-R280K with *in vivo* p53-dependent anti-tumor activity (Soares et al., 2016). In order to search for new mutp53 reactivators, a small library of SLMP53-1 derivatives was synthesized. The activity of the compounds as potential mutp53 reactivators was investigated by analysis of their anti-proliferative effect on p53-null NCI-H1299 tumor cells ectopically expressing four of the most prevalent mutp53. By SRB assay, the compound SLMP53-2 (**Figure 4.1A**) was selected based on its marked reduction of the IC_{50} values in NCI-H1299 cells expressing mutp53-R175H, -Y220C, or -G245S, compared to cells transfected with the empty vector (**Figure 4.1B**).

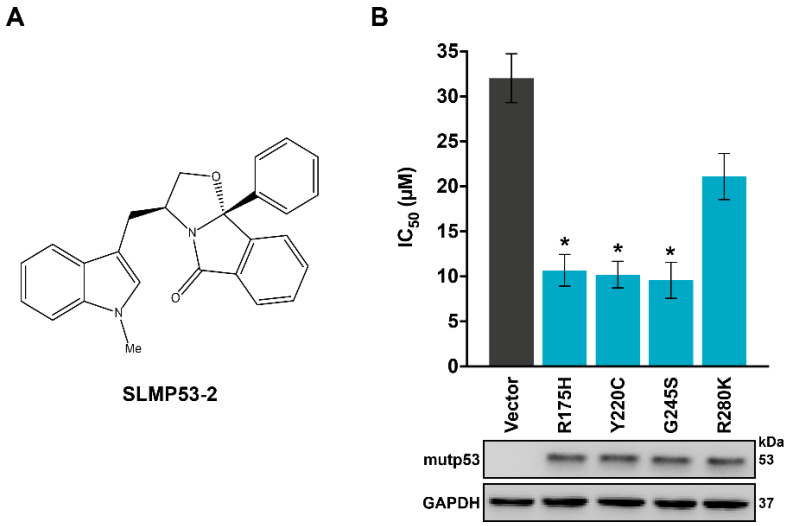

Figure 4.1 Growth inhibitory effect of SLMP53-2 in human tumour cells is dependent on structural mutp53. (A) Chemical structure of SLMP53-2. **(B)** IC_{50} values of SLMP53-2, in p53-null H1299 cells transfected with pcDNA3 expressing different mutp53 or empty vector, were determined by SRB assay after 48 h treatment with 3.12-50 μM SLMP53-2; data are mean±SEM (n=5); values significantly different from pcDNA3-Empty: **p*<0.05, one-way ANOVA with Dunnett's multiple comparison test. Mutp53 expression was confirmed by western blot; GAPDH was used as loading control. Immunoblots represent one of three independent experiments.

For in-depth analysis of the molecular mechanism of SLMP53-2, we focused on mutp53-Y220C, known to have a druggable hydrophobic pocket (Boeckler et al., 2008). First, the growth inhibitory effect of SLMP53-2 against HuH-7 and HCC1419 cells endogenously expressing mutp53-Y220C was evaluated by SRB assay. As expected, SLMP53-2 inhibited the growth of both tumor cells with similar IC_{50} values (**Figure 4.2A**), and higher potency than APR-246 (**Figure 4.2B**). Notably, the growth inhibitory activity of SLMP53-2 against non-tumoral HFF-1 cells (IC_{50} of 50 µM) was significantly lower compared to tumor cells (**Figure 4.2A**). In HuH-7 cells, SLMP53-2 displayed a concentration-dependent growth inhibitory effect on colony formation (**Figure 4.2C**). We next assessed whether the growth inhibitory effect of SLMP53-2 in HuH-7 cells was associated with DNA damage. However, unlike the positive control (50 µM etoposide, PC), no induction of H2AX phosphorylation (γH2AX) was detected after 14, 28, or 42 µM SLMP53-2 treatments (**Figure 4.2D**).

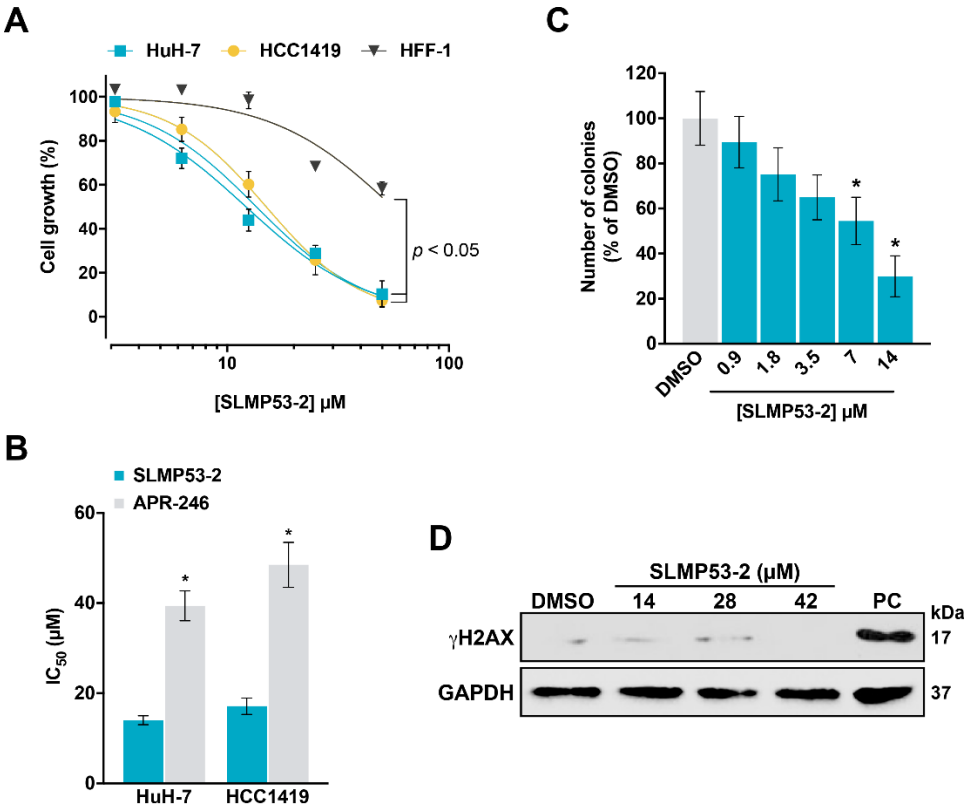

Figure 4.2 SLMP53-2 inhibits the growth of mutp53-Y220C-expressing tumor cells with no genotoxicity. (A) Concentration-response curves for SLMP53-2 in human non-tumoral HFF-1 and tumor mutp53-Y220C-expressing HuH-7 and HCC1419 cells, analyzed by SRB assay after 48 h treatment with 3.12-50 µM SLMP53-2. Data are mean±SEM (n=5); p<0.05, extra sum-of-squares F test. **(B)** IC_{50} values of SLMP53-2 and APR-246 in HuH-7 and HCC1419 cells were determined by SRB assay after 48 h treatment with 3.12-50 µM SLMP53-2 or APR-246. Data are mean±SEM (n=5);

*p<0.05, two-way ANOVA with Sidak's multiple comparison test. **(C)** Effect of SLMP53-2 in HuH-7 cell colony formation, analyzed after 14 days incubation with SLMP53-2. Data are mean±SEM (n=5); values significantly different from DMSO: *p<0.05, one-way ANOVA with Dunnett's multiple comparison test. **(D)** Levels of γH2AX in HuH-7 cells treated with SLMP53-2; 50 μM etoposide was used as a positive control (PC). Immunoblots represent one of three independent experiments; GAPDH was used as a loading control.

A microarray analysis (GEO: GSE124021) indicated that 28 and 42 μM SLMP53-2 led to the differential expression of more than 700 genes (adjusted p value <0.05, $\log_2$ fold change >0.6 and <-0.6) in HuH-7 cells (**Figure 4.3A, B**; **Figure C.2**). Pathway and upstream regulator analyses (Ingenuity Pathway, Metascape and Enrichr) identified signatures consistent with downregulation of cell cycle progression, upregulation of lipid metabolism and cell death, and ER stress induction (**Figure 4.3C-E**; **Figure C.1**; **Figure C.2**). In SLMP53-2-treated HuH-7 cells, *NUPR1*, *TP53* and *ATF4* were among the top scoring upstream regulators inferred from the gene expression dataset. *NUPR1* is an *ATF4* target and can contribute to ER stress responses, cell proliferation and apoptosis (Niessner et al., 2017).

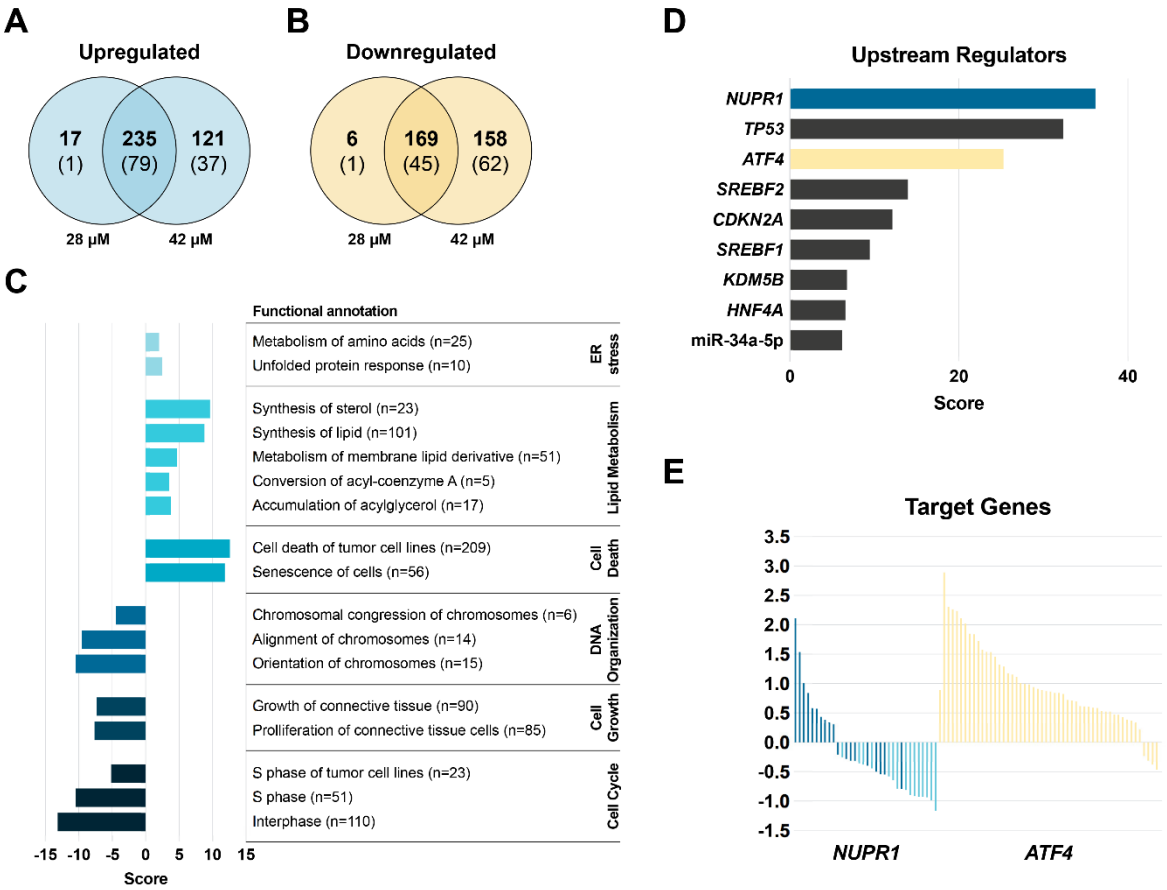

Figure 4.3 SLMP53-2 induces differential expression of genes involved in cell cycle and death, lipid metabolism, and ER stress. (A, B) Venn Diagram presenting the number of DEGs (adj p value <0.05) for 28 or 42 μM SLMP53-2 and the overlap. For upregulated **(A)** and downregulated **(B)** genes

there is a dose dependency on the number of DEGs with a large common core of genes. Besides the *p* value cut-off, a $\log_2$ fold change greater or equal to 0.6 or less than -0.6 was used. Number in parenthesis are relative to a more stringent cut-off ($\log_2$ fold change cut off >1 or <-1). **(C)** Top enriched biological pathways grouped by broad categories based on IPA starting from the dataset of DEGs from HuH-7 cells treated with 28 μM SLMP53-2. The number of features for each functional annotation is given in parenthesis. The score combines the $\log_{10}$ *p*-value and predicted pathway activation or repression status of the corresponding pathway/process, respectively for positive and negative score. The different colours correspond to the different functional annotation categories. **(D)** Top scoring upstream regulators inferred from the same gene expression dataset. The score is the $\log_{10}$ *p*-value of the predicted activation status. **(E)** Gene expression changes of *NUPR1* (blue) and *ATF4* (yellow) target genes in SLMP53-2-treated HuH-7 cells.

Gene expression changes showed that most *ATF4* target genes were upregulated, while the majority of *NUPR1* targets were downregulated (**Figure 4.3E**). This was expected as several *NUPR1* targets are involved in cell cycle and proliferation. Interestingly, downregulated genes were enriched for targets of miR-34a, a well-established p53-inducible microRNA (Raver-Shapira et al., 2007), (**Figure C.2**). Gene expression changes identified by microarray analysis were confirmed by qPCR for selected genes (**Figure C.2**). The gene expression signature had similarities with molecules inducing apoptosis, autophagy or inhibiting the proteasome, based on Connectivity Map (**Figure C.3**). In addition, cytotoxic chemotherapeutics are not present in the top scoring molecules, consistent with the results showing SLMP53-2 is not activating an overt DNA damage response (**Figure 4.2D**).

In accordance with microarray data, 14 and 28 μM SLMP53-2 induced G_0/G_1-phase cell cycle arrest (**Figure 4.4A**) and apoptosis (**Figure 4.4B**), in HuH-7 cells. Moreover, consistently with the induction of an ER stress response, 28 μM SLMP53-2 increased the levels of XBP1 nuclear protein (**Figure 4.4C, D**), spliced XBP1 (sXBP1) mRNA (**Figure 4.4E**), and phosphorylated eIF2α (**Figure 4.4F**).

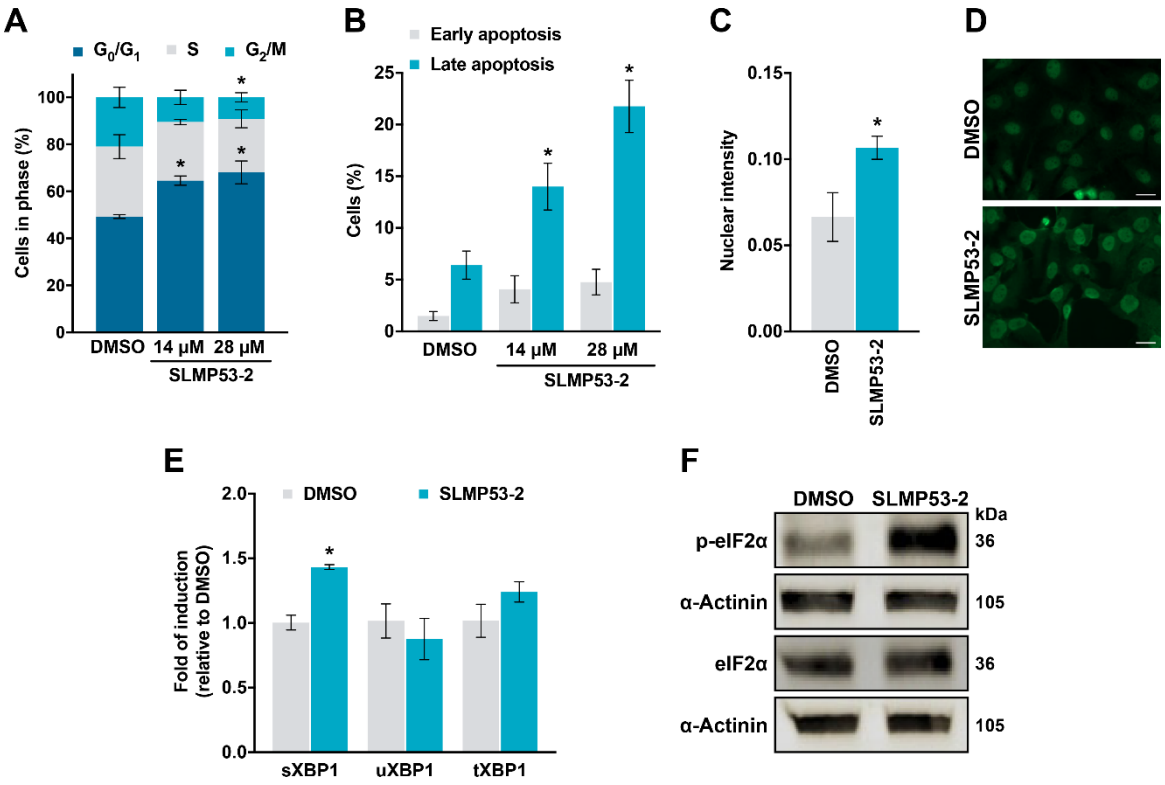

Figure 4.4 Growth inhibitory effect of SLMP53-2 in HCC cells is associated with cell cycle arrest, apoptosis, and ER stress. (A) Effect of SLMP53-2 on cell cycle progression of HuH-7 cells after 48 h treatment. Data are mean±SEM (n=5); values significantly different from DMSO: **p*<0.05, two-way ANOVA with Dunnett's multiple comparison test. **(B)** Effect of SLMP53-2 on apoptosis of HuH-7 cells, after 72 h treatment. Data are mean±SEM (n=5); values significantly different from DMSO: **p*<0.05, one-way ANOVA with Dunnett's multiple comparison test. **(C)** Quantification of nuclear fluorescence intensity of XBP1 in HuH-7 cells after 24 h treatment with 28µM SLMP53-2. Data are mean±SEM (n=3); values significantly different from DMSO: **p*<0.05, unpaired Student's *t*-test. **(D)** Representative images of XBP1 immunofluorescence in HuH-7 cells treated with 28 µM SLMP53-2 or DMSO for 24 h (scale bar = 10 µm). **(E)** mRNA levels of spliced (sXBP1), unspliced (uXBP1), and total (tXBP1) XBP1 in HuH-7 cells after 24 h treatment with 28 µM SLMP53-2, determined by RT-qPCR; fold of induction is relative to DMSO. Data are mean±SEM (n=3); values significantly different from DMSO: **p*<0.05, two-way ANOVA with Dunnett's multiple comparison test. **(F)** Protein levels of phosphorylated and total eIF2α in HuH-7 cells, after 24 h treatment with 28 µM SLMP53-2. Immunoblots represent one of three independent experiments; α-actinin was used as a loading control.

4.1.2. SLMP53-2 restores wt-like conformation and transcriptional activity to mutp53-Y220C in HCC cells

We next evaluated the effect of SLMP53-2 on the expression levels of several p53 target genes. By western blot, it was observed that 14 µM SLMP53-2 increased the protein levels of MDM2, p21, GADD45, BAX, and KILLER, while downregulating survivin and VEGF, an effect abolished in HuH-7 p53KO cells (**Figure 4.5A**). The regulation of p53 target genes by 14 and 28 µM SLMP53-2 in HuH-7 cells was further confirmed at mRNA level with

the upregulation of *BAX*, *GADD45*, *CDKN1A* (p21), and *TNFRSF10B* (KILLER), and the downregulation of *BIRC5* (survivin) (**Figure 4.5B**). Consistently with the microarray analysis, 28 μM SLMP53-2 also upregulated miR-34a in HuH-7, but not in HuH-7-p53KO cells (**Figure 4.5C**). Moreover, 28 μM SLMP53-2 significantly enhanced the expression of p53 target genes involved in the ER stress response, namely *CHOP* and *DDIT4*, and of *TRB3* (a *CHOP* target gene (Ohoka et al., 2005; Liu et al., 2007; Riley et al., 2008)) in HuH-7, but not in HuH-7-p53KO cells (**Figure 4.5D**). The reestablishment of mutp53-Y220C transcriptional activity was further supported by ChIP. In fact, 28 μM SLMP53-2 significantly increased mutp53-Y220C occupancy at the p21 promoter (**Figure 4.5E**), reflecting the restoration of p53 DNA-binding ability.

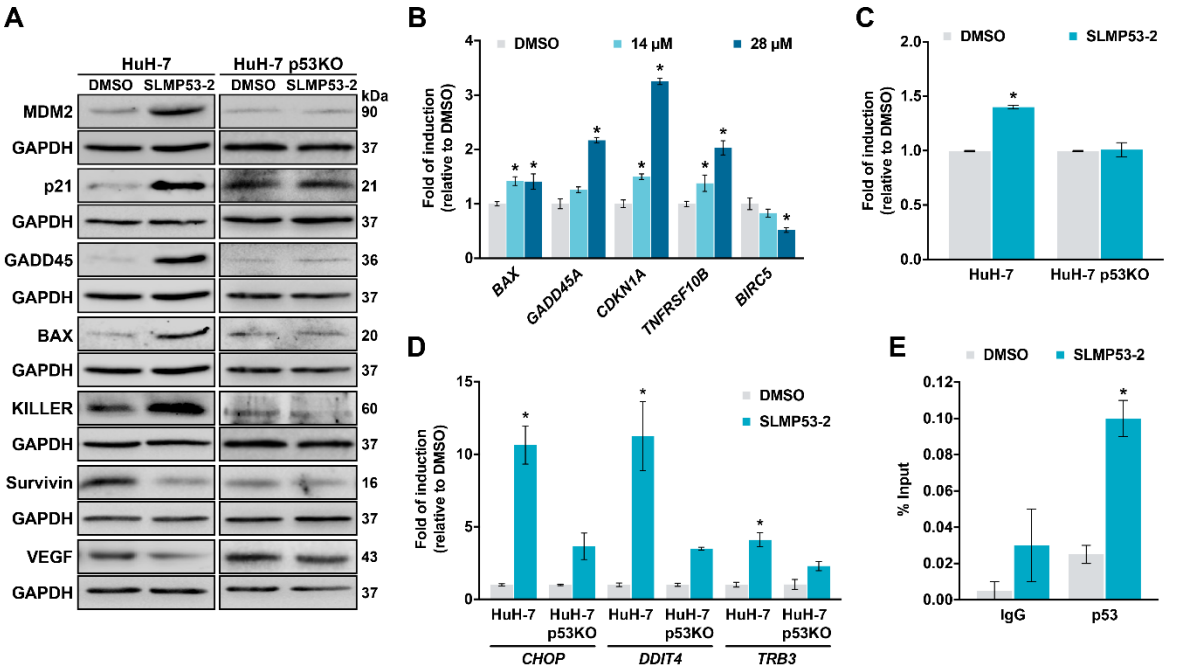

Figure 4.5 SLMP53-2 induces p53 transcriptional targets, including miR-34a and genes involved in ER stress response, and restores DNA-binding ability to mutp53-Y220C in HCC cells. (A) Protein levels of p53 target genes in parental and p53KO HuH-7 cells, after 16 h (p21), 24 h (survivin, VEGF) or 48 h (MDM2, GADD45, BAX, KILLER) treatment with 14 μM SLMP53-2. Immunoblots represent one of three independent experiments; GAPDH was used as a loading control. **(B)** mRNA levels of p53 target genes, in HuH-7 cells, after 24 h treatment with 14 and 28 μM SLMP53-2, determined by RT-qPCR; fold of induction is relative to DMSO. **(C)** miR-34a levels in parental and p53KO HuH-7 cells, after 24 h treatment with 28 μM SLMP53-2, determined by RT-qPCR; fold of induction is relative to DMSO. **(D)** mRNA levels of genes involved in the ER stress response, in parental and p53KO HuH-7 cells, after 24 h treatment with 28 μM SLMP53-2, determined by RT-qPCR; fold of induction is relative to DMSO. **(E)** Analysis of the occupancy of mutp53-Y220C on the p21 promoter in HuH-7 cells, determined by ChIP, after 24 h treatment with 28 μM SLMP53-2 or DMSO; immunoprecipitation was performed with an anti-p53 antibody (p53) or an anti-mouse IgG as a negative control (IgG); the enrichment of DNA fragments was analysed by RT-qPCR using site-specific primers. In **B-E**, data are mean±SEM (n=3); values significantly different from DMSO (B-E): **p*<0.05, two-way ANOVA with Dunnett's **(B, E)** or Sidak's **(D)** multiple comparison test; **p*<0.05, unpaired Student's *t*-test **(C)**.

As a structural mutp53, we investigated the ability of SLMP53-2 to restore wt-like folding to mutp53-Y220C, through IP using PAb1620 (wt/folded) and PAb240 (mut/unfolded) conformation-specific antibodies. The results showed that 28 and 42 μM SLMP53-2 visibly increased the amount of p53 precipitated with PAb1620, while decreasing the amount of p53 precipitated with PAb240 (**Figure 4.6A**). Consistently, SLMP53-2 visibly increased PAb1620 and decreased PAb240 immunofluorescence staining in HuH-7 cells (**Figure 4.6B**).

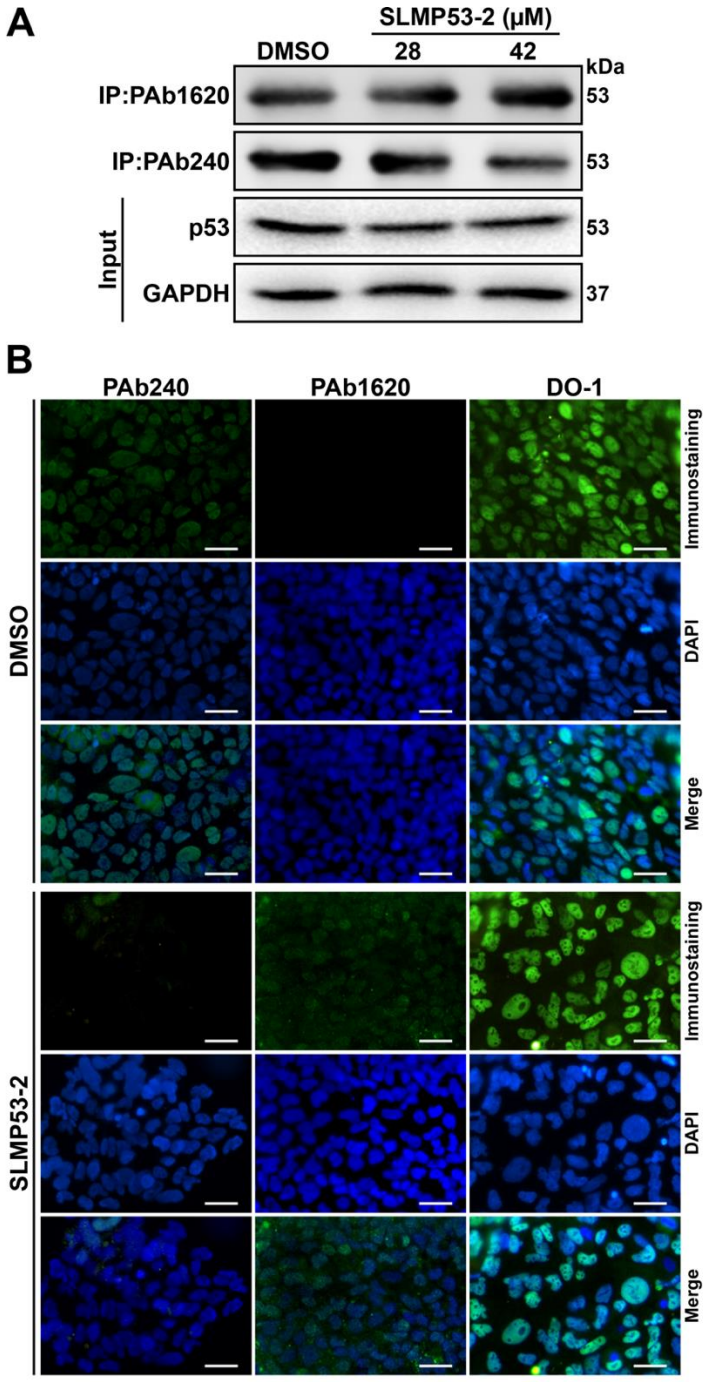

Figure 4.6 SLMP53-2 restores wt-like folding to mutp53 Y220C. (A) Immunoprecipitation of p53 in HuH-7 cells treated with 28 and 42 μM SLMP53-2 for 36 h, using the conformation-specific

antibodies PAb240 (mut/unfolded) and PAb1620 (wt/folded), followed by immunoblotting with anti-p53 antibody (DO-1); whole cell lysate (input). Immunoblots represent one of three independent experiments; GAPDH was used as a loading control. **(B)** Representative images of p53 immunofluorescence staining of HuH-7 cells treated with 42 µM SLMP53-2 or DMSO for 36 h. Cells were labelled with conformation-specific antibodies PAb240 (unfolded/mutant) and PAb1620 (folded/wild-type), or with DO-1 (total p53) (scale bar = 20 µm).

4.1.3. Hsp70 is a potential mediator of mutp53-Y220C reactivation by SLMP53-2

To determine the mechanism by which SLMP53-2 would affect mutp53-Y220C function, we checked whether SLMP53-2 could bind to this mutp53. To this end, the recombinant human mutp53-Y220C DBD was produced and purified from *Escherichia coli* and used to carry out the HSQC-NMR experiments. However, despite the presence of a druggable hydrophobic pocket in mutp53-Y220C, no binding of SLMP53-2 to recombinant mutp53-Y220C DBD was detected (**Figure 4.7**).

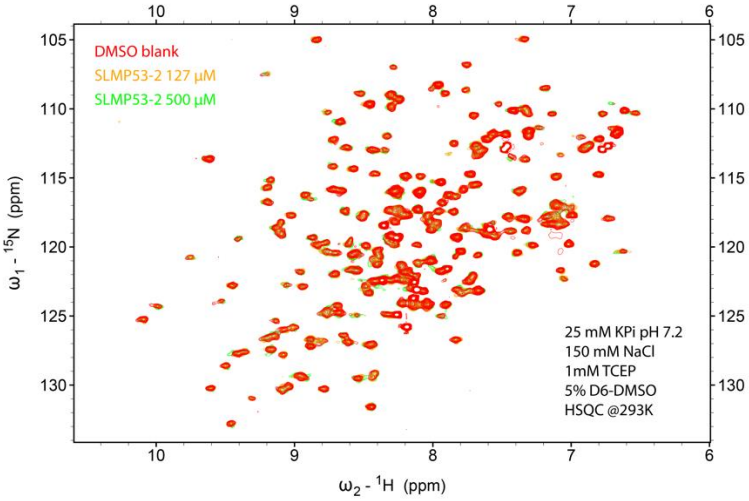

Figure 4.7 Overlay of $^{1}H/^{15}N$-HSQC NMR spectra of T-p53C-Y220C with varying concentrations of SLMP53-2, showing no significant chemical shift.

Chaperones from the Hsp40, Hsp70, and Hsp90 families have long been recognized as mutp53-binding partners capable of folding mutp53 to the wt-like conformation (Hainaut and Milner, 1992; Walerych et al., 2009; Wawrzynow et al., 2018). Therefore, we interrogated whether SLMP53-2 could reactivate mutp53-Y220C by promoting its interaction with these chaperones. To investigate potential interactions between mutp53-Y220C and Hsp40/Hsp70/Hsp90, co-IP experiments were performed in HuH-7 cells.

Conversely to that observed with Hsp40 and Hsp90, 28 and 42 μM SLMP53-2 visibly increased the amount of Hsp70 precipitated with p53 (**Figure 4.8A**), indicating an enhancement of Hsp70 binding to p53. This was further supported by IP of p53 with the mutp53-conformation-specific PAb240 antibody, showing the increased interaction between Hsp70 and mutp53-Y220C (**Figure 4.8B**). Moreover, in Hsp70 siRNA silenced HuH-7 cells (**Figure 4.8C**), the inhibitory effect of SLMP53-2 on colony formation was significantly reduced (**Figure 4.8D**). Therefore, SLMP53-2 may restore wt-like conformation to mutp53-Y220C through enhancement of its interaction with Hsp70.

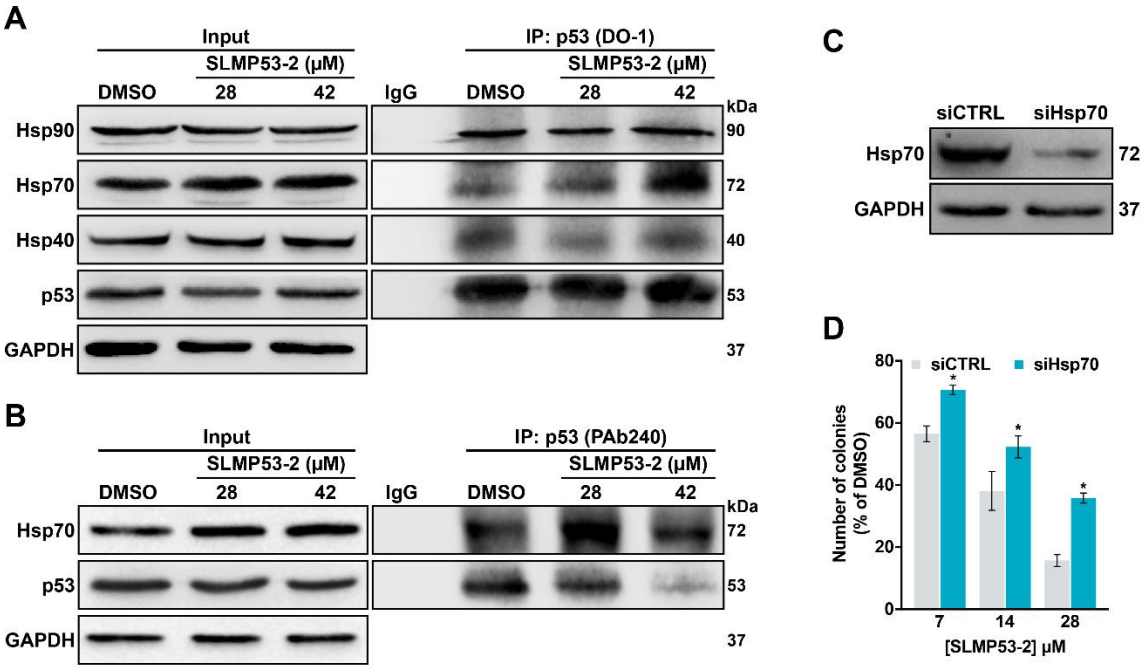

Figure 4.8 SLMP53-2 promotes mutp53-Y220C interaction with Hsp70. (A) Co-immunoprecipitation of Hsp40, Hsp70, and Hsp90 with p53 in HuH-7 cells treated with 28 and 42 μM SLMP53-2 or DMSO for 36 h, using anti-p53 antibody (DO-1), followed by immunoblotting with anti-Hsp40, anti-Hsp70, anti-Hsp90, and anti-p53 antibodies. **(B)** Co-immunoprecipitation of Hsp70 with p53 in HuH-7 cells treated with 28 and 42 μM SLMP53-2 or DMSO for 36 h, using anti-p53 antibody (Pab240), followed by immunoblotting with anti-Hsp70 and anti-p53 antibodies. **(C)** Western blot analysis of Hsp70 protein levels in HuH7 cells transfected with siRNA against Hsp70 (siHsp70) or control siRNA (siCTRL). **(D)** Effect of SLMP53-2 in the cell colony formation of HuH-7 cells transfected with siHsp70 or siCTRL, analyzed after 14 days incubation with SLMP53-2; data are mean±SEM (n=5); values significantly different from siCTRL: **p*<0.05, one-way ANOVA with Dunnett's multiple comparison test. In **A-C**, immunoblots represent one of three independent experiments; whole cell lysate (input); GAPDH was used as a loading control.

4.1.4.SLMP53-2 sensitizes HCC cells to sorafenib

A potential synergistic association between SLMP53-2 and sorafenib was assessed by SRB assay, in HuH-7 cells. When combined with 1.5 µM SLMP53-2, sorafenib displayed significantly higher growth inhibitory effect compared to its effect as a single agent (**Figure 4.9A**). Consistently, a synergistic effect (CI<1) was obtained for all tested sorafenib concentrations in combination with 1.5 µM SLMP53-2 (**Figure 4.9B**).

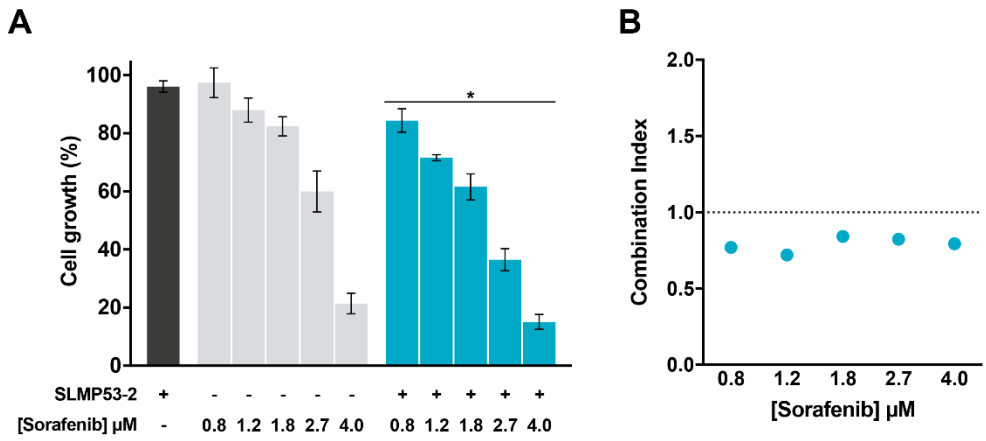

Figure 4.9 SLMP53-2 synergizes with sorafenib in HCC cells. HuH-7 cells were treated with increasing concentrations of sorafenib, alone and in combination with 1.5 µM SLMP53-2. **(A)** Cell growth was measured by SRB assay after 48 h treatment; data are mean±SEM (n=4); values significantly different from chemotherapeutic alone: *p<0.05, two-way ANOVA. **(B)** Combination index (CI) values calculated using the CompuSyn software for each combined treatment. CI<1, synergy; 1<CI<1.1, additive effect; CI>1.1, antagonism. CI values were calculated using a mean value effect (n=4).

4.1.5.SLMP53-2 displays *in vivo* anti-tumor activity in HCC xenograft mouse models, with no apparent toxic side effects

The toxicity profile of SLMP53-2 was evaluated in rats subjected to five intraperitoneal administrations of 50 mg/kg SLMP53-2 or vehicle, followed by analysis of hematological and biochemical parameters from blood samples (**Table 4.1**). Although a slight reduction of the red cell distribution width and mean platelet volume was observed upon SLMP53-2 treatment, these values were within the reference range (Giknis and Clifford, 2008). Therefore, no undesirable hematological and biochemical toxicity was induced by SLMP53-2 *in vivo*.

Table 4.1 Biochemical and hematological data of SLMP53-2 in Wistar rats.

	Control	Treated
Biochemical data		
Blood glucose (mg/dL)	165.83 ± 8.91	193.33 ± 19.63
Urea (mg/dL)	18.38 ± 0.45	19.07 ± 0.62
Creatinine (mg/dL)	0.32 ± 0.01	0.32 ± 0.01
Uric Acid (mg/dL)	2.8 ± 0.33	1.9 ± 0.15
Total protein (g/dL)	6.68 ± 0.24	6.43 ± 0.03
Albumin (g/dL)	3.25 ± 0.08	3.4 ± 0.06
Sodium (mmol/L)	146.83 ± 0.83	148.33 ± 1.33
Potassium (mmol/L)	5.98 ± 0.23	5.83 ± 0.67
Osmolality (mOSM/Kg)	296.6 ± 1.97	302.67 ± 1.76
Phosphorous (mg/dL)	7.83 ± 0.47	8.43 ± 0.17
ALT (U/L)	38.67 ± 2.5	34.33 ± 3.84
AST (U/L)	73.83 ± 8.68	67.67 ± 5.46
Total cholesterol (mg/dL)	65.33 ± 7.44	68.67 ± 2.96
Cholesterol-HDL (mg/dL)	42.33 ± 4.78	44 ± 2.08
Cholesterol-LDL (mg/dL)	20.83 ± 2.79	19.67 ± 1.45
Triglycerides (mg/dL)	153.33 ± 27.72	183 ± 10.07
Atherogenic index	1.53 ± 0.04	1.57 ± 0.03
Hematological data		
WBC ($\times 10^3$/µL)	1.78 ± 0.42	2.33 ± 0.87
RBC ($\times 10^6$/µL)	8.5 ± 0.32	8.14 ± 0.49
HGB (g/dL)	14.72 ± 0.55	14.9 ± 0.15
HCT (%)	44.07 ± 1.69	44.7 ± 0.61
MCV (fL)	51.85 ± 0.58	55.23 ± 3.47
MCH (pg)	17.3 ± 0.21	18.4 ± 1.11
MCHC (g/dL)	33.38 ± 0.3	33.33 ± 0.15
RDW (%)	14.73 ± 0.31	13.3 ± 0.55*
PLT ($\times 10^3$/µL)	552.98 ± 152.92	781.67 ± 29.04
MPV (fL)	7.92 ± 0.02	6.23 ± 0.83*
RET (%)	3.09 ± 0.31	3.66 ± 0.16
IRF	0.7 ± 0.03	0.71 ± 0.01
Lymphocytes (%)	77.3 ± 1.03	81 ± 3.91
Lymphocytes ($\times 10^3$/µL))	1.4 ± 0.32	1.83 ± 0.61

Data from blood samples were analysed for saline (control), and 50mg/kg SLMP53-2 (treated) rat groups, after five intraperitoneal administrations (twice a week). Results are shown as mean±SEM (n=5; values significantly different from control: *p<0.05; unpaired Student's t-test). ALT, alanine aminotransferase; AST, aspartate aminotransferase; HCT, hematocrit; HGB, Hemoglobin concentration; IRF, immature reticulocyte fraction; MCH, mean corpuscular hemoglobin; MCHC, mean corpuscular hemoglobin concentration; MCV, mean corpuscular volume; MPV, mean platelet volume; PLT, platelet; RBC, red blood cell count; RDW, red cell distribution width; RET, reticulocytes; WBC, white blood cells.

To evaluate the *in vivo* anti-tumor activity of SLMP53-2, five intraperitoneal administrations of 50 mg/kg SLMP53-2 or vehicle were performed in nude mice carrying HuH-7 xenografts. A pronounced reduction of tumor volume (**Figure 4.10A**) and weight (**Figure 4.10B**) was observed in SLMP53-2-treated mice compared to vehicle. Moreover, nude mice showed no significant variation of body weight throughout the experiment (**Figure 4.10C**), and no significant differences were observed between the weight of spleen, liver, heart, and kidneys of SLMP53-2-treated mice and vehicle (**Figure 4.10D**). These results further supported a favorable therapeutic index of SLMP53-2 *in vivo*.

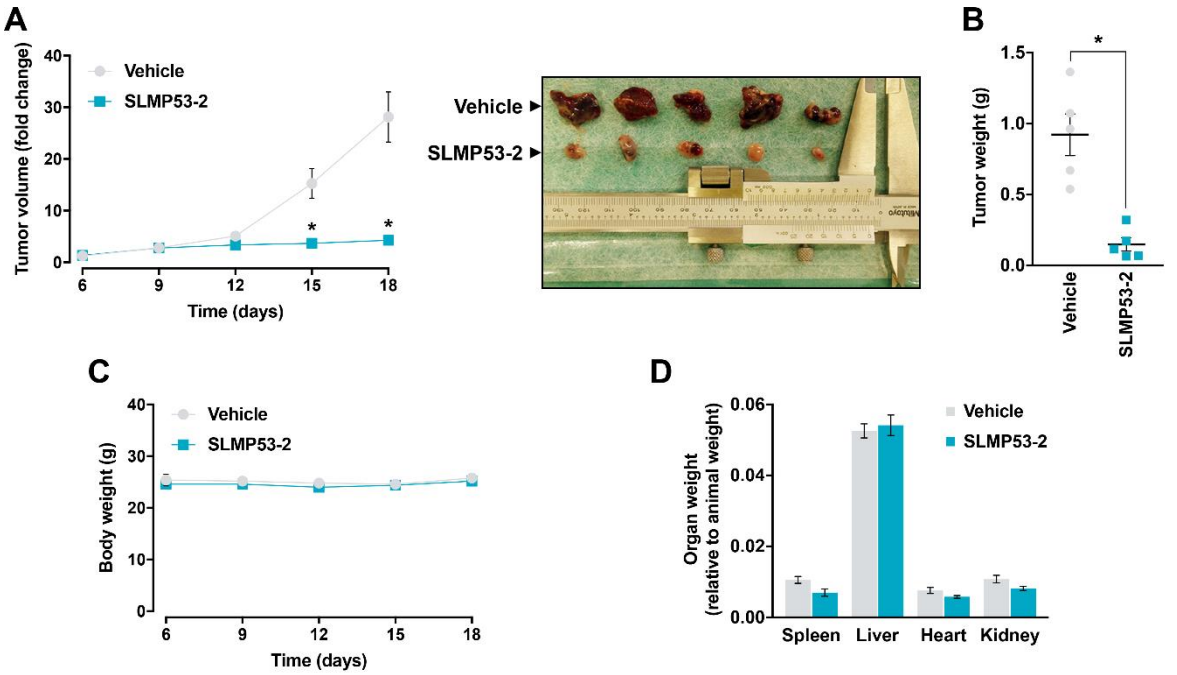

Figure 4.10 *In vivo* anti-tumor activity of SLMP53-2. Swiss nude mice carrying HuH-7 xenografts were treated with 50 mg/kg SLMP53-2 or vehicle, by intraperitoneal injection twice a week, for a total of five administrations. (A) Tumor volume curves of mice carrying HuH-7 xenografts treated with SLMP53-2 or vehicle; image of vehicle and SLMP53-2-treated tumors; values significantly different from vehicle: **p*<0.05, two-way ANOVA with Sidak's multiple comparison test. **(B)** Tumor weights measured at the end of the experiment; value significantly different from vehicle: **p*<0.05, unpaired Student's *t*-test. **(C)** Mice body weight during treatment with SLMP53-2 or vehicle. **(D)** Weight of spleen, liver, heart and kidneys, relative to animal weight, in animals treated with SLMP53-2 or vehicle. In **A-D** data are mean±SEM (n=5). In **C** and **D**, values not significantly different from vehicle: *p*>0.05, two-way ANOVA with Sidak's multiple comparison test.

Additionally, the IHC staining of tumor sections revealed that SLMP53-2 decreased Ki-67 and VEGF, and increased BAX staining (**Figure 4.11A-C**), compared to vehicle. Altogether, these results unveiled a potent *in vivo* anti-tumor activity of SLMP53-2 through induction of apoptosis and inhibition of cell proliferation and angiogenesis.

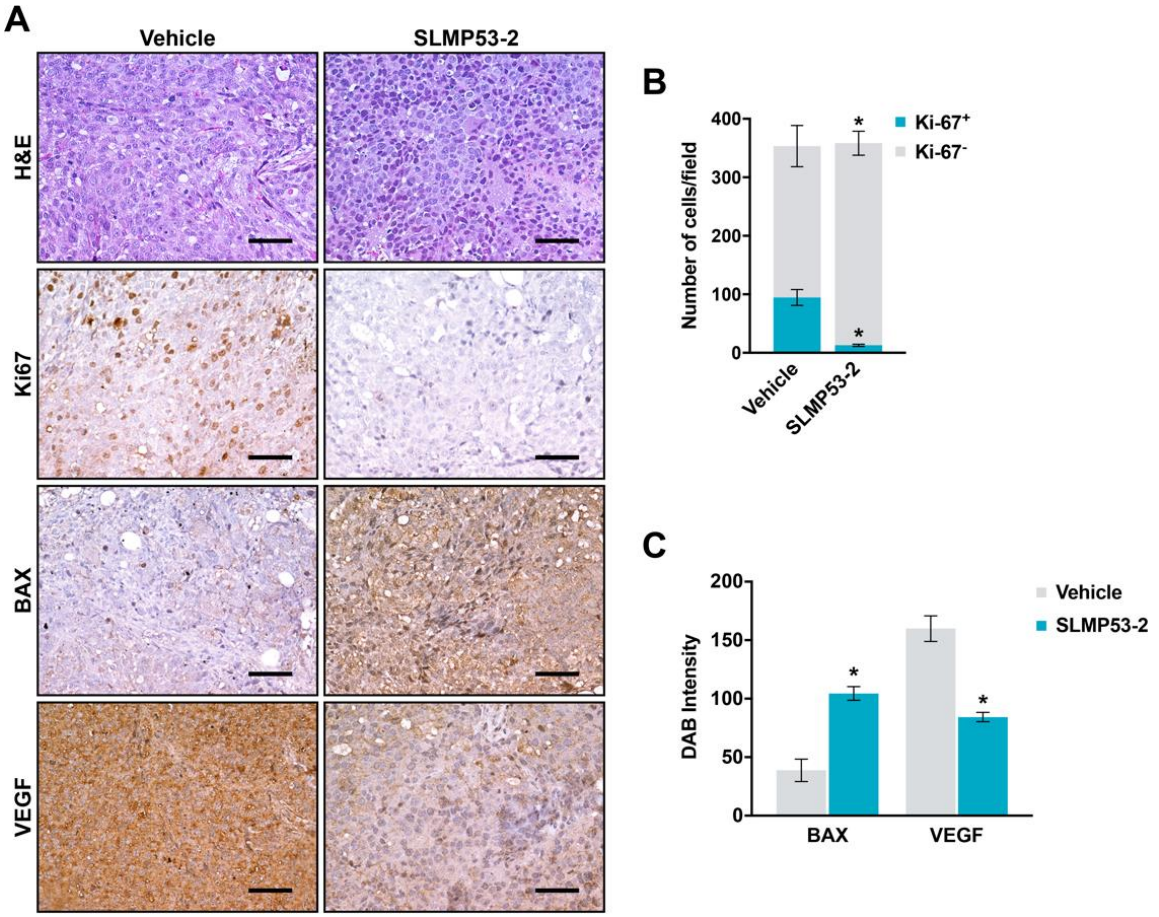

Figure 4.11 Immunohistochemical analysis of xenograft tumor tissue. (A) Representative images of Ki-67, BAX, and VEGF detection in tumor tissues of HuH-7 xenografts treated with SLMP53-2 or vehicle, collected at the end of treatment (scale bar = 20 μm; magnification = 200×); hematoxylin and eosin (H&E). **(B, C**) Quantification of immunohistochemistry of HuH-7 xenograft tumor tissues treated with SLMP53-2 or vehicle; in **B**, quantification of the number of Ki-67 positive and negative cells (n=5); values significantly different from vehicle: **p*<0.05, two-way ANOVA with Sidak's multiple comparison test; in **C**, BAX and VEGF staining were quantified by evaluation of DAB intensity (n=5); values significantly different from vehicle: **p*<0.05, unpaired Student's *t*-test.

4.2. Discussion

In this chapter, the identification of SLMP53-2 as a novel reactivator of structural mutp53 is reported. Interestingly, unlike SLMP53-1 (Soares et al., 2016), SLMP53-2 did not significantly interfere with the activity of contact mutp53-R280K. In fact, the results evidenced the selectivity of SLMP53-2 to reactivate multiple structural mutp53. SLMP53-2 shows p53-dependent growth inhibitory effect on human tumor cells through induction of cell cycle arrest and apoptosis. In addition, it stimulates the ER stress response by inducing the expression of several ER stress markers, including the p53 target gene *CHOP*, which triggers ER stress-related cell death (Kim et al., 2008). ER stress occurs when the tightly-regulated protein folding environment of the ER is disrupted, causing accumulation of unfolded proteins. This triggers the UPR, a mechanism intended to re-establish ER homeostasis. When the UPR fails to restore ER homeostasis, cell death is triggered (Kim et al., 2008). In fact, ER stress exacerbation for cell death induction has been proposed as a relevant anticancer therapeutic strategy, specifically against HCC (Gorrini et al., 2013).

Herein, SLMP53-2 is also shown to restore wt-like folding and DNA-binding ability to mutp53-Y220C. In fact, SLMP53-2 reactivates p53 transcriptional activity, regulating the expression of several p53 transcriptional targets involved in cell cycle arrest (p21, GADD45), apoptosis (BAX, KILLER, survivin), ER stress response (CHOP, DDIT4), and angiogenesis (VEGF). Interestingly, SLMP53-2 causes p53-dependent reduction of the expression levels of survivin, which is frequently overexpressed in HCC, correlating with increased invasion and metastasis, and decreased overall and relapse-free survival (Liu et al., 2013a; Jin et al., 2014; Su, 2016). Additionally, SLMP53-2 upregulates miR-34a, a p53 transcriptional target. Consistently, the microarray data revealed that SLMP53-2 leads to downregulation of several miR-34a targets. miR-34a is a crucial tumor suppressor that controls cellular processes including proliferation, apoptosis, senescence, and stemness (Slabakova et al., 2017). This is of particular interest in HCC, in which miR-34a downregulation is commonly associated with invasion and metastasis (Li et al., 2009). Consistently, MRX34, a liposomal miR-34a mimic, has displayed promising anti-tumor activity in orthotopic HCC models (Daige et al., 2014), having recently completed phase I clinical trials for advanced solid tumors, including HCC (Beg et al., 2017).

Despite its inability to bind to mutp53-Y220C, SLMP53-2 enhances the mutp53-Y220C interaction with chaperone Hsp70, known to bind to mutp53, leading to its refolding and protein stabilization, with subsequent restoration of DNA-binding and transcriptional activity (Hainaut and Milner, 1992; Walerych et al., 2009; Wawrzynow et al., 2018). A similar mutp53 reactivation mechanism was recently reported for CTM, which restores wt-like function to mutp53-R175H by enhancing its interaction with Hsp40 (Hiraki et al., 2015).

Interestingly, the requirement of Hsp70 for mutp53-R175H stabilization, and its contribution to the pancreatic cells malignant transformation have been recently reported (Polireddy et al., 2019). However, these results were obtained in non-tumoral cells, which might justify the distinct observations made in the current work.

Considering the relevance of mutp53 in the HCC pathogenesis and the lack of therapeutic alternatives (Bevant and Coulouarn, 2017), this work also paves the way to a potential application of SLMP53-2 (alone or in combination therapy) in HCC treatment. It is worth to note that SLMP53-2 also shows antitumor activity against wtp53-expressing HCC cells, namely HepG2 cells (IC_{50} of 12.5±0.8 μM). This is consistent with the proposed mechanism of action of SLMP53-2, since the stabilization of wtp53 by Hsp70 has also been reported (Walerych et al., 2009). Moreover, besides its growth inhibitory activity against HCC cells [superior to that of APR-246, currently in phase Ib/II clinical trials (Bykov et al., 2018)], SLMP53-2 also sensitizes HCC cells to sorafenib, the only drug currently approved for the treatment of advanced HCC (Lin et al., 2012a; Vogel et al., 2018). Importantly, in the HCC xenograft mouse model, SLMP53-2 displays pronounced antitumor activity associated with induction of apoptosis and inhibition of cell proliferation and angiogenesis. Interestingly, the crucial role of angiogenesis in HCC development and dissemination has been widely explored for the development of targeted therapies (Raoul et al., 2017). In fact, antiangiogenic agents, like sorafenib, have been the only effective targeted drugs in clinical trials for HCC (Raoul et al., 2017). Notably, SLMP53-2 also displays a favorable toxicological profile *in vivo*, with no significant alteration of toxicological parameters related to liver function. This is of particular importance in HCC, as patients often display liver cirrhosis that can lead to impaired liver function and consequently increased drug toxicity (Kudo, 2017).

As a whole, this work unveils SLMP53-2 as a new mutp53 reactivator with great potential as an anticancer drug, particularly in HCC treatment, or as astarting material for the development of improved anticancer mutp53-targeting therapeutic alternatives.

Chapter 5. General discussion and future perspectives

It is widely accepted that the development of new targeted anticancer drugs is of the utmost importance in personalized cancer treatment. The majority of conventional chemotherapeutic drugs target rapidly dividing cells by interfering with cell cycle or DNA synthesis. While tumor cells display increased susceptibility towards these chemotherapeutic agents, rapidly dividing normal cells are also affected, justifying the frequent severe side effects experienced by patients subjected to these therapeutic approaches (Baudino, 2015). In contrast, targeted anticancer agents interfere with proteins or pathways that are specifically altered in tumors, minimizing the effect on normal cells, and consequently, their adverse side effects (Baudino, 2015). This is the basis of personalized cancer treatment, through which each patient would be treated with targeted agents suited to the particular molecular and genetic features of their tumor, maximizing antitumor response while limiting undesirable toxicity (Huang et al., 2014). In this context, p53 family proteins arise as highly attractive therapeutic targets. In fact, the therapeutic targeting of p53 family proteins produces antitumor effects through interference with multiple hallmarks of cancer. In addition, p53 family proteins are often inactivated in human cancers, either by mutation, or by overexpression of negative regulators. Since these cellular alterations are highly specific of tumor cells, p53 family-targeting agents are expected to display selective growth inhibitory activity towards cancer cells, with limited undesirable effects on non-tumoral cells. It is also important to note that many of the chemotherapeutics currently available for cancer treatment rely on the presence of a functional p53-pathway to elicit antitumor response. Considering this, p53 family-activating drugs are expected to be valuable in combination therapy, by sensitizing p53-impaired tumors to currently available chemotherapeutic drugs.

Based on the exposed above, the present thesis focused on the identification of small molecules with antitumor activity in p53-impaired tumors, by targeting TAp73 and mutp53 (**Figure 5.1**).

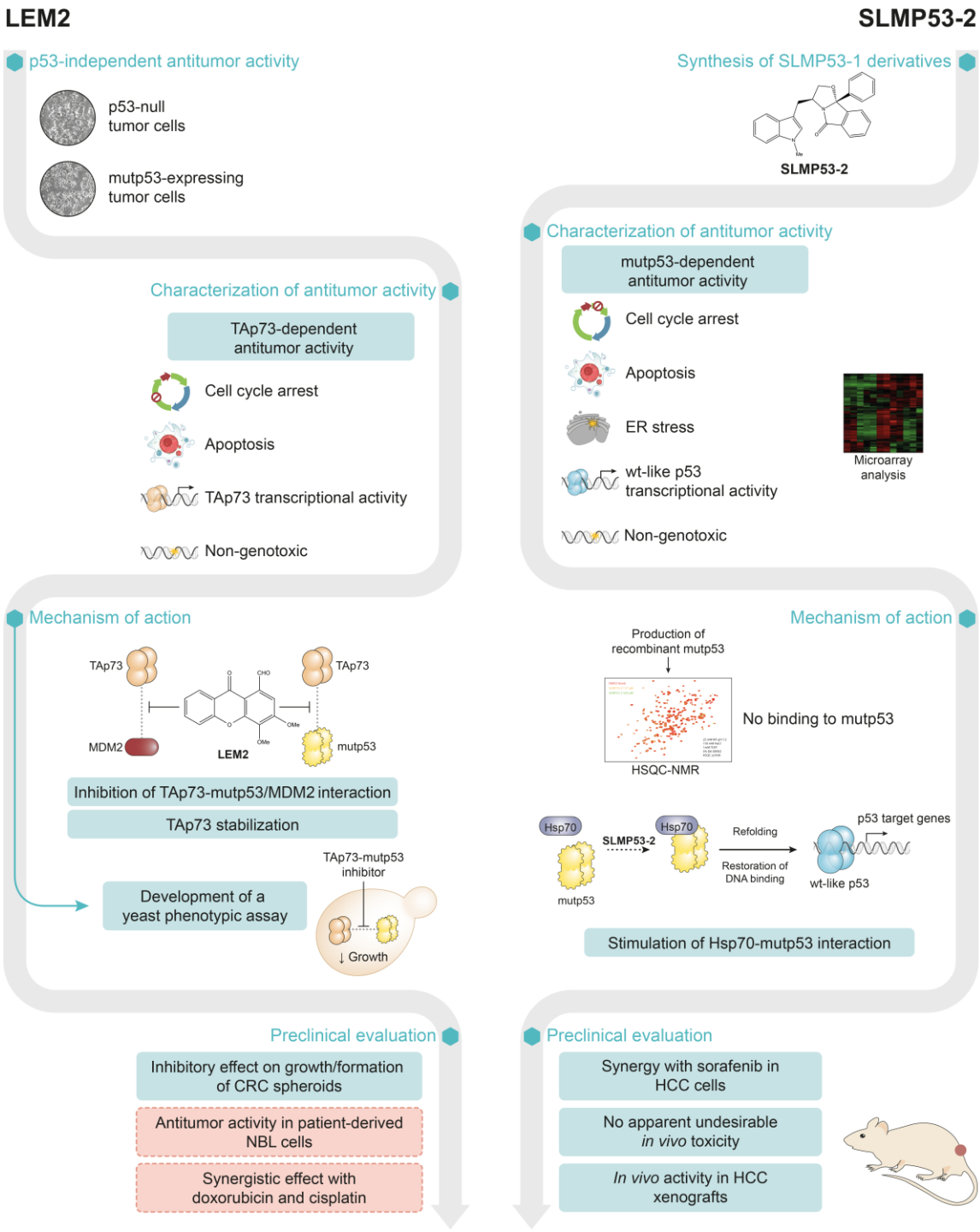

Figure 5.1 Schematic representation of the major outcomes achieved in the present thesis. (Chapter 3) LEM2 displays p53-independent antitumor activity in both p53-null and mutp53-expressing cells. The growth inhibitory effect of LEM2 is TAp73-dependent, and associated with cell cycle arrest, apoptosis, and induction of TAp73 target genes, but not with genotoxicity. LEM2 is an activator of TAp73 through disruption of its interaction with MDM2 and mutp53, and TAp73 stabilization. A new yeast phenotypic assay to search for inhibitors of the TAp73-mutp53 interaction was developped. The potential application of LEM2 for colorectal cancer (CRC) and neuroblatoma (NBL) treatment was evidenced. **(Chapter 4)** SLMP53-2 was selected from a small library of synthetized SLMP53-1 derivatives, based on its mutp53-dependent growth inhibitory effect. The antitumor activity of SLMP53-2 in mutp53-expressing cells was studied, and molecular pathways

altered by SLMP53-2 were assessed by microarray analysis. SLMP53-2 growth inhibitory effect is associated with cell cycle arrest, apoptosis, ER stress, and regulation of wtp53 target genes, but not with genotoxicity. SLMP53 does not bind to mutp53, instead promoting its interaction with Hsp70, which results in refolding and re-estabishment of wt-like DNA binding. The potential of SLMP53-2 for clinical application, in particular for HCC treatment, was evidenced; SLMP53-2 sensitizes HCC cells to sorafenib, and displays *in vivo* antitumor activity with no apparent undesirable toxicity.

The work developed in **Chapter 3** allowed the identification of 1-carbaldehyde-3,4-dimethoxyxanthone (LEM2) as a new activator of TAp73, through inhibition of its interaction with both MDM2 and mutp53. This compound enhances TAp73 transcriptional activity, triggering cell cycle arrest and apoptosis in both p53-null and mutp53-expressing tumor cells. It is important to note that another relevant outcome arising from this work was the development of a new yeast phenotypic assay that mimics the GOF of mutp53 through its inhibitory effect on TAp73. In fact, this work supports the suitability of the yeast model to screen for small molecule inhibitors of the TAp73-mutp53 interaction. While the present work focused on mutp53-R273H, this assay may be easily extended to other mutp53 forms. Notably, a remarkable antitumor activity of LEM2 against patient-derived neuroblastoma cells, consistent with the activation of a TAp73 pathway was demonstrated in a work complementary to this thesis (Gomes et al., 2019b). In fact, TAp73 has been proposed as a promising therapeutic target in neuroblastoma (Wolter et al., 2010). In these tumors, p53 is often sequestered in the cytoplasm, and therefore inactivated, while TAp73 retains normal nuclear location, allowing it to execute normal transcriptional functions (Nikolaev et al., 2003). Despite this, MDM2 amplification has been reported in neuroblastoma (Slack et al., 2005), constituting one of the mechanisms of TAp73 inactivation in this type of cancer. In addition, while p53 mutations are rare in primary neuroblastoma (Vogan et al., 1993), they have been observed in relapsed tumors, and are thought to occur as a mechanism of therapeutic resistance (Carr et al., 2006). Considering this, the ability of LEM2 to release TAp73 from inhibitory interactions with both MDM2 and mutp53 arises as a promising strategy against neuroblastoma. Furthermore, besides compensating for the lack of a functional p53 pathway, TAp73 has been reported to induce p53 nuclear translocation and downregulate N-myc in neuroblastoma (Goldschneider et al., 2004; Horvilleur et al., 2008). Importantly, the ability of LEM2 to sensitize patient-derived neuroblastoma cells to doxorubicin and cisplatin was also shown (Gomes et al., 2019b), which is of particular relevance in neuroblastoma treatment. Both doxorubicin and cisplatin are included in chemotherapy regimens for neuroblastoma therapy, with significant toxic side effects and high relapse rates. Interestingly, both these molecules have been reported to downregulate ΔNp73, which is frequently overexpressed in neuroblastoma, leading to TAp73 inactivation. Therefore, the synergistic association observed between LEM2 and cisplatin/doxorubicin

may be due to the downregulation of distinct negative regulators of TAp73. As a whole, besides its potential as an anticancer drug, LEM2 may also be a promising starting point for the development of improved TAp73-activating agents for anticancer therapy, particularly against neuroblastoma.

The work developed in **Chapter 4** led to the identification of the tryptophanol-derived oxazoloisoindolinone SLMP53-2 as a new mutp53-reactivating compound. SLMP53-2 induces cell cycle arrest, apoptosis, and ER stress in mutp53-expressing HCC cells. ER stress inducing compounds have been reported as potential anticancer agents. Particularly, the prodrug of thapsigargin, mipsagargin (a known ER stress inducer through interference with ER calcium levels) was tested in patients with solid tumors, including HCC (Mahalingam et al., 2016). Moreover, zebularine (a DNA methyltransferase inhibitor) has been reported to induce p53-dependent ER stress-mediated cell death in colorectal cancer (Yang et al., 2013). Interestingly, the mutp53 reactivators APR-246 and PK11007 have also been reported to induce ER stress-mediated cell death in mutp53-expressing tumor cells (Lambert et al., 2009b; Bauer et al., 2016). Furthermore, SLMP53-2 restores wt-like conformation and transcriptional activity to mutp53-Y220C, through enhancement of its interaction with the chaperone Hsp70. This work also highlighted the antitumor potential of SLMP53-2 against HCC, for which therapeutic alternatives are insufficient. HCC, the most common histologic type of primary liver cancer, is associated with unfavorable prognosis, mainly due to high chemoresistance and recurrence rates (Lin et al., 2012a; Vogel et al., 2018). The majority of patients are diagnosed at advanced- or terminal-stage, and available therapeutic options are restricted to symptomatic treatment (for terminal HCC) or sorafenib, a multi-target kinase inhibitor (Lin et al., 2012a; Vogel et al., 2018) (for advanced-stage HCC). Nonetheless, the increase of median overall survival of HCC patients treated with sorafenib is only 2.8 months (Vogel et al., 2018), making the identification of effective therapeutic alternatives a high priority. About 30% of HCC harbor p53 mutations, correlating with increased invasiveness, recurrence, and lower survival rates (Bevant and Coulouarn, 2017). This makes mutp53 a privileged therapeutic target in HCC. Consistently, SLMP53-2 sensitizes HCC cells to sorafenib. Most importantly, SLMP53-2 demonstrates potent *in vivo* antitumor activity in a human HCC xenograft mouse model. As a whole, SLMP53-2 represents a new mutp53-reactivating agent with a mechanism of action different from those reported to date. It may also represent a new effective anticancer therapeutic option, particularly against HCC, or it may be the basis for new derivatives with increased efficacy.

In conclusion, the work developed under the scope of this thesis provides a significant contribution to p53 family pharmacology and personalized cancer treatment, with the identification of new TAp73- and mutp53-activating agents and with promising anticancer properties.

In spite of the potential of LEM2 and SLMP53-2 as anticancer drug candidates, further research will be relevant to their successful translation to a clinical setting. In particular, although the mechanism of action of both compounds has been deeply explored in this thesis, it would be important to validate the molecular target to which the compounds bind to exert their antitumor effects. In fact, the characterization of the binding mode to their molecular targets would enable the rational design of SLMP53-2 and LEM2 derivatives with improved antitumor activity and selectivity towards tumor cells. In addition, considering the wide diversity of *TP53* mutations in human tumors, it would be relevant to study the impact of both SLMP53-2 and LEM2 on tumor cells expressing mutp53 forms beyond those addressed in this thesis. In fact, since both compounds interfere with mutp53-interacting proteins, it is plausible that they may target tumor cells expressing different forms of mutp53. This is of particular interest considering the concept of tumor heterogeneity, based on which the same tumor may express more than one mutp53 form. Taking this into consideration, it would also be valuable to assess the antitumor activity of SLMP53-2 against more physiologically-relevant model systems that account for tumor heterogeneity, namely in patient-derived xenograft (PDX) models. Regarding LEM2, despite its promising effect on patient-derived tumor cells, it would be crucial to analyze its antitumor effect in *in vivo* models, in view of a clinical application. However, its low aqueous solubility has hindered the assessment of LEM2 *in vivo* antitumor activity, a limitation that might be circumvented through the design of derivatives with improved solubility or through the development of nanotechnology-based formulations for LEM2 delivery.

Finally, since the successful clinical translation of any drug requires appropriate characterization of absorption, distribution, metabolism, and elimination (ADME) characterization, these pharmacokinetic properties should also be assessed for both LEM2 and SLMP53-2. In addition, although neither of the compounds displayed apparent unspecific toxicity in the model systems tested, an in-depth toxicological assessment of LEM2 and SLMP53-2 would be required.

References

Aggarwal, M., Saxena, R., Sinclair, E., Fu, Y., Jacobs, A., Dyba, M., et al., 2016, Reactivation of mutant p53 by a dietary-related compound phenethyl isothiocyanate inhibits tumor growth. Cell Death and Differentiation **23**(10): 1615-1627.

Alessandrini, F., Pezze, L., Menendez, D., Resnick, M. A. and Ciribilli, Y., 2018, ETV7-Mediated DNAJC15 Repression Leads to Doxorubicin Resistance in Breast Cancer Cells. Neoplasia **20**(8): 857-870.

Alexandrova, E. M., Yallowitz, A. R., Li, D., Xu, S., Schulz, R., Proia, D. A., et al., 2015, Improving survival by exploiting tumour dependence on stabilized mutant p53 for treatment. Nature **523**(7560): 352-356.

Andreeff, M., Kelly, K. R., Yee, K., Assouline, S., Strair, R., Popplewell, L., et al., 2016, Results of the Phase I Trial of RG7112, a Small-Molecule MDM2 Antagonist in Leukemia. Clinical Cancer Research **22**(4): 868-876.

Andreotti, V., Ciribilli, Y., Monti, P., Bisio, A., Lion, M., Jordan, J., et al., 2011, p53 transactivation and the impact of mutations, cofactors and small molecules using a simplified yeast-based screening system. PLoS One **6**(6): e20643.

Arai, Y., Honda, S., Haruta, M., Kasai, F., Fujiwara, Y., Ohshima, J., et al., 2010, Genome-wide analysis of allelic imbalances reveals 4q deletions as a poor prognostic factor and MDM4 amplification at 1q32.1 in hepatoblastoma. Genes Chromosomes Cancer **49**(7): 596-609.

Balint, E., Phillips, A. C., Kozlov, S., Stewart, C. L. and Vousden, K. H., 2002, Induction of p57(KIP2) expression by p73beta. Proceedings of the National Academy of Sciences of the United States of America **99**(6): 3529-3534.

Barak, Y., Gottlieb, E., Juven-Gershon, T. and Oren, M., 1994, Regulation of mdm2 expression by p53: alternative promoters produce transcripts with nonidentical translation potential. Genes & Development **8**(15): 1739-1749.

Bartel, F., Schulz, J., Bohnke, A., Blumke, K., Kappler, M., Bache, M., et al., 2005, Significance of HDMX-S (or MDM4) mRNA splice variant overexpression and HDMX gene amplification on primary soft tissue sarcoma prognosis. International Journal of Cancer **117**(3): 469-475.

Baud, M. G. J., Bauer, M. R., Verduci, L., Dingler, F. A., Patel, K. J., Horil Roy, D., et al., 2018, Aminobenzothiazole derivatives stabilize the thermolabile p53 cancer mutant Y220C and show anticancer activity in p53-Y220C cell lines. European Journal of Medicinal Chemistry **152**: 101-114.

Baudino, T. A., 2015, Targeted Cancer Therapy: The Next Generation of Cancer Treatment. Current Drug Discovery Technololgies **12**(1): 3-20.

Bauer, M. R., Joerger, A. C. and Fersht, A. R., 2016, 2-Sulfonylpyrimidines: Mild alkylating agents with anticancer activity toward p53-compromised cells. Proceedings of the National Academy of Sciences of the United States of America **113**(36): E5271-E5280.

Beg, M. S., Brenner, A. J., Sachdev, J., Borad, M., Kang, Y. K., Stoudemire, J., et al., 2017, Phase I study of MRX34, a liposomal miR-34a mimic, administered twice weekly in patients with advanced solid tumors. Investigational New Drugs **35**(2): 180-188.

Bell, H. S., Dufes, C., O'Prey, J., Crighton, D., Bergamaschi, D., Lu, X., et al., 2007, A p53-derived apoptotic peptide derepresses p73 to cause tumor regression in vivo. Journal of Clinical Investigation **117**(4): 1008-1018.

Belyi, V. A., Ak, P., Markert, E., Wang, H., Hu, W., Puzio-Kuter, A., et al., 2010, The origins and evolution of the p53 family of genes. Cold Spring Harbor Perspectives in Biology **2**(6): a001198.

Bergamaschi, D., Gasco, M., Hiller, L., Sullivan, A., Syed, N., Trigiante, G., et al., 2003, p53 polymorphism influences response in cancer chemotherapy via modulation of p73-dependent apoptosis. Cancer Cell **3**(4): 387-402.

Bessa, C., Soares, J., Raimundo, L., Loureiro, J. B., Gomes, C., Reis, F., et al., 2018, Discovery of a small-molecule protein kinase Cδ-selective activator with promising application in colon cancer therapy. Cell Death & Disease **9**(2): 1-16.

Bevant, K. and Coulouarn, C., 2017, Landscape of genomic alterations in hepatocellular carcinoma: current knowledge and perspectives for targeted therapies. Hepatobiliary Surgery and Nutrition **6**(6): 404-407.

Bieging, K. T., Mello, S. S. and Attardi, L. D., 2014, Unravelling mechanisms of p53-mediated tumour suppression. Nature Reviews Cancer **14**(5): 359-370.

Bisio, A., Ciribilli, Y., Fronza, G., Inga, A. and Monti, P., 2014, TP53 Mutants in the Tower of Babel of Cancer Progression. Human Mutation **35**(6): 689-701.

Boeckler, F. M., Joerger, A. C., Jaggi, G., Rutherford, T. J., Veprintsev, D. B. and Fersht, A. R., 2008, Targeted rescue of a destabilized mutant of p53 by an in silico screened drug. Proceedings of the National Academy of Sciences of the United States of America **105**(30): 10360-10365.

Bouaoun, L., Sonkin, D., Ardin, M., Hollstein, M., Byrnes, G., Zavadil, J., et al., 2016, TP53 Variations in Human Cancers: New Lessons from the IARC TP53 Database and Genomics Data. Human Mutation **37**(9): 865-876.

Bougeard, G., Sesboue, R., Baert-Desurmont, S., Vasseur, S., Martin, C., Tinat, J., et al., 2008, Molecular basis of the Li-Fraumeni syndrome: an update from the French LFS families. Journal of Medical Genetics **45**(8): 535-538.

Bourdon, J. C., Renzing, J., Robertson, P. L., Fernandes, K. N. and Lane, D. P., 2002, Scotin, a novel p53-inducible proapoptotic protein located in the ER and the nuclear membrane. Journal of Cell Biology **158**(2): 235-246.

Brachmann, R. K., Vidal, M. and Boeke, J. D., 1996, Dominant-negative p53 mutations selected in yeast hit cancer hot spots. Proceedings of the National Academy of Sciences of the United States of America **93**(9): 4091-4095.

Brandt, T., Petrovich, M., Joerger, A. C. and Veprintsev, D. B., 2009, Conservation of DNA-binding specificity and oligomerisation properties within the p53 family. BMC Genomics **10**: 628.

Bray, F., Ferlay, J., Soerjomataram, I., Siegel, R. L., Torre, L. A. and Jemal, A., 2018, Global cancer statistics 2018: GLOBOCAN estimates of incidence and mortality worldwide for 36 cancers in 185 countries. CA: A Cancer Journal for Clinicians **68**(6): 394-424.

Brooks, C. L. and Gu, W., 2011, p53 regulation by ubiquitin. FEBS Letters **585**(18): 2803-2809.

Brown, J. P., Wei, W. and Sedivy, J. M., 1997, Bypass of senescence after disruption of p21CIP1/WAF1 gene in normal diploid human fibroblasts. Science **277**(5327): 831-834.

Bruckner, A., Polge, C., Lentze, N., Auerbach, D. and Schlattner, U., 2009, Yeast two-hybrid, a powerful tool for systems biology. International Journal of Molecular Sciences **10**(6): 2763-2788.

Brush, M. H., Weiser, D. C. and Shenolikar, S., 2003, Growth arrest and DNA damage-inducible protein GADD34 targets protein phosphatase 1 alpha to the endoplasmic reticulum and promotes dephosphorylation of the alpha subunit of eukaryotic translation initiation factor 2. Molecular and Cellular Biology **23**(4): 1292-1303.

Burgess, A., Chia, K. M., Haupt, S., Thomas, D., Haupt, Y. and Lim, E., 2016, Clinical Overview of MDM2/X-Targeted Therapies. Frontiers in Oncology **6**(1): 661-667.

Bustin, S. A., Benes, V., Garson, J. A., Hellemans, J., Huggett, J., Kubista, M., et al., 2009, The MIQE Guidelines: Minimum Information for Publication of Quantitative Real-Time PCR Experiments. Clinical Chemistry **55**(4): 611-622.

Bykov, V. J. N., 2005, Reactivation of Mutant p53 and Induction of Apoptosis in Human Tumor Cells by Maleimide Analogs. Journal of Biological Chemistry **280**(34): 30384-30391.

Bykov, V. J. N., Eriksson, S. E., Bianchi, J. and Wiman, K. G., 2018, Targeting mutant p53 for efficient cancer therapy. Nature Reviews Cancer **18**(2): 89-102.

Bykov, V. J. N., Issaeva, N., Shilov, A., Hultcrantz, M., Pugacheva, E., Chumakov, P., et al., 2002, Restoration of the tumor suppressor function to mutant p53 by a low-molecular-weight compound. Nature Medicine **8**(3): 282-288.

Bykov, V. J. N. and Wiman, K. G., 2014, Mutant p53 reactivation by small molecules makes its way to the clinic. FEBS Letters: 1-6.

Calabro, V., Mansueto, G., Parisi, T., Vivo, M., Calogero, R. A. and La Mantia, G., 2002, The Human MDM2 Oncoprotein Increases the Transcriptional Activity and the Protein Level of the p53 Homolog p63. Journal of Biological Chemistry **277**(4): 2674-2681.

Campisi, J., 2005, Senescent cells, tumor suppression, and organismal aging: good citizens, bad neighbors. Cell **120**(4): 513-522.

Candi, E., Agostini, M., Melino, G. and Bernassola, F., 2014, How the TP53 family proteins TP63 and TP73 contribute to tumorigenesis: regulators and effectors. Human Mutation **35**(6): 702-714.

Candi, E., Rufini, A., Terrinoni, A., Giamboi-Miraglia, A., Lena, A. M., Mantovani, R., et al., 2007, DeltaNp63 regulates thymic development through enhanced expression of FgfR2 and Jag2. Proceedings of the National Academy of Sciences of the United States of America **104**(29): 11999-12004.

Carr, J., Bell, E., Pearson, A. D. J., Kees, U. R., Beris, H., Lunec, J., et al., 2006, Increased Frequency of Aberrations in the p53/MDM2/p14ARF Pathway in Neuroblastoma Cell Lines Established at Relapse. Cancer Research **66**(4): 2138-2145.

Chan, W. M., Siu, W. Y., Lau, A. and Poon, R. Y., 2004, How many mutant p53 molecules are needed to inactivate a tetramer? Molecular and Cellular Biology **24**(8): 3536-3551.

Chen, I. T., Smith, M. L., O'Connor, P. M. and Fornace, A. J., Jr., 1995, Direct interaction of Gadd45 with PCNA and evidence for competitive interaction of Gadd45 and p21Waf1/Cip1 with PCNA. Oncogene **11**(10): 1931-1937.

Chen, J., 2016, The Cell-Cycle Arrest and Apoptotic Functions of p53 in Tumor Initiation and Progression. Cold Spring Harbor Perspectives in Medicine **6**(3): a026104.

Chène, P., 1998, In vitro analysis of the dominant negative effect of p53 mutants. Journal of Molecular Biology **281**(2): 205-209.

Chin, P. L., Momand, J. and Pfeifer, G. P., 1997, In vivo evidence for binding of p53 to consensus binding sites in the p21 and GADD45 genes in response to ionizing radiation. Oncogene **15**(1): 87-99.

Chou, T.-C. and Talalay, P., 1984, Quantitative analysis of dose-effect relationships: the combined effects of multiple drugs or enzyme inhibitors. Advances in Enzyme Regulation **22**: 27-55.

Ciribilli, Y., Monti, P., Bisio, A., Nguyen, H. T., Ethayathulla, A. S., Ramos, A., et al., 2013, Transactivation specificity is conserved among p53 family proteins and depends on a response element sequence code. Nucleic Acids Research **41**(18): 8637-8653.

Clegg, H. V., Itahana, K. and Zhang, Y., 2008, Unlocking the Mdm2-p53 loop: ubiquitin is the key. Cell Cycle **7**(3): 287-292.

Cross, B., Chen, L., Cheng, Q., Li, B., Yuan, Z. M. and Chen, J., 2011, Inhibition of p53 DNA binding function by the MDM2 protein acidic domain. Journal of Biological Chemistry **286**(18): 16018-16029.

Daige, C. L., Wiggins, J. F., Priddy, L., Nelligan-Davis, T., Zhao, J. and Brown, D., 2014, Systemic delivery of a miR34a mimic as a potential therapeutic for liver cancer. Molecular Cancer Therapeutics **13**(10): 2352-2360.

De Laurenzi, V., Costanzo, A., Barcaroli, D., Terrinoni, A., Falco, M., Annicchiarico-Petruzzelli, M., et al., 1998, Two New p73 Splice Variants, γ and δ, with Different Transcriptional Activity. Journal of Experimental Medicine **188**(9): 1763-1768.

De Laurenzi, V. D., Catani, M. V., Terrinoni, A., Corazzari, M., Melino, G., Costanzo, A., et al., 1999, Additional complexity in p73: induction by mitogens in lymphoid cells and identification of two new splicing variants epsilon and zeta. Cell Death and Differentiation **6**(5): 389-390.

Dearth, L. R., Qian, H., Wang, T., Baroni, T. E., Zeng, J., Chen, S. W., et al., 2007, Inactive full-length p53 mutants lacking dominant wild-type p53 inhibition highlight loss of heterozygosity as an important aspect of p53 status in human cancers. Carcinogenesis **28**(2): 289-298.

Demma, M., Maxwell, E., Ramos, R., Liang, L., Li, C., Hesk, D., et al., 2010, SCH529074, a Small Molecule Activator of Mutant p53, Which Binds p53 DNA Binding Domain (DBD), Restores Growth-suppressive Function to Mutant p53 and Interrupts HDM2-mediated Ubiquitination of Wild Type p53. Journal of Biological Chemistry **285**(14): 10198-10212.

Di Agostino, S., Cortese, G., Monti, O., Dell'Orso, S., Sacchi, A., Eisenstein, M., et al., 2008, The disruption of the protein complex mutantp53/p73 increases selectively the response of tumor cells to anticancer drugs. Cell Cycle **7**(21): 3440-3447.

Di Como, C. J., Gaiddon, C. and Prives, C., 1999, p73 function is inhibited by tumor-derived p53 mutants in mammalian cells. Molecular and Cellular Biology **19**(2): 1438-1449.

Di Ventura, B., Funaya, C., Antony, C., Knop, M. and Serrano, L., 2008, Reconstitution of Mdm2-Dependent Post-Translational Modifications of p53 in Yeast. PLoS One **3**(1): e1507-1509.

Ding, Q., Zhang, Z., Liu, J. J., Jiang, N., Zhang, J., Ross, T. M., et al., 2013, Discovery of RG7388, a potent and selective p53-MDM2 inhibitor in clinical development. Journal of Medicinal Chemistry **56**(14): 5979-5983.

Dittmer, D., Pati, S., Zambetti, G., Chu, S., Teresky, A. K., Moore, M., et al., 1993, Gain of function mutations in p53. Nature Genetics **4**: 42-46.

Dominguez, G., Garcia, J. M., Pena, C., Silva, J., Garcia, V., Martinez, L., et al., 2006, DeltaTAp73 upregulation correlates with poor prognosis in human tumors: putative in vivo network involving p73 isoforms, p53, and E2F-1. Journal of Clinical Oncology **24**(5): 805-815.

Donehower, L. A., Harvey, M., Slagle, B. L., McArthur, M. J., Montgomery, C. A., Jr., Butel, J. S., et al., 1992, Mice deficient for p53 are developmentally normal but susceptible to spontaneous tumours. Nature **356**(6366): 215-221.

Dötsch, V., Bernassola, F., Coutandin, D., Candi, E. and Melino, G., 2010, p63 and p73, the Ancestors of p53. Cold Spring Harbor Perspectives in Biology **2**(9): a004887-a004887.

Duffy, M. J., Synnott, N. C., McGowan, P. M. and Crown, J., 2014, p53 as a target for the treatment of cancer. Cancer Treatment Reviews **40**(10): 1153-1160.

el-Deiry, W. S., Tokino, T., Velculescu, V. E., Levy, D. B., Parsons, R., Trent, J. M., et al., 1993, WAF1, a potential mediator of p53 tumor suppression. Cell **75**(4): 817-825.

Epstein, R. J., 2013, The unpluggable in pursuit of the undruggable: tackling the dark matter of the cancer therapeutics universe. Front Oncol **3**: 304.

Erster, S., Palacios, G., Rosenquist, T., Chang, C. and Moll, U. M., 2006, Deregulated expression of DeltaNp73alpha causes early embryonic lethality. Cell Death and Differentiation **13**(1): 170-173.

Ferlay, J., Colombet, M., Soerjomataram, I., Mathers, C., Parkin, D. M., Pineros, M., et al., 2019, Estimating the global cancer incidence and mortality in 2018: GLOBOCAN sources and methods. International Journal of Cancer **144**(8): 1941-1953.

Flores, E. R., Sengupta, S., Miller, J. B., Newman, J. J., Bronson, R., Crowley, D., et al., 2005, Tumor predisposition in mice mutant for p63 and p73: evidence for broader tumor suppressor functions for the p53 family. Cancer Cell **7**(4): 363-373.

Foster, B. A., 1999, Pharmacological Rescue of Mutant p53 Conformation and Function. Science **286**(5449): 2507-2510.

Freedman, D. A., Epstein, C. B., Roth, J. C. and Levine, A. J., 1997, A genetic approach to mapping the p53 binding site in the MDM2 protein. Journal of Molecular Medicine **3**(4): 248-259.

Friedler, A., Hansson, L. O., Veprintsev, D. B., Freund, S. M. V., Rippin, T. M., Nikolova, P. V., et al., 2002, A peptide that binds and stabilizes p53 core domain: chaperone strategy for rescue of oncogenic mutants. Proceedings of the National Academy of Sciences of the United States of America **99**(2): 937-942.

Fronza, G., Inga, A., Monti, P., Scott, G., Campomenosi, P., Menichini, P., et al., 2000, The yeast p53 functional assay: a new tool for molecular epidemiology. Hopes and facts. Mutation Research/Reviews in Mutation Research **462**(2-3): 293-301.

Fukazawa, T., Fujiwara, T., Morimoto, Y., Shao, J., Nishizaki, M., Kadowaki, Y., et al., 1999, Differential involvement of the CD95 (Fas/APO-1) receptor/ligand system on apoptosis induced by the wild-type p53 gene transfer in human cancer cells. Oncogene **18**(13): 2189-2199.

Gaiddon, C., Lokshin, M., Ahn, J., Zhang, T. and Prives, C., 2001, A subset of tumor-derived mutant forms of p53 down-regulate p63 and p73 through a direct interaction with the p53 core domain. Molecular and Cellular Biology **21**(5): 1874-1887.

Gallagher, W. M., Argentini, M., Sierra, V., Bracco, L., Debussche, L. and Conseiller, E., 1999, MBP1: a novel mutant p53-specific protein partner with oncogenic properties. Oncogene **18**(24): 3608-3616.

Gembarska, A., Luciani, F., Fedele, C., Russell, E. A., Dewaele, M., Villar, S., et al., 2012, MDM4 is a key therapeutic target in cutaneous melanoma. Nature Medicine **18**(8): 1239-1247.

Ghioni, P., Bolognese, F., Duijf, P. H., Van Bokhoven, H., Mantovani, R. and Guerrini, L., 2002, Complex transcriptional effects of p63 isoforms: identification of novel activation and repression domains. Molecular and Cellular Biology **22**(24): 8659-8668.

Giaccia, A. J. and Kastan, M. B., 1998, The complexity of p53 modulation: emerging patterns from divergent signals. Genes & Development **12**(19): 2973-2983.

Gietz, R. D. and Schiestl, R. H., 2007, High-efficiency yeast transformation using the LiAc/SS carrier DNA/PEG method. Nature Protocols **2**(1): 31-34.

Giknis, M. and Clifford, C. B., 2008, Clinical laboratory parameters for Crl: WI (Han). Charles River Laboratories.

Giorgi, C., Bonora, M., Sorrentino, G., Missiroli, S., Poletti, F., Suski, J. M., et al., 2015, p53 at the endoplasmic reticulum regulates apoptosis in a Ca2+-dependent manner. Proceedings of the National Academy of Sciences of the United States of America **112**(6): 1779-1784.

Global Burden of Disease Cancer Collaboration, Fitzmaurice, C., Akinyemiju, T. F., Al Lami, F. H., Alam, T., Alizadeh-Navaei, R., et al., 2018, Global, Regional, and National Cancer Incidence, Mortality, Years of Life Lost, Years Lived With Disability, and Disability-Adjusted Life-Years for 29 Cancer Groups, 1990 to 2016. JAMA Oncology **4**(11): 1553-1516.

Goldschneider, D., Blanc, E., Raguénez, G., Barrois, M., Legrand, A., Le Roux, G., et al., 2004, Differential response of p53 target genes to p73 overexpression in SH-SY5Y neuroblastoma cell line. Journal of Cell Science **117**(Pt 2): 293-301.

Gomes, A. S., Brandao, P., Fernandes, C. S. G., da Silva, M. R. P. C., de Sousa, M. E. P. and Pinto, M. M. d. M., 2016, Drug-like Properties and ADME of Xanthone Derivatives: The Antechamber of Clinical Trials. Current Medicinal Chemistry **23**(32): 3654-3686.

Gomes, A. S., Ramos, H., Gomes, S., Loureiro, J. B., Soares, J., Barcherini, V., et al., 2019a, SLMP53-1 reactivates mutant p53 by targeting DNA-binding domain. Structure.

Gomes, S., Raimundo, L., Soares, J., Loureiro, J. B., Leão, M., Ramos, H., et al., 2019b, New inhibitor of the TAp73 interaction with MDM2 and mutant p53 with promising antitumor activity against neuroblastoma. Cancer Letters **446**: 90-102.

Gorrini, C., Harris, I. S. and Mak, T. W., 2013, Modulation of oxidative stress as an anticancer strategy. Nature Reviews Drug Discovery **12**(12): 931-947.

Graves, B., Thompson, T., Xia, M., Janson, C., Lukacs, C., Deo, D., et al., 2012, Activation of the p53 pathway by small-molecule-induced MDM2 and MDMX dimerization. Proceedings of the National Academy of Sciences of the United States of America **109**(29): 11788-11793.

Guaragnella, N., Palermo, V., Galli, A., Moro, L., Mazzoni, C. and Giannattasio, S., 2014, The expanding role of yeast in cancer research and diagnosis: insights into the function of the oncosuppressors p53 and BRCA1/2. FEMS Yeast Research **14**(1): 2-16.

Guo, X., Keyes, W. M., Papazoglu, C., Zuber, J., Li, W., Lowe, S. W., et al., 2009a, TAp63 induces senescence and suppresses tumorigenesis in vivo. Nature Publishing Group **11**(12): 1451-1457.

Guo, X., Keyes, W. M., Papazoglu, C., Zuber, J., Li, W., Lowe, S. W., et al., 2009b, TAp63 induces senescence and suppresses tumorigenesis in vivo. Nature Cell Biology **11**(12): 1451-1457.

Hainaut, P. and Milner, J., 1992, Interaction of heat-shock protein 70 with p53 translated in vitro: evidence for interaction with dimeric p53 and for a role in the regulation of p53 conformation. The EMBO Journal **11**(10): 3513-3520.

Hainaut, P., Olivier, M. and Wiman, K. G., 2012. P53 in the Clinics.

Hanahan, D. and Weinberg, R. A., 2000, The hallmarks of cancer. Cell **100**(1): 57-70.

Hanahan, D. and Weinberg, R. A., 2011, Hallmarks of cancer: the next generation. Cell **144**(5): 646-674.

Harper, J. W., Adami, G. R., Wei, N., Keyomarsi, K. and Elledge, S. J., 1993, The p21 Cdk-interacting protein Cip1 is a potent inhibitor of G1 cyclin-dependent kinases. Cell **75**(4): 805-816.

Hassan, N. M. M., Tada, M., Hamada, J.-I., Kashiwazaki, H., Kameyama, T., Akhter, R., et al., 2008, Presence of dominant negative mutation of TP53 is a risk of early recurrence in oral cancer. Cancer Letters **270**(1): 108-119.

He, C., Li, L., Guan, X., Xiong, L. and Miao, X., 2017, Mutant p53 Gain of Function and Chemoresistance: The Role of Mutant p53 in Response to Clinical Chemotherapy. Chemotherapy **62**(1): 43-53.

Hermeking, H., Lengauer, C., Polyak, K., He, T. C., Zhang, L., Thiagalingam, S., et al., 1997, 14-3-3sigma is a p53-regulated inhibitor of G2/M progression. Molecular Cell **1**(1): 3-11.

Hiraki, M., Hwang, S.-Y., Cao, S., Ramadhar, T. R., Byun, S., Yoon, K. W., et al., 2015, Small-Molecule Reactivation of Mutant p53 to Wild-Type-like p53 through the p53-Hsp40 Regulatory Axis. Chemistry & Biology **22**(9): 1206-1216.

Hollander, M. C., Alamo, I., Jackman, J., Wang, M. G., McBride, O. W. and Fornace, A. J., Jr., 1993, Analysis of the mammalian gadd45 gene and its response to DNA damage. Journal of Biological Chemistry **268**(32): 24385-24393.

Hong, B., Prabhu, V. V., Zhang, S., van den Heuvel, A. P. J., Dicker, D. T., Kopelovich, L., et al., 2014, Prodigiosin rescues deficient p53 signaling and antitumor effects via upregulating p73 and disrupting its interaction with mutant p53. Cancer Research **74**(4): 1153-1165.

Horvilleur, E., Bauer, M., Goldschneider, D., Mergui, X., de La Motte, A., Bénard, J., et al., 2008, p73α isoforms drive opposite transcriptional and post-transcriptional regulation of MYCN expression in neuroblastoma cells. Nucleic Acids Research **36**(13): 4222-4232.

Hu, W., Feng, Z. and Levine, A. J., 2012, The Regulation of Multiple p53 Stress Responses is Mediated through MDM2. Genes Cancer **3**(3-4): 199-208.

Huang, M., Shen, A., Ding, J. and Geng, M., 2014, Molecularly targeted cancer therapy: some lessons from the past decade. Trends in Pharmacological Sciences **35**(1): 41-50.

Ikawa, S., Nakagawara, A. and Ikawa, Y., 1999, p53 family genes: structural comparison, expression and mutation. Cell Death and Differentiation **6**(12): 1154-1161.

INE, I. P., 2019, Causas de Morte - 2017. I. P. Instituto Nacional de Estatística. Portugal, Instituto Nacional de Estatística, I.P.

Inga, A., Cresta, S., Monti, P., Aprile, A., Scott, G., Abbondandolo, A., et al., 1997, Simple identification of dominant p53 mutants by a yeast functional assay. Carcinogenesis **18**(10): 2019-2021.

Innocente, S. A. and Lee, J. M., 2005, p73 is a p53-independent, Sp1-dependent repressor of cyclin B1 transcription. Biochemical and Biophysical Research Communications **329**(2): 713-718.

Institute for Health Metrics and Evaluation. (2017). "GBD Compare | Viz Hub." Retrieved March 2019, from https://vizhub.healthdata.org/gbd-compare/.

International Agency for Research on Cancer. (2018a). "Global Cancer Observatory: Cancer Today." Retrieved March 2019, from http://gco.iarc.fr/today/home.

International Agency for Research on Cancer. (2018b). "Global Cancer Observatory: Cancer Tomorrow." Retrieved March 2019, from http://gco.iarc.fr/tomorrow/home.

Ishioka, C., Frebourg, T., Yan, Y. X., Vidal, M., Friend, S. H., Schmidt, S., et al., 1993, Screening patients for heterozygous p53 mutations using a functional assay in yeast. Nature Genetics **5**(2): 124-129.

Iwabuchi, K., Li, B., Bartel, P. and Fields, S., 1993, Use of the two-hybrid system to identify the domain of p53 involved in oligomerization. Oncogene **8**(6): 1693-1696.

Iwakuma, T. and Lozano, G., 2003, MDM2, an introduction. Molecular Cancer Research **1**(14): 993-1000.

Jain, A. K. and Barton, M. C., 2010, Making sense of ubiquitin ligases that regulate p53. Cancer Biology & Therapy **10**(7): 665-672.

Jin, Y., Chen, J., Feng, Z., Fan, W., Wang, Y., Li, J., et al., 2014, The expression of Survivin and NF-kappaB associated with prognostically worse clinicopathologic variables in hepatocellular carcinoma. Tumor Biology **35**(10): 9905-9910.

Joerger, A. C. and Fersht, A. R., 2008, Structural Biology of the Tumor Suppressor p53. Annual Review of Biochemistry **77**(1): 557-582.

Joerger, A. C. and Fersht, A. R., 2016, The p53 Pathway: Origins, Inactivation in Cancer, and Emerging Therapeutic Approaches. Annual Review of Biochemistry **85**: 375-404.

Joerger, A. C., Rajagopalan, S., Natan, E., Veprintsev, D. B., Robinson, C. V. and Fersht, A. R., 2009, Structural evolution of p53, p63, and p73: implication for heterotetramer formation. Proceedings of the National Academy of Sciences of the United States of America **106**(42): 17705-17710.

Jones, S. N., Hancock, A. R., Vogel, H., Donehower, L. A. and Bradley, A., 1998, Overexpression of Mdm2 in mice reveals a p53-independent role for Mdm2 in tumorigenesis. Proceedings of the National Academy of Sciences of the United States of America **95**(26): 15608-15612.

Jordan, J. J., Menendez, D., Inga, A., Noureddine, M., Bell, D. A. and Resnick, M. A., 2008, Noncanonical DNA motifs as transactivation targets by wild type and mutant p53. PLoS Genetics **4**(6): e1000104.

Jost, C. A., Marin, M. C. and Kaelin, W. G., Jr., 1997, p73 is a simian [correction of human] p53-related protein that can induce apoptosis. Nature **389**(6647): 191-194.

Kadakia, M., Slader, C. and Berberich, S. J., 2001, Regulation of p63 function by Mdm2 and MdmX. DNA and Cell Biology **20**(6): 321-330.

Kaghad, M., Bonnet, H., Yang, A., Creancier, L., Biscan, J. C., Valent, A., et al., 1997, Monoallelically expressed gene related to p53 at 1p36, a region frequently deleted in neuroblastoma and other human cancers. Cell **90**(4): 809-819.

Keyes, W. M., Vogel, H., Koster, M. I., Guo, X., Qi, Y., Petherbridge, K. M., et al., 2006, p63 heterozygous mutant mice are not prone to spontaneous or chemically induced tumors. Proceedings of the National Academy of Sciences of the United States of America **103**(22): 8435-8440.

Khoo, K. H., Hoe, K. K., Verma, C. S. and Lane, D. P., 2014, Drugging the p53 pathway: understanding the route to clinical efficacy. Nature Reviews Drug Discovery **13**(3): 217-236.

Kim, I., Xu, W. and Reed, J. C., 2008, Cell death and endoplasmic reticulum stress: disease relevance and therapeutic opportunities. Nature Reviews Drug Discovery **7**(12): 1013-1030.

Kimura, T., Gotoh, M., Nakamura, Y. and Arakawa, H., 2003, hCDC4b, a regulator of cyclin E, as a direct transcriptional target of p53. Cancer Science **94**(5): 431-436.

Kinzler, K. W. and Vogelstein, B., 1997, Cancer-susceptibility genes. Gatekeepers and caretakers. Nature **386**(6627): 761-763.

Kojima, T., Ikawa, Y. and Katoh, I., 2001, Analysis of Molecular Interactions of the p53-Family p51(p63) Gene Products in a Yeast Two-Hybrid System: Homotypic and Heterotypic Interactions and Association with p53-Regulatory Factors. Biochemical and Biophysical Research Communications **281**(5): 1170-1175.

Kortlever, R. M., Higgins, P. J. and Bernards, R., 2006, Plasminogen activator inhibitor-1 is a critical downstream target of p53 in the induction of replicative senescence. Nature Cell Biology **8**(8): 877-884.

Krause, K., Wasner, M., Reinhard, W., Haugwitz, U., Dohna, C. L., Mossner, J., et al., 2000, The tumour suppressor protein p53 can repress transcription of cyclin B. Nucleic Acids Research **28**(22): 4410-4418.

Kravchenko, J. E., Ilyinskaya, G. V., Komarov, P. G., Agapova, L. S., Kochetkov, D. V., Strom, E., et al., 2008, Small-molecule RETRA suppresses mutant p53-bearing cancer cells through a p73-dependent salvage pathway. Proceedings of the National Academy of Sciences of the United States of America **105**(17): 6302-6307.

Kudo, M., 2017, Systemic Therapy for Hepatocellular Carcinoma: 2017 Update. Oncology **93**(1): 135-146.

Kulikov, R., Letienne, J., Kaur, M., Grossman, S. R., Arts, J. and Blattner, C., 2010, Mdm2 facilitates the association of p53 with the proteasome. Proceedings of the National Academy of Sciences of the United States of America **107**(22): 10038-10043.

Kussie, P. H., Gorina, S., Marechal, V., Elenbaas, B., Moreau, J., Levine, A. J., et al., 1996, Structure of the MDM2 oncoprotein bound to the p53 tumor suppressor transactivation domain. Science **274**(5289): 948-953.

Lambert, J. M. R., Gorzov, P., Veprintsev, D. B., SOderqvist, M., SegerbAck, D., Bergman, J., et al., 2009a, PRIMA-1 Reactivates Mutant p53 by Covalent Binding to the Core Domain. Cancer Cell **15**(5): 376-388.

Lambert, J. M. R., Moshfegh, A., Hainaut, P., Wiman, K. G. and Bykov, V. J. N., 2009b, Mutant p53 reactivation by PRIMA-1MET induces multiple signaling pathways converging on apoptosis. Nature Publishing Group **29**(9): 1329-1338.

Lane, D. P. and Crawford, L. V., 1979, T antigen is bound to a host protein in SV40-transformed cells. Nature **278**(5701): 261-263.

Lang, G. A., Iwakuma, T., Suh, Y. A., Liu, G., Rao, V. A., Parant, J. M., et al., 2004, Gain of function of a p53 hot spot mutation in a mouse model of Li-Fraumeni syndrome. Cell **119**(6): 861-872.

Laptenko, O., Shiff, I., Freed-Pastor, W., Zupnick, A., Mattia, M., Freulich, E., et al., 2015, The p53 C terminus controls site-specific DNA binding and promotes structural changes within the central DNA binding domain. Molecular Cell **57**(6): 1034-1046.

Lau, L. M., Wolter, J. K., Lau, J. T., Cheng, L. S., Smith, K. M., Hansford, L. M., et al., 2009, Cyclooxygenase inhibitors differentially modulate p73 isoforms in neuroblastoma. Oncogene **28**(19): 2024-2033.

Lau, L. M. S., Nugent, J. K., Zhao, X. and Irwin, M. S., 2007, HDM2 antagonist Nutlin-3 disrupts p73-HDM2 binding and enhances p73 function. Oncogene **27**(7): 997-1003.

Laurie, N. A., Donovan, S. L., Shih, C. S., Zhang, J., Mills, N., Fuller, C., et al., 2006, Inactivation of the p53 pathway in retinoblastoma. Nature **444**(7115): 61-66.

Leão, M., Gomes, S., Bessa, C., Soares, J., Raimundo, L., Monti, P., et al., 2015a, Studying p53 family proteins in yeast: Induction of autophagic cell death and modulation by interactors and small molecules. Experimental Cell Research **330**(1): 164-177.

Leão, M., Gomes, S., Pedraza-Chaverri, J., Machado, N., Sousa, E., Pinto, M., et al., 2013a, α-Mangostin and Gambogic Acid as Potential Inhibitors of the p53–MDM2 Interaction Revealed by a Yeast Approach. Journal of Natural Products **76**(4): 774-778.

Leão, M., Gomes, S., Soares, J., Bessa, C., Maciel, C., Ciribilli, Y., et al., 2013b, Novel simplified yeast-based assays of regulators of p53-MDMX interaction and p53 transcriptional activity. FEBS Journal **280**(24): 6498-6507.

Leão, M., Pereira, C., Bisio, A., Ciribilli, Y., Paiva, A. M., Machado, N., et al., 2013c, Discovery of a new small-molecule inhibitor of p53–MDM2 interaction using a yeast-based approach. Biochemical Pharmacology **85**(9): 1234-1245.

Leão, M., Soares, J., Gomes, S., Raimundo, L., Ramos, H., Bessa, C., et al., 2015b, Enhanced cytotoxicity of prenylated chalcone against tumour cells via disruption of the p53-MDM2 interaction. Life Sciences **142**: 60-65.

Lee, A. H., Iwakoshi, N. N. and Glimcher, L. H., 2003, XBP-1 regulates a subset of endoplasmic reticulum resident chaperone genes in the unfolded protein response. Molecular and Cellular Biology **23**(21): 7448-7459.

Leong, C. O., Vidnovic, N., DeYoung, M. P., Sgroi, D. and Ellisen, L. W., 2007, The p63/p73 network mediates chemosensitivity to cisplatin in a biologically defined subset of primary breast cancers. Journal of Clinical Investigation **117**(5): 1370-1380.

Levrero, M., De Laurenzi, V., Costanzo, A., Gong, J., Wang, J. Y. and Melino, G., 2000, The p53/p63/p73 family of transcription factors: overlapping and distinct functions. Journal of Cell Science **113 (Pt 10)**: 1661-1670.

Li, D., Marchenko, N. D. and Moll, U. M., 2011, SAHA shows preferential cytotoxicity in mutant p53 cancer cells by destabilizing mutant p53 through inhibition of the HDAC6-Hsp90 chaperone axis. Cell Death and Differentiation **18**(12): 1904-1913.

Li, N., Fu, H., Tie, Y., Hu, Z., Kong, W., Wu, Y., et al., 2009, miR-34a inhibits migration and invasion by down-regulation of c-Met expression in human hepatocellular carcinoma cells. Cancer Lett. **275**(1): 44-53.

Liedtke, C., Groger, N., Manns, M. P. and Trautwein, C., 2003, The human caspase-8 promoter sustains basal activity through SP1 and ETS-like transcription factors and can be up-regulated by a p53-dependent mechanism. Journal of Biological Chemistry **278**(30): 27593-27604.

Lin, S., Hoffmann, K. and Schemmer, P., 2012a, Treatment of Hepatocellular Carcinoma: A Systematic Review. Liver Cancer **1**(3-4): 144-158.

Lin, W. C., Chuang, Y. C., Chang, Y. S., Lai, M. D., Teng, Y. N., Su, I. J., et al., 2012b, Endoplasmic reticulum stress stimulates p53 expression through NF-kappaB activation. PLoS One **7**(7): e39120.

Linzer, D. I. and Levine, A. J., 1979, Characterization of a 54K dalton cellular SV40 tumor antigen present in SV40-transformed cells and uninfected embryonal carcinoma cells. Cell **17**(1): 43-52.

Liu, J. L., Zhang, X. J., Zhang, Z., Zhang, A. H., Wang, W. and Dong, J. H., 2013a, Meta-analysis: prognostic value of survivin in patients with hepatocellular carcinoma. PLoS One **8**(12): e83350.

Liu, T., Laurell, C., Selivanova, G., Lundeberg, J., Nilsson, P. and Wiman, K. G., 2007, Hypoxia induces p53-dependent transactivation and Fas/CD95-dependent apoptosis. Cell Death and Differentiation **14**(3): 411-421.

Liu, X., Wilcken, R., Joerger, A. C., Chuckowree, I. S., Amin, J., Spencer, J., et al., 2013b, Small molecule induced reactivation of mutant p53 in cancer cells. Nucleic Acids Research **41**(12): 6034-6044.

Liu, Y., Hu, X., Han, C., Wang, L., Zhang, X., He, X., et al., 2015, Targeting tumor suppressor genes for cancer therapy. BioEssays **37**(12): 1277-1286.

Maas, A.-M., Bretz, A. C., Mack, E. and Stiewe, T., 2013, Targeting p73 in cancer. Cancer Letters **332**(2): 229-236.

Madan, E., Parker, T. M., Bauer, M. R., Dhiman, A., Pelham, C. J., Nagane, M., et al., 2018, The curcumin analog HO-3867 selectively kills cancer cells by converting mutant p53 protein to transcriptionally active wildtype p53. Journal of Biological Chemistry: jbc.RA117.000950-000931.

Maddocks, O. D. and Vousden, K. H., 2011, Metabolic regulation by p53. Journal of Journal of Molecular Medicine **89**(3): 237-245.

Mahalingam, D., Wilding, G., Denmeade, S., Sarantopoulas, J., Cosgrove, D., Cetnar, J., et al., 2016, Mipsagargin, a novel thapsigargin-based PSMA-activated prodrug: results of a first-in-man phase I clinical trial in patients with refractory, advanced or metastatic solid tumours. British Journal of Cancer **114**(9): 986-994.

Maleki Vareki, S., Salim, K. Y., Danter, W. R. and Koropatnick, J., 2018, Novel anti-cancer drug COTI-2 synergizes with therapeutic agents and does not induce resistance or exhibit cross-resistance in human cancer cell lines. PLoS One **13**(1): e0191766.

Malkin, D., 1993, p53 and the Li-Fraumeni syndrome. Cancer Genetics and Cytogenetics **66**(2): 83-92.

Marcel, V., Petit, I., Murray-Zmijewski, F., Goullet de Rugy, T., Fernandes, K., Meuray, V., et al., 2012, Diverse p63 and p73 isoforms regulate Delta133p53 expression through modulation of the internal TP53 promoter activity. Cell Death and Differentiation **19**(5): 816-826.

Marciniak, S. J., Garcia-Bonilla, L., Hu, J., Harding, H. P. and Ron, D., 2006, Activation-dependent substrate recruitment by the eukaryotic translation initiation factor 2 kinase PERK. Journal of Cell Biology **172**(2): 201-209.

McCullough, K. D., Martindale, J. L., Klotz, L. O., Aw, T. Y. and Holbrook, N. J., 2001, Gadd153 sensitizes cells to endoplasmic reticulum stress by down-regulating Bcl2 and perturbing the cellular redox state. Molecular and Cellular Biology **21**(4): 1249-1259.

Meek, D. W. and Anderson, C. W., 2009, Posttranslational Modification of p53: Cooperative Integrators of Function. Cold Spring Harbor Perspectives in Biology **1**(6): a000950-a000950.

Melino, G., 2011, p63 is a suppressor of tumorigenesis and metastasis interacting with mutant p53. Cell Death and Differentiation **18**(9): 1487-1499.

Melino, G., De Laurenzi, V. and Vousden, K. H., 2002, p73: Friend or foe in tumorigenesis. Nature Reviews Cancer **2**(8): 605-615.

Mendelsohn, J., Howley, P. M., Israel, M. A., Gray, J. W. and Thompson, C. B., 2014. The Molecular Basis of Cancer, Elsevier Health Sciences.

Merkel, O., Taylor, N., Prutsch, N., Staber, P. B., Moriggl, R., Turner, S. D., et al., 2017, When the guardian sleeps: Reactivation of the p53 pathway in cancer. Mutation Research/Reviews in Mutation Research **773**: 1-13.

Mihara, M., Erster, S., Zaika, A., Petrenko, O., Chittenden, T., Pancoska, P., et al., 2003, p53 has a direct apoptogenic role at the mitochondria. Molecular Cell **11**(3): 577-590.

Mills, A. A., Zheng, B., Wang, X. J., Vogel, H., Roop, D. R. and Bradley, A., 1999, p63 is a p53 homologue required for limb and epidermal morphogenesis. Nature **398**(6729): 708-713.

Moll, U. M. and Slade, N., 2004, p63 and p73: roles in development and tumor formation. Molecular Cancer Research **2**(7): 371-386.

Monti, P., Campomenosi, P., Ciribilli, Y., Iannone, R., Aprile, A., Inga, A., et al., 2003, Characterization of the p53 mutants ability to inhibit p73β transactivation using a yeast-based functional assay. Oncogene **22**(34): 5252-5260.

Monti, P., Campomenosi, P., Ciribilli, Y., Iannone, R., Inga, A., Abbondandolo, A., et al., 2002, Tumour p53 mutations exhibit promoter selective dominance over wild type p53. Oncogene **21**(11): 1641-1648.

Monti, P., Perfumo, C., Bisio, A., Ciribilli, Y., Menichini, P., Russo, D., et al., 2011, Dominant-Negative Features of Mutant TP53 in Germline Carriers Have Limited Impact on Cancer Outcomes. Molecular Cancer Research **9**(3): 271-279.

Morris, L. G. T. and Chan, T. A., 2014, Therapeutic targeting of tumor suppressor genes. Cancer **121**(9): 1357-1368.

Muller, P. A. and Vousden, K. H., 2013, p53 mutations in cancer. Nature Cell Biology **15**(1): 2-8.

Murray-Zmijewski, F., Lane, D. P. and Bourdon, J. C., 2006, p53/p63/p73 isoforms: an orchestra of isoforms to harmonise cell differentiation and response to stress. Cell Death and Differentiation **13**(6): 962-972.

Neilsen, P. M., Noll, J. E., Suetani, R. J., Schulz, R. B., Al-Ejeh, F., Evdokiou, A., et al., 2011, Mutant p53 uses p63 as a molecular chaperone to alter gene expression and induce a pro-invasive secretome. Oncotarget **2**(12): 1203-1217.

Niessner, H., Sinnberg, T., Kosnopfel, C., Smalley, K. S. M., Beck, D., Praetorius, C., et al., 2017, BRAF Inhibitors Amplify the Proapoptotic Activity of MEK Inhibitors by Inducing ER Stress in NRAS-Mutant Melanoma. Clinical Cancer Research **23**(20): 6203-6214.

Nikolaev, A. Y., Li, M., Puskas, N., Qin, J. and Gu, W., 2003, Parc: a cytoplasmic anchor for p53. Cell **112**(1): 29-40.

Nikolova, P. V., Henckel, J., Lane, D. P. and Fersht, A. R., 1998, Semirational design of active tumor suppressor p53 DNA binding domain with enhanced stability. Proceedings of the National Academy of Sciences of the United States of America **95**(25): 14675-14680.

North, S., Pluquet, O., Maurici, D., El Ghissassi, F. and Hainaut, P., 2002, Restoration of wild-type conformation and activity of a temperature-sensitive mutant of p53 (p53V272M) by the

cytoprotective aminothiol WR1065 in the esophageal cancer cell line TE-1. Molecular Carcinogenesis **33**(3): 181-188.

O'Brien, P. J., Siraki, A. G. and Shangari, N., 2005, Aldehyde Sources, Metabolism, Molecular Toxicity Mechanisms, and Possible Effects on Human Health. Critical Reviews in Toxicology **35**(7): 609-662.

Obrador-Hevia, A., Martinez-Font, E., Felipe-Abrio, I., Calabuig-Farinas, S., Serra-Sitjar, M., Lopez-Guerrero, J. A., et al., 2015, RG7112, a small-molecule inhibitor of MDM2, enhances trabectedin response in soft tissue sarcomas. Cancer Invest **33**(9): 440-450.

Ohoka, N., Yoshii, S., Hattori, T., Onozaki, K. and Hayashi, H., 2005, TRB3, a novel ER stress-inducible gene, is induced via ATF4-CHOP pathway and is involved in cell death. The EMBO Journal **24**(6): 1243-1255.

Olive, K. P., Tuveson, D. A., Ruhe, Z. C., Yin, B., Willis, N. A., Bronson, R. T., et al., 2004, Mutant p53 gain of function in two mouse models of Li-Fraumeni syndrome. Cell **119**(6): 847-860.

Ongkeko, W. M., Wang, X. Q., Siu, W. Y., Lau, A. W., Yamashita, K., Harris, A. L., et al., 1999, MDM2 and MDMX bind and stabilize the p53-related protein p73. Current Biology **9**(15): 829-832.

Ou, H. D., Lohr, F., Vogel, V., Mantele, W. and Dotsch, V., 2007, Structural evolution of C-terminal domains in the p53 family. The EMBO Journal **26**(14): 3463-3473.

Owen-Schaub, L. B., Zhang, W., Cusack, J. C., Angelo, L. S., Santee, S. M., Fujiwara, T., et al., 1995, Wild-type human p53 and a temperature-sensitive mutant induce Fas/APO-1 expression. Molecular and Cellular Biology **15**(6): 3032-3040.

Parant, J., Chavez-Reyes, A., Little, N. A., Yan, W., Reinke, V., Jochemsen, A. G., et al., 2001, Rescue of embryonic lethality in Mdm4-null mice by loss of Trp53 suggests a nonoverlapping pathway with MDM2 to regulate p53. Nature Genetics **29**(1): 92-95.

Paris, M., Rouleau, M., Puceat, M. and Aberdam, D., 2012, Regulation of skin aging and heart development by TAp63. Cell Death and Differentiation **19**(2): 186-193.

Park, B. J., Lee, S. J., Kim, J. I., Lee, S. J., Lee, C. H., Chang, S. G., et al., 2000, Frequent alteration of p63 expression in human primary bladder carcinomas. Cancer Research **60**(13): 3370-3374.

Patton, J. T., Mayo, L. D., Singhi, A. D., Gudkov, A. V., Stark, G. R. and Jackson, M. W., 2006, Levels of HdmX expression dictate the sensitivity of normal and transformed cells to Nutlin-3. Cancer Research **66**(6): 3169-3176.

Pereira, N. A. L., Monteiro, A., Machado, M., Gut, J., Molins, E., Perry, M. J., et al., 2015, Enantiopure Indolizinoindolones with in vitro Activity against Blood- and Liver-Stage Malaria Parasites. ChemMedChem **10**(12): 2080-2089.

Petitjean, A., Mathe, E., Kato, S., Ishioka, C., Tavtigian, S. V., Hainaut, P., et al., 2007, Impact of mutant p53 functional properties on TP53 mutation patterns and tumor phenotype: lessons from recent developments in the IARC TP53 database. Human Mutation **28**(6): 622-629.

Pluquet, O. and Hainaut, P., 2001, Genotoxic and non-genotoxic pathways of p53 induction. Cancer Letters **174**(1): 1-15.

Pluquet, O., Qu, L. K., Baltzis, D. and Koromilas, A. E., 2005, Endoplasmic reticulum stress accelerates p53 degradation by the cooperative actions of Hdm2 and glycogen synthase kinase 3beta. Molecular and Cellular Biology **25**(21): 9392-9405.

Polireddy, K., Singh, K., Pruski, M., Jones, N. C., Manisundaram, N. V., Ponnela, P., et al., 2019, Mutant p53(R175H) promotes cancer initiation in the pancreas by stabilizing HSP70. Cancer Letters **453**: 122-130.

Pozniak, C. D., Barnabe-Heider, F., Rymar, V. V., Lee, A. F., Sadikot, A. F. and Miller, F. D., 2002, p73 is required for survival and maintenance of CNS neurons. Journal of Neuroscience **22**(22): 9800-9809.

Punganuru, S. R., Madala, H. R., Arutla, V. and Srivenugopal, K. S., 2018, Selective killing of human breast cancer cells by the styryl lactone (R)-goniothalamin is mediated by glutathione conjugation, induction of oxidative stress and marked reactivation of the R175H mutant p53 protein. Carcinogenesis **39**(11): 1399-1410.

Punganuru, S. R., Madala, H. R., Venugopal, S. N., Samala, R., Mikelis, C. and Srivenugopal, K. S., 2016, Design and synthesis of a C7-aryl piperlongumine derivative with potent antimicrotubule and mutant p53-reactivating properties. European Journal of Medicinal Chemistry **107**(C): 233-244.

Purdie, C. A., Harrison, D. J., Peter, A., Dobbie, L., White, S., Howie, S. E., et al., 1994, Tumour incidence, spectrum and ploidy in mice with a large deletion in the p53 gene. Oncogene **9**(2): 603-609.

Raimundo, L., Espadinha, M., Soares, J., Loureiro, J. B., Alves, M. G., Santos, M. M. M., et al., 2018, Improving anticancer activity towards colon cancer cells with a new p53-activating agent. British Journal of Pharmacology **175**(20): 3947-3962.

Ramadan, S., Terrinoni, A., Catani, M. V., Sayan, A. E., Knight, R. A., Mueller, M., et al., 2005, p73 induces apoptosis by different mechanisms. Biochemical and Biophysical Research Communications **331**(3): 713-717.

Raoul, J.-L., Gilabert, M., Adhoute, X. and Edeline, J., 2017, An in-depth review of chemical angiogenesis inhibitors for treating hepatocellular carcinoma. Expert Opinion on Pharmacotherapy **18**(14): 1467-1476.

Ratovitski, E. A., Patturajan, M., Hibi, K., Trink, B., Yamaguchi, K. and Sidransky, D., 2001, p53 associates with and targets Delta Np63 into a protein degradation pathway. Proceedings of the National Academy of Sciences of the United States of America **98**(4): 1817-1822.

Raver-Shapira, N., Marciano, E., Meiri, E., Spector, Y., Rosenfeld, N., Moskovits, N., et al., 2007, Transcriptional activation of miR-34a contributes to p53-mediated apoptosis. Molecular Cell **26**(5): 731-743.

Ray-Coquard, I., Blay, J. Y., Italiano, A., Le Cesne, A., Penel, N., Zhi, J., et al., 2012, Effect of the MDM2 antagonist RG7112 on the P53 pathway in patients with MDM2-amplified, well-differentiated or dedifferentiated liposarcoma: an exploratory proof-of-mechanism study. The Lancet Oncology **13**(11): 1133-1140.

Reed, D., Shen, Y., Shelat, A. A., Arnold, L. A., Ferreira, A. M., Zhu, F., et al., 2010, Identification and Characterization of the First Small Molecule Inhibitor of MDMX. Journal of Biological Chemistry **285**(14): 10786-10796.

Resnick-Silverman, L., St Clair, S., Maurer, M., Zhao, K. and Manfredi, J. J., 1998, Identification of a novel class of genomic DNA-binding sites suggests a mechanism for selectivity in target gene activation by the tumor suppressor protein p53. Genes & Development **12**(14): 2102-2107.

Riley, T., Sontag, E., Chen, P. and Levine, A., 2008, Transcriptional control of human p53-regulated genes. Nature Reviews Molecular and Cellular Biology **9**(5): 402-412.

Rippin, T. M., Bykov, V. J., Freund, S. M., Selivanova, G., Wiman, K. and Fersht, A. R., 2002, Characterization of the p53-rescue drug CP-31398 in vitro and in living cells. Oncogene **21**: 2119-2129.

Rocco, J. W., Leong, C.-O., Kuperwasser, N., DeYoung, M. P. and Ellisen, L. W., 2006, p63 mediates survival in squamous cell carcinoma by suppression of p73-dependent apoptosis. Cancer Cell **9**(1): 45-56.

Rossi, M., De Laurenzi, V., Munarriz, E., Green, D. R., Liu, Y. C., Vousden, K. H., et al., 2005, The ubiquitin-protein ligase Itch regulates p73 stability. The EMBO Journal **24**(4): 836-848.

Rossi, M., De Simone, M., Pollice, A., Santoro, R., La Mantia, G., Guerrini, L., et al., 2006, Itch/AIP4 associates with and promotes p63 protein degradation. Cell Cycle **5**(16): 1816-1822.

Salim, K. Y., Maleki Vareki, S., Danter, W. R., San-Marina, S. and Koropatnick, J., 2016, COTI-2, a novel small molecule that is active against multiple human cancer cell lines in vitro and in vivo. Oncotarget **7**: 41363-41379.

Schwartz, H., Alvares, C. P., White, M. B. and Fields, S., 1998, Mutation detection by a two-hybrid assay. Human Molecular Genetics **7**(6): 1029-1032.

Scian, M. J., Carchman, E. H., Mohanraj, L., Stagliano, K. E., Anderson, M. A., Deb, D., et al., 2008, Wild-type p53 and p73 negatively regulate expression of proliferation related genes. Oncogene **27**(18): 2583-2593.

Shadfan, M., Lopez-Pajares, V. and Yuan, Z. M., 2012, MDM2 and MDMX: Alone and together in regulation of p53. Translational Cancer Research **1**(2): 88-89.

Sharp, D. A., Kratowicz, S. A., Sank, M. J. and George, D. L., 1999a, Stabilization of the MDM2 oncoprotein by interaction with the structurally related MDMX protein. Journal of Biological Chemistry **274**(53): 38189-38196.

Sharp, D. A., Kratowicz, S. A., Sank, M. J. and George, D. L., 1999b, Stabilization of the MDM2 oncoprotein by interaction with the structurally related MDMX protein. Journal of Biological Chemistry **274**(53): 38189-38196.

Shi, X.-B., Nesslinger, N. J., Deitch, A. D., Gumerlock, P. H. and deVere White, R. W., 2002, Complex functions of mutantp53 alleles from human prostate cancer. The Prostate **51**(1): 59-72.

Slabakova, E., Culig, Z., Remsik, J. and Soucek, K., 2017, Alternative mechanisms of miR-34a regulation in cancer. Cell Death & Disease **8**(10): e3100.

Slack, A., Chen, Z., Tonelli, R., Pule, M., Hunt, L., Pession, A., et al., 2005, The p53 regulatory gene MDM2 is a direct transcriptional target of MYCN in neuroblastoma. Proceedings of the National Academy of Sciences of the United States of America **102**(3): 731-736.

Smits, V. A., Klompmaker, R., Vallenius, T., Rijksen, G., Makela, T. P. and Medema, R. H., 2000, p21 inhibits Thr161 phosphorylation of Cdc2 to enforce the G2 DNA damage checkpoint. Journal of Biological Chemistry **275**(39): 30638-30643.

Sniezek, J. C., Matheny, K. E., Westfall, M. D. and Pietenpol, J. A., 2004, Dominant negative p63 isoform expression in head and neck squamous cell carcinoma. The Laryngoscope **114**(12): 2063-2072.

Soares, J., Espadinha, M., Raimundo, L., Ramos, H., Gomes, A. S., Gomes, S., et al., 2017, DIMP53-1: A novel small-molecule dual inhibitor of p53-MDM2/X interactions with multifunctional p53-dependent anticancer properties. Molecular Oncology **19**: 329.

Soares, J., Pereira, N. A. L., Monteiro, A., Leão, M., Bessa, C., Dos Santos, D. J. V. A., et al., 2014, Oxazoloisoindolinones with in vitro antitumor activity selectively activate a p53-pathway

through potential inhibition of the p53-MDM2 interaction. European Journal of Pharmaceutical Sciences **66C**: 138-147.

Soares, J., Raimundo, L., Pereira, N. A., dos Santos, D. J., Perez, M., Queiroz, G., et al., 2015, A tryptophanol-derived oxazolopiperidone lactam is cytotoxic against tumors via inhibition of p53 interaction with murine double minute proteins. Pharmacological Research **95-96**: 42-52.

Soares, J., Raimundo, L., Pereira, N. A., Monteiro, A., Gomes, S., Bessa, C., et al., 2016, Reactivation of wild-type and mutant p53 by tryptophanolderived oxazoloisoindolinone SLMP53-1, a novel anticancer small-molecule. Oncotarget **7**(4): 4326-4343.

Soragni, A., Janzen, D. M., Johnson, L. M., Lindgren, A. G., Thai-Quynh Nguyen, A., Tiourin, E., et al., 2016, A Designed Inhibitor of p53 Aggregation Rescues p53 Tumor Suppression in Ovarian Carcinomas. Cancer Cell **29**(1): 90-103.

Stindt, M. H., Muller, P. A. J., Ludwig, R. L., Kehrloesser, S., Dötsch, V. and Vousden, K. H., 2015, Functional interplay between MDM2, p63/p73 and mutant p53. Nature Publishing Group **34**(33): 4300-4310.

Su, C., 2016, Survivin in survival of hepatocellular carcinoma. Cancer Letters **379**(2): 184-190.

Su, X., Chakravarti, D., Cho, M. S., Liu, L., Gi, Y. J., Lin, Y. L., et al., 2010, TAp63 suppresses metastasis through coordinate regulation of Dicer and miRNAs. Nature **467**(7318): 986-990.

Suh, E. K., Yang, A., Kettenbach, A., Bamberger, C., Michaelis, A. H., Zhu, Z., et al., 2006, p63 protects the female germ line during meiotic arrest. Nature **444**(7119): 624-628.

Tabas, I. and Ron, D., 2011, Integrating the mechanisms of apoptosis induced by endoplasmic reticulum stress. Nature Cell Biology **13**(3): 184-190.

Takimoto, R. and El-Deiry, W. S., 2000, Wild-type p53 transactivates the KILLER/DR5 gene through an intronic sequence-specific DNA-binding site. Oncogene **19**(14): 1735-1743.

Tanimura, S., Ohtsuka, S., Mitsui, K., Shirouzu, K., Yoshimura, A. and Ohtsubo, M., 1999, MDM2 interacts with MDMX through their RING finger domains. FEBS Letters **447**(1): 5-9.

Taylor, W. R., Schonthal, A. H., Galante, J. and Stark, G. R., 2001, p130/E2F4 binds to and represses the cdc2 promoter in response to p53. Journal of Biological Chemistry **276**(3): 1998-2006.

Terrinoni, A., Ranalli, M., Cadot, B., Leta, A., Bagetta, G., Vousden, K. H., et al., 2004, p73-alpha is capable of inducing scotin and ER stress. Oncogene **23**(20): 3721-3725.

Thanos, C. D. and Bowie, J. U., 1999, p53 Family members p63 and p73 are SAM domain-containing proteins. Protein Science **8**(8): 1708-1710.

Tomasini, R., Tsuchihara, K., Wilhelm, M., Fujitani, M., Rufini, A., Cheung, C. C., et al., 2008, TAp73 knockout shows genomic instability with infertility and tumor suppressor functions. Genes & Development **22**(19): 2677-2691.

Urist, M. J., Di Como, C. J., Lu, M. L., Charytonowicz, E., Verbel, D., Crum, C. P., et al., 2002, Loss of p63 expression is associated with tumor progression in bladder cancer. American Journal of Pathology **161**(4): 1199-1206.

Uversky, V. N., Dave, V., Iakoucheva, L. M., Malaney, P., Metallo, S. J., Pathak, R. R., et al., 2014, Pathological unfoldomics of uncontrolled chaos: intrinsically disordered proteins and human diseases. Chemical Reviews **114**(13): 6844-6879.

Vassilev, L. T., Vu, B. T., Graves, B., Carvajal, D., Podlaski, F., Filipovic, Z., et al., 2004, In Vivo Activation of the p53 Pathway by Small-Molecule Antagonists of MDM2. Science **303**(5659): 844-848.

Veerakumarasivam, A., Scott, H. E., Chin, S. F., Warren, A., Wallard, M. J., Grimmer, D., et al., 2008, High-resolution array-based comparative genomic hybridization of bladder cancers identifies mouse double minute 4 (MDM4) as an amplification target exclusive of MDM2 and TP53. Clinical Cancer Research **14**(9): 2527-2534.

Verfaillie, T., Jäger, R., Samali, A. and Agostinis, P., 2012. ER stress signaling pathways in cell survival and death. Endoplasmic Reticulum Stress in Health and Disease, Springer**:** 41-73.

Vieler, M. and Sanyal, S., 2018, p53 Isoforms and Their Implications in Cancer. Cancers **10**(9): 288.

Vigano, M. A., Lamartine, J., Testoni, B., Merico, D., Alotto, D., Castagnoli, C., et al., 2006, New p63 targets in keratinocytes identified by a genome-wide approach. The EMBO Journal **25**(21): 5105-5116.

Vilgelm, A. E., Washington, M. K., Wei, J., Chen, H., Prassolov, V. S. and Zaika, A. I., 2010, Interactions of the p53 protein family in cellular stress response in gastrointestinal tumors. Molecular Cancer Therapeutics **9**(3): 693-705.

Vogan, K., Bernstein, M., Leclerc, J. M., Brisson, L., Brossard, J., Brodeur, G. M., et al., 1993, Absence of p53 gene mutations in primary neuroblastomas. Cancer Research **53**(21): 5269-5273.

Vogel, A., Cervantes, A., Chau, I., Daniele, B., Llovet, J., Meyer, T., et al., 2018, Hepatocellular carcinoma: ESMO Clinical Practice Guidelines for diagnosis, treatment and follow-up†. Annals of Oncology **29**(Supplement_4): iv238-iv255.

Vogelstein, B. and Kinzler, K. W., 2004, Cancer genes and the pathways they control. Nature Medicine **10**(8): 789-799.

Vousden, K. H. and Prives, C., 2009, Blinded by the Light: The Growing Complexity of p53. Cell **137**(3): 413-431.

Wade, M. and Wahl, G. M., 2009, Targeting Mdm2 and Mdmx in cancer therapy: better living through medicinal chemistry? Molecular Cancer Research **7**(1): 1-11.

Wager, M., Guilhot, J., Blanc, J. L., Ferrand, S., Milin, S., Bataille, B., et al., 2006, Prognostic value of increase in transcript levels of Tp73 DeltaEx2-3 isoforms in low-grade glioma patients. British Journal of Cancer **95**(8): 1062-1069.

Walerych, D., Olszewski, M. B., Gutkowska, M., Helwak, A., Zylicz, M. and Zylicz, A., 2009, Hsp70 molecular chaperones are required to support p53 tumor suppressor activity under stress conditions. Oncogene **28**(48): 4284-4294.

Wang, X., Arooz, T., Siu, W. Y., Chiu, C. H., Lau, A., Yamashita, K., et al., 2001, MDM2 and MDMX can interact differently with ARF and members of the p53 family. FEBS Letters **490**(3): 202-208.

Wang, X., Wang, J. and Jiang, X., 2011, MdmX protein is essential for Mdm2 protein-mediated p53 polyubiquitination. Journal of Biological Chemistry **286**(27): 23725-23734.

Wassman, C. D., Baronio, R., Demir, Ö., Wallentine, B. D., Chen, C.-K., Hall, L. V., et al., 2013, Computational identification of a transiently open L1/S3 pocket for reactivation of mutant p53. Nature Communications **4**: 1407.

Wawrzynow, B., Zylicz, A. and Zylicz, M., 2018, Chaperoning the guardian of the genome. The two-faced role of molecular chaperones in p53 tumor suppressor action. Biochimica et Biophysica Acta (BBA) - Reviews on Cancer **1869**(2): 161-174.

Weber, A., Bellmann, U., Bootz, F., Wittekind, C. and Tannapfel, A., 2002, Expression of p53 and its homologues in primary and recurrent squamous cell carcinomas of the head and neck. International Journal of Cancer **99**(1): 22-28.

Wei, C.-L., Wu, Q., Vega, V. B., Chiu, K. P., Ng, P., Zhang, T., et al., 2006a, A Global Map of p53 Transcription-Factor Binding Sites in the Human Genome. Cell **124**(1): 207-219.

Wei, C. L., Wu, Q., Vega, V. B., Chiu, K. P., Ng, P., Zhang, T., et al., 2006b, A global map of p53 transcription-factor binding sites in the human genome. Cell **124**(1): 207-219.

Wei, J., Zaika, E. and Zaika, A., 2012, p53 Family: Role of Protein Isoforms in Human Cancer. Journal of Nucleic Acids **2012**(7221): 1-19.

Weinmann, L., Wischhusen, J., Demma, M. J., Naumann, U., Roth, P., Dasmahapatra, B., et al., 2008, A novel p53 rescue compound induces p53-dependent growth arrest and sensitises glioma cells to Apo2L/TRAIL-induced apoptosis. Cell Death and Differentiation **15**(4): 718-729.

Weisz, L., Oren, M. and Rotter, V., 2007, Transcription regulation by mutant p53. Oncogene **26**(15): 2202-2211.

Westfall, M. D. and Pietenpol, J. A., 2004, p63: Molecular complexity in development and cancer. Carcinogenesis **25**(6): 857-864.

Wilhelm, M. T., Rufini, A., Wetzel, M. K., Tsuchihara, K., Inoue, S., Tomasini, R., et al., 2010, Isoform-specific p73 knockout mice reveal a novel role for delta Np73 in the DNA damage response pathway. Genes & Development **24**(6): 549-560.

Willis, A. C., Pipes, T., Zhu, J. and Chen, X., 2003, p73 can suppress the proliferation of cells that express mutant p53. Oncogene **22**(35): 5481-5495.

Wolf, E. R., McAtarsney, C. P., Bredhold, K. E., Kline, A. M. and Mayo, L. D., 2018, Mutant and wild-type p53 form complexes with p73 upon phosphorylation by the kinase JNK. Science Signaling **11**(524): eaao4170.

Wolter, J., Angelini, P. and Irwin, M., 2010, p53 family: therapeutic targets in neuroblastoma. Future Oncology **6**(3): 429-444.

Wu, G., Osada, M., Guo, Z., Fomenkov, A., Begum, S., Zhao, M., et al., 2005, DeltaNp63alpha up-regulates the Hsp70 gene in human cancer. Cancer Research **65**(3): 758-766.

Wu, H. and Leng, R. P., 2015, MDM2 mediates p73 ubiquitination: a new molecular mechanism for suppression of p73 function. Oncotarget **6**(25): 21479-21492.

Wu, H., Pomeroy, S. L., Ferreira, M., Teider, N., Mariani, J., Nakayama, K. I., et al., 2011, UBE4B promotes Hdm2-mediated degradation of the tumor suppressor p53. Nature Medicine: 1-10.

Wu, X., Bayle, J. H., Olson, D. and Levine, A. J., 1993, The p53-mdm-2 autoregulatory feedback loop. Genes & Development **7**(7A): 1126-1132.

Xie, B., Nagalingam, A., Kuppusamy, P., Muniraj, N., Langford, P., Győrffy, B., et al., 2016, Benzyl Isothiocyanate potentiates p53 signaling and antitumor effects against breast cancer through activation of p53-LKB1 and p73-LKB1 axes. Scientific Reports **7**: 1-14.

Xiong, S., Pant, V., Suh, Y. A., Van Pelt, C. S., Wang, Y., Valentin-Vega, Y. A., et al., 2010, Spontaneous tumorigenesis in mice overexpressing the p53-negative regulator Mdm4. Cancer Research **70**(18): 7148-7154.

Xu, J., Reumers, J., Couceiro, J. R., De Smet, F., Gallardo, R., Rudyak, S., et al., 2011, Gain of function of mutant p53 by coaggregation with multiple tumor suppressors. Nature Chemical Biology **7**(5): 285-295.

Yamamoto, K., Sato, T., Matsui, T., Sato, M., Okada, T., Yoshida, H., et al., 2007, Transcriptional induction of mammalian ER quality control proteins is mediated by single or combined action of ATF6alpha and XBP1. Developmental Cell **13**(3): 365-376.

Yang, A., Kaghad, M., Wang, Y., Gillett, E., Fleming, M. D., Dötsch, V., et al., 1998, p63, a p53 homolog at 3q27-29, encodes multiple products with transactivating, death-inducing, and dominant-negative activities. Molecular Cell **2**(3): 305-316.

Yang, A., Schweitzer, R., Sun, D., Kaghad, M., Walker, N., Bronson, R. T., et al., 1999, p63 is essential for regenerative proliferation in limb, craniofacial and epithelial development. Nature **398**(6729): 714-718.

Yang, A., Walker, N., Bronson, R., Kaghad, M., Oosterwegel, M., Bonnin, J., et al., 2000, p73-deficient mice have neurological, pheromonal and inflammatory defects but lack spontaneous tumours. Nature **404**(6773): 99-103.

Yang, P.-M., Lin, Y.-T., Shun, C.-T., Lin, S.-H., Wei, T.-T., Chuang, S.-H., et al., 2013, Zebularine inhibits tumorigenesis and stemness of colorectal cancer via p53-dependent endoplasmic reticulum stress. Scientific Reports **3**(1): 505-511.

Yu, X., Narayanan, S., Vazquez, A. and Carpizo, D. R., 2014, Small molecule compounds targeting the p53 pathway: are we finally making progress? Apoptosis **19**(7): 1055-1068.

Yu, X., Vazquez, A., Levine, A. J. and Carpizo, D. R., 2012, Allele-Specific p53 Mutant Reactivation. Cancer Cell **21**(5): 614-625.

Yun, J., Chae, H. D., Choy, H. E., Chung, J., Yoo, H. S., Han, M. H., et al., 1999, p53 negatively regulates cdc2 transcription via the CCAAT-binding NF-Y transcription factor. Journal of Biological Chemistry **274**(42): 29677-29682.

Zache, N., Lambert, J. M. R., Rökaeus, N., Shen, J., Hainaut, P., Bergman, J., et al., 2008, Mutant p53 targeting by the low molecular weight compound STIMA-1. Molecular Oncology **2**(1): 70-80.

Zaika, A. I., Slade, N., Erster, S. H., Sansome, C., Joseph, T. W., Pearl, M., et al., 2002, DeltaNp73, a dominant-negative inhibitor of wild-type p53 and TAp73, is up-regulated in human tumors. Journal of Experimental Medicine **196**(6): 765-780.

Zdzalik, M., Pustelny, K., Kedracka-Krok, S., Huben, K., Pecak, A., Wladyka, B., et al., 2010, Interaction of regulators Mdm2 and Mdmx with transcription factors p53, p63 and p73. Cell Cycle **9**(22): 4584-4591.

Zerdoumi, Y., Aury-Landas, J., Bonaiti-Pellie, C., Derambure, C., Sesboue, R., Renaux-Petel, M., et al., 2013, Drastic effect of germline TP53 missense mutations in Li-Fraumeni patients. Human Mutation **34**(3): 453-461.

Zhang, Y., Wang, J., Yuan, Y., Zhang, W., Guan, W., Wu, Z., et al., 2010, Negative regulation of HDM2 to attenuate p53 degradation by ribosomal protein L26. Nucleic Acids Research **38**(19): 6544-6554.

Zhu, J., Jiang, J., Zhou, W. and Chen, X., 1998, The potential tumor suppressor p73 differentially regulates cellular p53 target genes. Cancer Research **58**(22): 5061-5065.

Zilfou, J. T. and Lowe, S. W., 2009, Tumor suppressive functions of p53. Cold Spring Harbor Perspectives in Biology **1**(5): a001883-a001883.

Zocchi, L., Bourdon, J.-C., Codispoti, A., Knight, R., Lane, D. P., Melino, G., et al., 2008, Scotin: A new p63 target gene expressed during epidermal differentiation. Biochemical and Biophysical Research Communications **367**(2): 271-276.

Appendices

Appendix A. Synthesis of LEM2 and putative metabolites

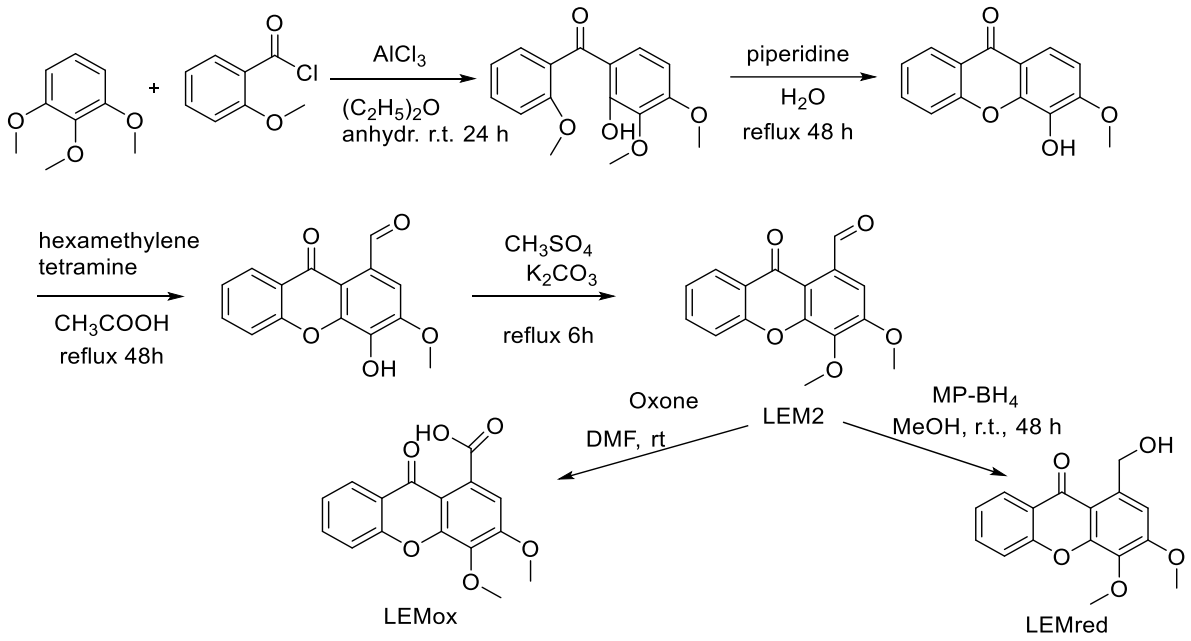

Figure A.1 Synthetic pathway and reaction conditions to obtain 1-carbaldehyde-3,4-dimethoxyxanthone (LEM2) and putative metabolites LEMred and LEMox.

Synthesis of 1-carbaldehyde-3,4-dimethoxy-9*H*-xanthen-9-one (LEM2): 2-Methoxybenzoyl chloride (3.6 g, 27 mmol), 1,2,3-trimethoxybenzene (5.0 g, 30 mmol), and $AlCl_3$ (15.0 g, 110 mmol) in dry diethyl ether (250 mL) were stirred at room temperature for 24 h. The solvent was evaporated to dryness and the crude solid poured on to ice. The aqueous suspension was acidified with 10% HCl and extracted with chloroform (3×200 mL). The organic layers were collected and dried (Na_2SO_4) and the solvent was evaporated to dryness. The crude product (2.6 g, 9 mmol) in piperidine (30 mL, 32 mmol) and water (50 mL) was heated under reflux for 48 h. After this period, the mixture was cooled and poured into 4 M HCl (300 mL). The mixture was extracted with dichloromethane (3×200 mL) and dried (Na_2SO_4) The solvent was evaporated to dryness and the product thus obtained was purified by column chromatography [petroleum ether (40-60 ºC)-ethyl acetate] yielding 1.7 g of 4-hydroxy-3-methoxyxanthone (m.p. 194-196 ºC) in 38%. To a solution of 1-carbaldehyde-4-hydroxy-3-methoxyxanthone (0.67 mmol), obtained by a Duff reaction from 4-hydroxy-3-methoxyxanthone according to a previously described procedure (Cruz et al., 2017) in acetone (10 mL), potassium carbonate (1.2 mmol) was added, followed by methyl sulfate (0.12 mL). This was heated at reflux, with magnetic stirring, for 6 h. After the reaction, the suspension was filtered, the residue was washed with acetone and the solvent was evaporated. The residue obtained was dissolved in ethyl ether (20 mL) and washed several

times with sodium hydroxide 5% (3×15 mL) and water (2×15 mL). After dehydration with anhydrous Na_2SO_4, the solvent was evaporated giving a brown oily residue. The residue was crystallized from ethyl acetate: *n*-hexane, giving light brown crystals of 1-carbaldehyde-3,4-dimetoxyxanthone (80%). IR vmax(cm^{-1}) (KBr): 3433, 2927, 1684, 1649, 1580, 1464, 1320, 1132, 758; ^{1}H NMR ($CDCl_3$): δ11.20 (s, 1H, CHO), 8.30 (dd, 1H, J= 8.0 Hz and J= 1.6 Hz, H-8), 7.76 (ddd, 1H, J= 8.5 Hz, J= 7.5 Hz and J= 1.6 Hz, H-6), 7.59 (d, 1H, J= 8.5 Hz, H-5), 7.54 (s, 1H, H-2), 7.42 (dd, 1H, J= 7.5 Hz and J= 7.5 Hz, H-7), 4.10 (s, 3H, OCH_3), 4.04 (s, 3H, OCH_3) ppm; ^{13}C NMR ($CDCl_3$): δ 192.7 (CHO); 177.8 (C-9), 156.3 (C-3), 155.4 (C-4b), 150.8 (C-4a), 140.6 (C-4), 134.7 (C-6), 133.5 (C-1), 126.7 (C-8), 124.4 (C-7), 122.0 (C-8b), 117.8 (C-5), 116.1 (C-8a), 108.4 (C-2) ppm; MS (EI): 284 (100), 299 (45), 342 (35) m/z; HRMS/ESI (+) m/z: Anal. calc. for $C_{16}H_{12}O_5$ $[M+H]^+$: 285.06847; found: 285.07627.

Synthesis of 1-(hydroxymethyl)-3,4-dimethoxy-9*H*-xanthen-9-one (LEMred): LEM2 (40 mg, 0.141 mmol) was dissolved/suspended in methanol and 4.0 equimolar quantity of Biotage® MP-Borohydride (MP-BH_4, 225.2 mg, 0,563 mmol, loading 2,5 mmol/g) was added. The resulting mixture was stirred at room temperature for 48 h. After the solution was concentrated under reduced pressure, a solid phase extraction using a cation exchange cartridge Discovery® DSC-SCX was applied to purify the crude product. Initially, an activation of the cartridge with methanol (100 mL) was carried out followed by loading the cartridge with the sample. Then, the elution was performed with the following solvents/solutions: (i) dichloromethane/methanol (5:5) and (ii) methanol. The fractions obtained from the elution with (i) were gathered and the solvent was evaporated under reduced pressure. A flash cartridge chromatography with hexane/ethyl acetate in gradient was carried out to obtain 1-(hydroxymethyl)-3,4-dimethoxy-xanthone (**LEMred**, 21 mg, 52%) as a white solid. m.p. 187-189 °C; IR umax(cm^{-1}) (KBr): 3496, 2938, 1638, 1618, 1584, 1510, 1466, 1405, 1327, 1132, 1093, 1053, 993, 755; ^{1}H-NMR ($CDCl_3$, 300.13 MHz): δ = 8.32 (1H, dd, *J* = 8.0 and 1.7 Hz, H-8), 7.75 (1H, ddd, *J* = 8.5, 7.0, and 1.7 Hz, H-6), 7.59 (1H, dd, *J* = 8.4 and 0.9 Hz, H-5), 7.41 (1H, ddd, *J* = 8.0, 7.1 and 0.9 Hz, H-7), 6.98 (1H, s, H-2), 4.95 (2H, s, H-1'); 4.03 (3H, s, 4-OCH_3), 4.01 (3H, s, 3-OCH_3) ppm; ^{13}C-NMR ($CDCl_3$, 75.47 MHz): δ = 179.0 (C-9), 156.7 (C-3), 155.4 (C-10a), 152.3 (C-4a), 139.3 (C-1), 136.1 (C-1), 134.9 (C-6), 126.7 (C-8), 124.2 (C-7), 121.9 (C-8a), 117.7 (C-5), 114.8 (C-9a), 110.3 (C-2), 65.7 (C-1'), 61.6 (4-OCH_3), 56.4 (3-OCH_3) ppm. HRMS/ESI (+) m/z: Anal. calc. for $[C_{16}H_{15}O_5]$: 287.09140; found: 287.09122.

Synthesis of 3,4-dimethoxy-9-oxo-9*H*-xanthene-1-carboxylic acid (LEMox): LEM2 (50 mg, 0.176 mmol) was dissolved in DMF (1.759 ml). Oxone (108.1 mg, 0.176 mmol) was added in one portion and stirred at room temperature for 24 h. The crude was

dissolved with 1N HCl and after cooling, a precipitate was formed. The solid was filtered and crystallized from methanol giving a white solid corresponding to 3,4-dimethoxy-9-oxo-xanthone-1-carboxylic acid (**LEMox**, 60%). m.p. > 330 °C (ethyl acetate); ^{1}H NMR ($CDCl_3$, 300.13 MHz): δ = 8.43 (1H, dd, J = 8.0 and 1.6 Hz, H-8), 8.39 (1H, s, H2), 7.88 (1H, ddd, J = 8.6, 7.1, and 1.6 Hz, H-6), 7.66 (1H, dd, J = 8.1 and 1.6 Hz, H-5), 7.50 (1H, ddd, J = 8.6, 7.1 and 1.6 Hz, H-7), 4.13 (3H, s, H-4), 4.11 (3H, s, H-3) ppm; ^{13}CNMR ($CDCl_3$, 75.47 MHz): δ = 178.1 (C-9), 157.1 (C-3), 155.4 (C-10a), 149.6 (C-4a), 139.5 (C-4), 137.0 (C-6), 130.4 (C-1), 127.9 (C-8), 125.5 (C-7), 120.4 (C-8a), 117.9 (C-5 and C-9a), 107.3 (C-2), 62.1 (C-4''), 51.3 (C-3'') ppm. HRMS/ESI (+) m/z: Anal. calc. for $C_{16}H_{12}O_6$ $[M+H]^+$: 301.07066; found: 301.07053.

References

Cruz, I., Puthongking, P., Cravo, S., Palmeira, A., Cidade, H., Pinto, M., et al., 2017, Xanthone and flavone derivatives as dual agents with acetylcholinesterase inhibition and antioxidant activity as potential anti-alzheimer agents. Journal of Chemistry **2017**: 16.

Appendix B. NMR spectra of SLMP53-2

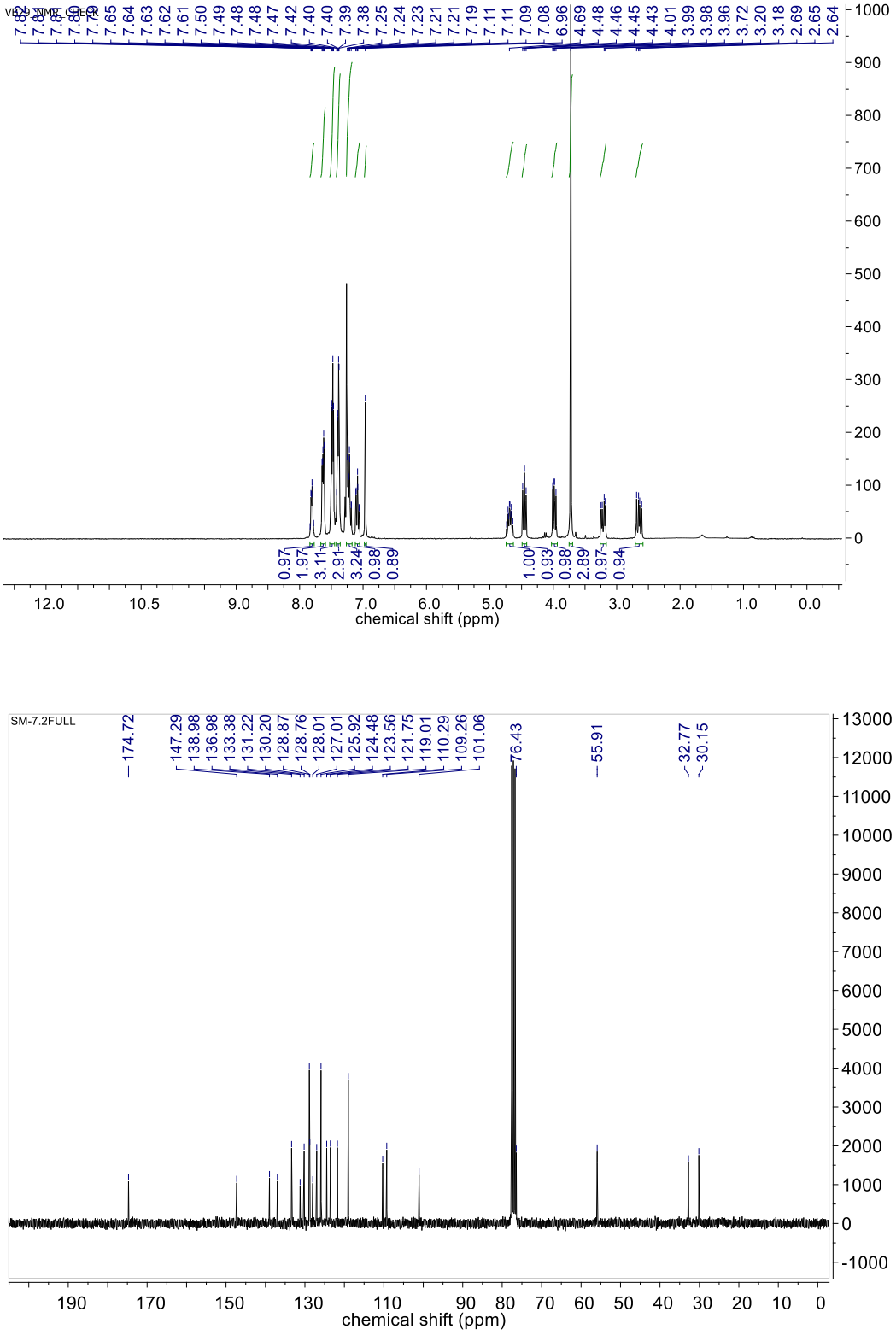

Figure B.1 ^{1}H NMR and ^{13}C NMR data for SLMP53-2

Appendix C. Supplemental microarray data

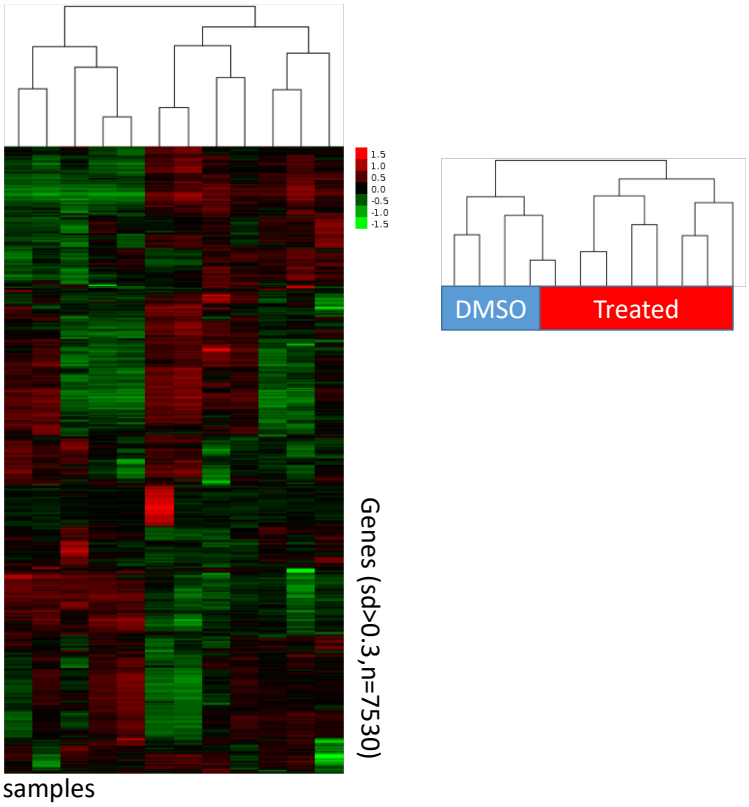

Figure C.1 Clustering analysis of the microarray data. The microarray experiment was performed in quadruplicate for 2×IC_{50} (28 μM) or 3×IC_{50} (42 μM) SLMP53-2 and control (DMSO). The overall result of the clustering analysis performed expression matrix of the genes with standard deviation higher than 0.3 (n=7530) indicates high level of reproducibility among the replicates. The microarray data has been deposited in GEO (GSE124021).

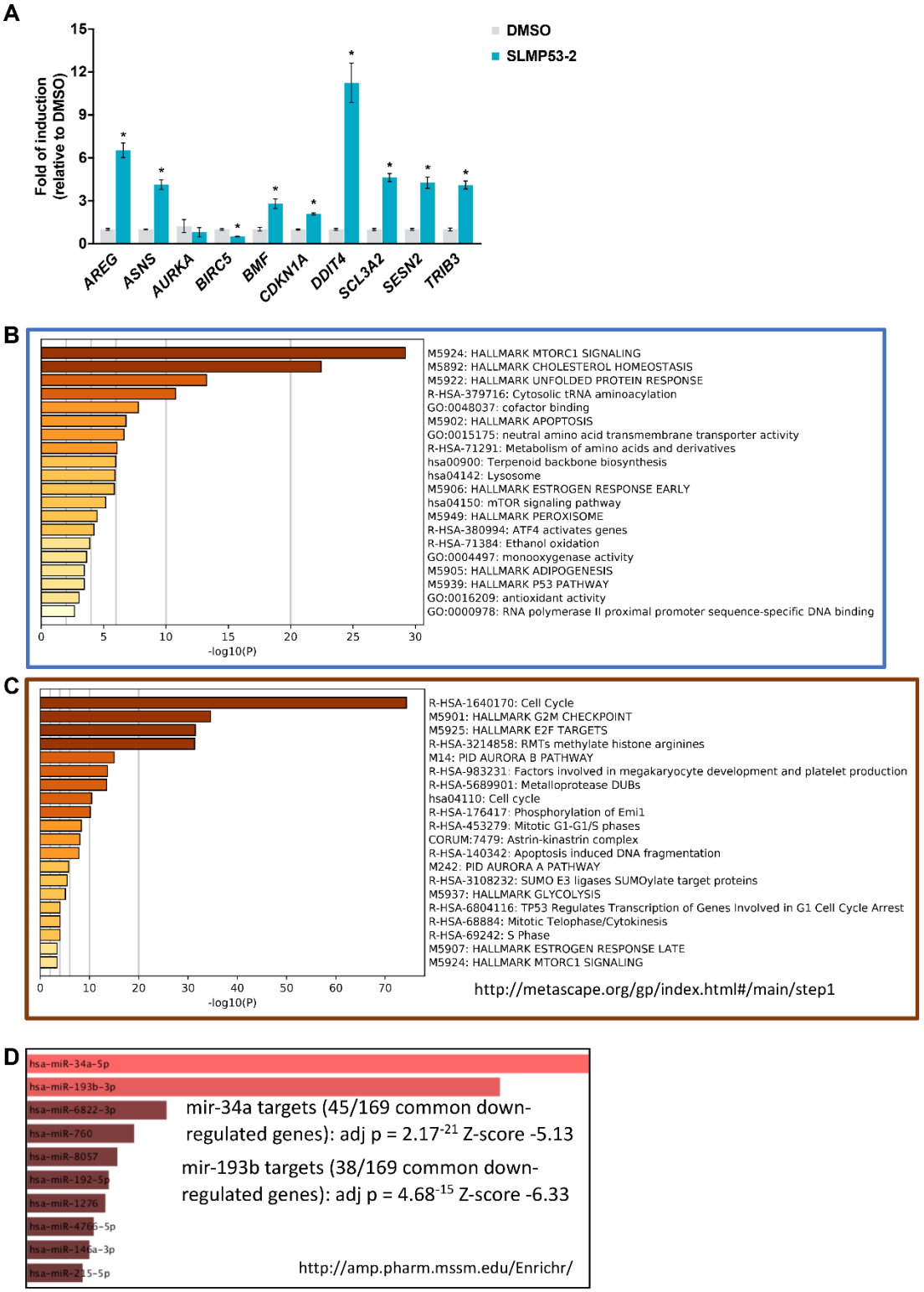

Figure C.2 Microarray data analysis related to Figure 4.3. (A) qPCR validation of the responsiveness of 10 DEGs for 28 µM SLMP53-2. Two of the ten genes (*AURKA* and *BIRC5*) were repressed by SLMP53-2 according to the microarray results. In all cases except *AURKA*, for which the difference is consistent but not significant, SLMP53-2 led to significant modulation of the genes (p<0.05, t-test). The highest fold change was seen for *DDIT4* that along with *SESN2* and *TRIB3* were included because of their involvement in the unfolded protein response. Presented are the average fold of induction relative to the DMSO treatment and the standard deviation of three replicates. B2M was used as reference genes. **(B, C)** Metascape was used to perform Gene Ontology analysis and

comparison of enriched pathways and molecular functions derived from the lists of DEGs in common between the two treatments. **(B)** Modulation of mTORC1 signalling, cholesterol homeostasis and unfolded protein response are the most significant enriched features from the up-regulated gene group, consistent with the results obtained by Ingenuity Pathway (**Figure C.1**). **(C)** Cell cycle, proliferation and cell division pathways are strongly enriched considering the repressed, differentially expressed genes. **(D)** SLMP53-2 repressed genes are enriched for mir-34a and mir-193b targets according to Enrichr. Presented are the results from miRTarBase-2017 starting from the list of 169 down-regulated, genes that are downregulated in the treatment with both SLMP53-2. The number of targets for each of the two microRNAs and the statistical analysis is provided.

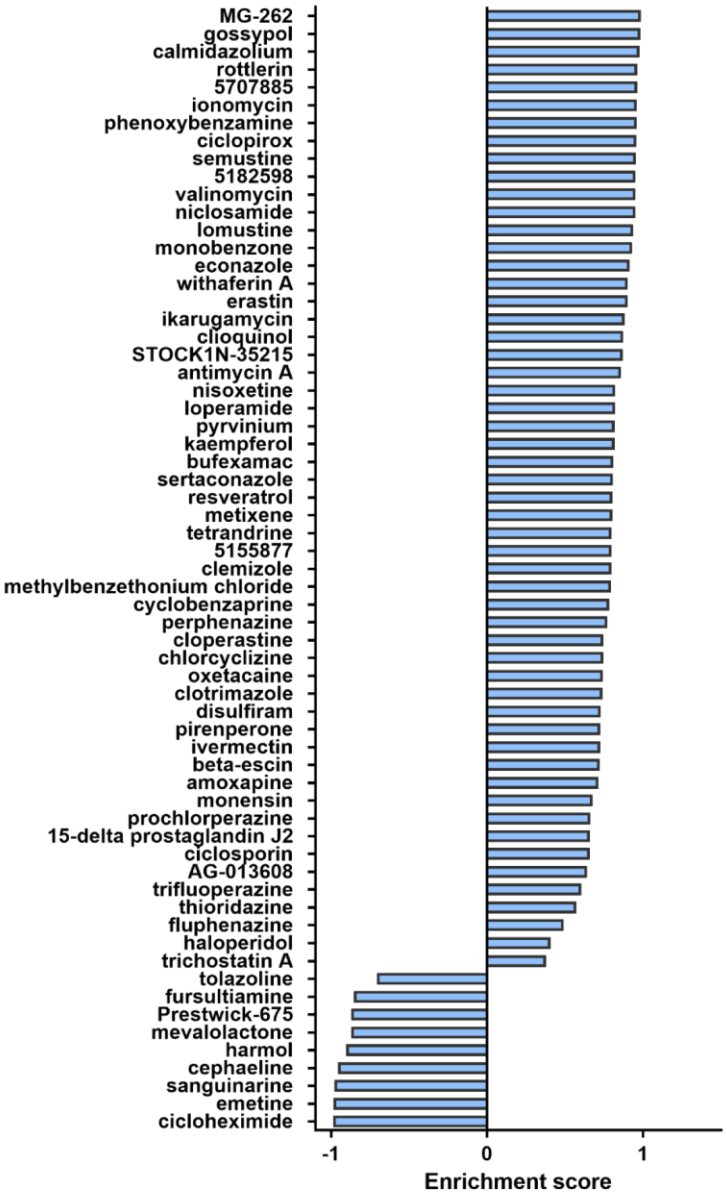

Figure C.3 Connectivity map results. Summary graph of the connectivity map results obtained using the gene expression results from the HuH-7 cells treated with 28 μM SLMP53-2. Results were filtered for p value and are ordered for decreasing enrichment score. As expected, given the strong cell cycle arrest and apoptosis phenotype induced by SLMP53-2, high enrichment score was observed with several drugs, although specificity was generally low. Interestingly, among the top scorer are molecules involved in autophagy and proteasome functions.